KUNGL
TEKNISKA
HÖGSKOLAN

TRITA - KRV- 2002-02
ISSN - 1100/7990
ISRN KTH-KRV-R-02-2-SE
ISBN 91-7283-358-0

Numerical Investigation of the Aerodynamic Vibration Excitation of High-Pressure Turbine Rotors

Markus Jöcker

Doctoral Thesis
2002

Department of Energy Technology
Division of Heat and Power Technology
Royal Institute of Technology

Akademisk avhandling som med tillstånd av Kungliga Tekniska Högskolan (Royal Institute of Technology) i Stockholm framlägges till offentlig granskning för avläggande av teknisk doktorexamen i energiteknik, måndagen den 14 oktober 2002, kl 10.00 i föreläsningssalen M2, Brinellvägen 64, Kungliga Tekniska Högskolan, Stockholm. Avhandlingen försvaras på engelska.

ABSTRACT

The design parameters axial gap and stator count of high pressure turbine stages are evaluated numerically towards their influence on the unsteady aerodynamic excitation of rotor blades. Of particular interest is if and how unsteady aerodynamic considerations in the design could reduce the risk of high cycle fatigue (HCF) failures of the turbine rotor.

A well-documented 2D/Q3D non-linear unsteady code (UNSFLO) is chosen to perform the stage flow analyses. The evaluated results are interpreted as aerodynamic excitation mechanisms on stream sheets neglecting 3D effects. Mesh studies and validations against measurements and 3D computations provide confidence in the unsteady results.

Three test cases are analysed. First, a typical aero-engine high pressure turbine stage is studied at subsonic and transonic flow conditions, with four axial gaps (37% - 52% of $c_{ax,rotor}$) and two stator configurations (43 and 70 NGV). Operating conditions are according to the resonant conditions of the blades used in accompanied experiments. Second, a subsonic high pressure turbine intended to drive the turbopump of a rocket engine is investigated. Four axial gap variations (10% - 29% of $c_{ax,rotor}$) and three stator geometry variations are analysed to extend and generalise the findings made on the first study. Third, a transonic low pressure turbine rotor, known as the International Standard Configuration 11, has been modelled to compute the unsteady flow due to blade vibration and compared to available experimental data.

Excitation mechanisms due to shock, potential waves and wakes are described and related to the work found in the open literature. The strength of shock excitation leads to increased pressure excitation levels by a factor 2 to 3 compared to subsonic cases. Potential excitations are of a typical wave type in all cases, differences in the propagation direction of the waves and the wave reflection pattern in the rotor passage lead to modifications in the time and space resolved unsteady pressures on the blade surface. The significant influence of operating conditions, axial gap and stator size on the wave propagation is discussed on chosen cases. The wake influence on the rotor blade unsteady pressure is small in the present evaluations, which is explicitly demonstrated on the turbopump turbine by a parametric study of wake and potential excitations. A reduction in stator size (towards $R \approx 1$) reduces the potential excitation part so that wake and potential excitation approach in their magnitude.

Potentials to reduce the risk of HCF excitation in transonic flow are the decrease of stator exit Mach number and the modification of temporal relations between shock and potential excitation events. A similar temporal tuning of wake excitation to shock excitation appears not efficient because of the small wake excitation contribution. The increase of axial gap does not necessarily decrease the shock excitation strength neither does the decrease of vane size because the shock excitation may remain strong even behind a smaller stator. The evaluation of the aerodynamic excitation towards a HCF risk reduction should only be done with regard to the excited mode shape, as demonstrated with parametric studies of the mode shape influence on excitability.

Keywords: Aeroelasticity, Aerodynamics, Stator-Rotor Interaction, Excitation Mechanism, Unsteady Flow Computation, Forced Response, High Cycle Fatigue, Turbomachinery, Gas-Turbine, High-Pressure Turbine, Turbopump, CFD, Design

PREFACE

This thesis is mainly based on the publications listed below, which are also enclosed in the Appendix.

I. **Fransson, T.H., Jöcker, M., Bölcs, A., Ott, P.; 1999**
"Viscous and Inviscid Linear/Nonlinear Calculations Versus Quasi 3D Experimental Cascade Data For a New Aeroelastic Turbine Standard Configuration", *Journal of Turbomachinery, Vol. 121, No. 4, Oct. 1999, pp. 717ff.*

II. **Freudenreich, K., Jöcker, M., Rheder, H.-J., Höhn, W., Fransson, T.H.; 1999**
"Aerodynamic Performance of Two Isolated Stators in Transonic Annular Cascade Flow", *Proceedings of the 3rd Euopean Conference on Turbomachinery – Fluid Dynamics and Thermodynamics, London, UK, March 2-5, 1999, Professional Engineering Publishing, ISBN: 1 86058 196 X*

III. **Jöcker, M.; Freudenreich, K.; Rehder, H.-J.; Fransson, T.H.; 2000b**
"Parametric Studies of the Aerodynamic Excitation in High Pressure Turbines.", *Proceedings of 9th International Symposium on Unsteady Aerodynamics, Aeroacoustics and Aeroelasticity of Turbomachines, Lyon, France, 2000, ISBN: 2 7061 1052 X*

IV. **Freudenreich, K.; Jöcker, M., Fransson, T.H.; 2001a**
"Gust and Forcing Function in a Transonic Turbine" *Conference Proceedings of the 4th European Conference on Turbomachinery - Fluid Dynamics and Thermodynamics Firenze, 20th-23rd March, 2001, S.G.E., ISBN: 88-86281-57-9*

V. **Jöcker, M.; Hillion, F.X.; Fransson, T.H.; Wåhlén, U.; 2001**
"Numerical Unsteady Flow Analysis of a Turbine Stage with Extremely Large Blade Loads", *46th ASME TURBO EXPO 2001, paper No. 2001-GT-0260 and J. of Turbomachinery, Vol. 124, No. 3, July 2002*

VI. **Jöcker, M.; Fransson, T.H.; 2002b**
"Modeshape Sensitivity of the High Pressure Turbine Rotor Excitation Due to Upstream Stators", *presented at the 47th ASME TURBO EXPO 2002, paper No. GT-2002-30452*

Not included in the Appendix is

VII. **Moyroud, F.; Cosme, N.; Jöcker, M.; Fransson, T.H.; Lornagex, D.; Jacquet-Richardet, G.; 2000**
"A Fluid-Structure Interfacing Technique for Computational Aeroelastic Simulations"; *Proceedings of 9th International Symposium on Unsteady Aerodynamics, Aeroacoustics and Aeroelasticity of Turbomachines, Lyon, France, 2000, ISBN: 2 7061 1052 X*

Professor Torsten H. Fransson has supervised all publications. The experimental work in publication 1 was performed by the research team at the Swiss Federal Institute of Technology (EPFL) in Lausanne, Switzerland in 1991. The main part of the experimental

work in publications 2, 3 and 4 was conducted and evaluated by Dr. Kai Freudenreich during our collaboration 1997 –2001, and minor parts by Mr. Hans-Jürgen Rheder at the German Aerospace Centre (DLR). A few numerical studies presented in the thesis and the publications were supported by colleagues, in particular to name Mr. Jerome Jeanpierre (UNSFLO installation and some early numerical studies), Mr. Francois Xavier Hillion (some studies with UNSFLO for Publication 5) and Dr. Wolfgang Höhn (Inst and Volsol computations in publications 1 and 2). Dr. Francois Moyroud, who is the main contributor to publication 7, maintained the post-processor, which was partly used and extended by the author. A large part of the work was conducted in the frame of a European research project (ADTurB, 1996 -2000) and a research collaboration between Volvo Aero Corporation in Sweden and the Royal Institute of Technology (KTH) in Stockholm (1997-2000) so that many details of the results are documented in confidential reports. These are listed below but not included in the Appendix.

Jeanpierre, J.; Fransson, T.; 1997
Brite EuRam ADTurB: "Task 2 Forced Response Analysis, Subtask A2.1.1: Prediction of the excitation level on the blades – 43 NGV", *Report ADTB-KTH-2005, Internal report No. 97/26, November 1997, Confidential*
Jöcker, M., Fransson, T.; 1998a
Brite EuRam ADTurB: "Task 2 Forced Response Analysis, Subtask A2.2.1: Prediction of the Blade Excitation Pressure Level - 70 NGV", *Report ADTB-KTH-2010, Internal report No. 98/29 November 1998, Confidential*
Jöcker, M., Fransson, T.; 1998b
KTH Study Part 2: Report on Unsflo Calculations: Numerical Parameter Study of the Axial Gap and Stator Pitch on the Forced Response, *Internal Report No. KTH-HPT-30/98, Confidential*
Jöcker, M.; Hillion, F.X.; Fransson, T.; 2000
"Final Report, Design and Analysis of a Turbine with Extremely Large Blade Loads, Phase 2"; *Internal Report No. 00/07, March 2000, Confidential*
Jöcker, M., Fransson, T.; 2002a
"Brite EuRam ADTurB: "Task 2 DLR Rig – Validation of Excitation Pressure Computations", *Report No. ADTB-KTH-2020, Internal Report No. KTH-HPT-25/02, Confidential*

Some results have been achieved during the following student works, which were supervised by the author:

Riewaldt, H.; 1999
"Numerical Study of the Forces Due to Blade Excitation and Rotor Blade Vibration to Estimate the Rotor Forced Response of a Stator-Rotor Turbine Stage Configuration*", KTH Stockholm, Avdelningen för Kraft- och Värme Teknologi, 12th March 99, Report No. 548*
Khalifa, A.; 1999
"Detailed Numerical Study of the Flutter Behaviour of a Turbine Blade (Standard Configuration 11) at Design and Off-Design Conditions with H-type Mesh using ICEMCFD" *KTH Stockholm, Avdelningen för Kraft- och Värme Teknologi, 17th Aug. 99, Rep. No. 552*
Limoa, A., 2001
"Test and Application of the unsteady aerodynamic code SLiQ at HPT", *4 months practice in the frame of the MSc. Curriculum at the University of Karlsruhe, April 2001, Internal Report No. 01/13*

ACKNOWLEDGEMENT

This work was initiated and supported by the European Community, Brite Euram Project “Aeromechanical Design of Turbine Blades”, (ADTurB), contract number BEPR-CT95-0124.

The opportunity to use the codes UNSFLO and SliQ provided by Rolls Royce and the code VOLSOL provided by Volvo Aero Corporation is gratefully acknowledged.

The work was supported with computing resources provided by the Centre of Parallel Computers (PDC) at KTH Stockholm and distributed by the Swedish National Allocations Committee (SNAC).

I would like to express my gratitude to Professor Dr. Torsten H. Fransson at the Chair of Heat and Power Technology, the Royal Institute of Technology (KTH) Stockholm, for making this work possible.

I also want to thank all colleagues at KTH Stockholm for the pleasant and stimulating time they shared with me. The contributions to the work by Mr. Jerome Jeanpierre and Mr. Francois Xavier Hillion are highly appreciated. Thanks also for the encouraging discussions on the aeroelastic subject to Mr. Andreas Krainer, Dr. Francois Moyroud, Dr. Wolfgang Höhn, Ms. Olga Tchernycheva and Mr. Björn Laumert. I gratefully enjoyed collaborating with Mr. Holger Riewaldt and Mr. Arif Khalifa, who contributed with their MSc thesis works and with Mr. Alvin Limoa, who did an internship.

Special thanks go to all the experimentalists, to name Dr. Kai Freudenreich (former KTH), Mr. Hans-Jürgen Rheder (DLR) and Dr. Holger Hennings (DLR), who provided the real data!

Many thanks to all fellows joining me running through the forests when sitting in the office was not to bear anymore, especially to Andreas, Thomas S., Samuel and Thomas B.

Last but not least I want to thank my family for supporting me performing this work. Great thanks to Eva, who had to withstand all the ups and downs and still gave birth to and is rising our son Ludvig, who has the great ability to distract all attention from everything else but him.

LIST OF CONTENTS

LIST OF FIGURES

LIST OF TABLES

NOMENCLATURE

A	Potential amplitude	[%]
A	Non-dimensional vibration amplitude (h/c for bending, α [rad] for torsion)	[-]
c	Chord length	[m]
c_p	Blade surface pressure coefficient	[-]
d	Damping	[Ns/m]
D	Damping ratio, damping/critical damping	[-]
D	Wake velocity deficit $(w_{max}-w_{mean})*100/w_{mean}$	[%]
f	Perturbation force	[N]
g_{ax}	Axial gap in percent of rotor axial chord	[-]
H	Blade height	[m]
h	Bending amplitude	[m]
k	Stiffness	[N/m]
k	Tangential wave number	[1/m]
k	Reduced frequency	[-]
K	Mean kinetik energy	
n	Traveling waver number, positive for backward (opposite rotational direction) traveling waves	[-]
$\vec{n}$	Normal blade surface vector	[m]
N	Number of vanes / blades	
M	Mach number	[-]
m	Perturbation blade moment	[Nm]
m	Mass	[kg]
p	Pressure	[Pa]
phi/phi_0	Stator relative angular position/ stator pitch angle	[-]
P	Pressure wave amplitude $(p_{max}-p_{mean})*100/p_{t2/rotor}$	[%]
R	Pitch ratio S_{stator}/S_{rotor}	[-]
R, r	Radius	[m]
S, s	Normalized curvilinear distance on blade, $s = \int_{x\min}^{x} ds\,, \quad ds = \sqrt{dx^2 + dy^2 + dz^2}$	[-]
S	Pitch	[m]
t	Time	[s]
T	Temperature	[K]
T	Time of period (T_{rotor} = vane passing period)	[-]
$\vec{u}$	Local airfoil vibration velocity	[m/s]
$\vec{w}$	Relative flow velocity	[m/s]
W	Aerodynamic work	[Nm]
W	Wake width normalized with S_s	[-]
x, y, z	Carthesian co-ordinates	[m]
α	Torsion vibration amplitude	[rad]
α	Flow angle	[º]
β	Relative flow angle	[º]
γ	Stagger angle	[º]
$\vec{\delta}$	Airfoil vibration displacement vector (mode shape)	[m]
$\partial(..)$	Spatial disturbance, derivative	[-]
ε	Phase shift between excitation and blade motion	[rad]

σ	Interblade phase angle	[rad]
λ	Axial wave number	[1/m]
ρ	Density	[kg/m^3]
Φ	Velocity potential (=$\nabla\vec{w}$)	[m^2/s]
Λ	Logarithmic decrement	[-]
Ξ	Aerodynamic damping	[-]
Ω	Excitation frequency, rotational speed	[rad/s]
ω	Circular frequency, eigenfrequency	[rad/s]

Subscripts

0	Reference value
1	Stage inlet
2	Between stator and rotor
3	Stage outlet
ax	Axial
c	Chordwise
e	Excitation
g	Generalised
h	Harmonic
iso	Isentropic
m	Motion
F	Flux averaged value
min, max ,mean	Minimum, maximum, average
p	Potential
r, rotor	Rotor
t	Total flow value
s, stator	Stator
W	Wake frame of reference
w	Vortical
x	Axial direction
y	Tangential direction

Superscripts

~	Unsteady (perturbation) value

Abbreviations

1F, 2F,.. 1E, 2E,.. 1T, 2T, ..	Mode shapes: orders of flap (F), edgewise (E) and torsion (T) modes
2D,Q3D, 3D	Two-, quasi three- and three dimensional
CFD	Computational fluid Dynamics
CS	Cebeci Smith turbulence model
CSD	Computational Structural Dynamics
EO	Excitation order
IBPA	Interblade phase angle
LE, TE	Leading edge, trailing edge
NGV	Nozzle guide vane
OP	Operating point
RPM	Rotations per minute
s	small axial gap cases

1 INTRODUCTION

1.1 General Background

1.1.1 "The driving forces for new developments"

"Today's aero gas turbine continues to have a promising future and is expected to capture an estimated market of $ 1 trillion over the next twenty years, spread across the four market sectors of civil and defence aerospace, marine and energy. However, advances in technology will be at the heart of its success in the future as in the past" [Ruffles 2001].

In the beginning of the 21st century gas-turbine technology is widely used both in propulsion engines and for stationary energy conversion in power plants. In the propulsion sector gas-turbines are commonly used in military and civil aircraft engines and also in marine propulsion and space propulsion engines. The future developments might also lead to vehicular-gas-turbine drives. On the energy market the gas turbine technology had a revival during the 1990s with the successful implementation of combined cycle power plants, which effectively rose the efficiency of energy conversion compared to single steam- or gas-turbine plants. Future power plants might use gas-turbine technology in new power-cycle developments as for example water or steam injected cycles, the air-bottoming cycle or the use of fuel cell technology. Another trend is the development of micro gas turbines reducing the engine to button size, which could be used as power units for a wide range of applications.

Because the energy retrieved from gas turbine engines usually requires fuel combustion the increase of engine efficiency is directly related to the decrease of air pollution and the decrease of driving costs, both major parameters for the competition with alternative energy and propulsion systems. Hence, a major research effort is put on the efficiency improvement and reduction of specific fuel consumption of gas-turbine engines by improving design and performance by means of reduced aerodynamic, thermal and mechanical losses, increased turbine inlet pressure and temperature, improved combustion efficiency, cooling performance and materials use.

However, component efficiencies of gas turbine engines nowadays offer only small margins for improvement because of the high technical standard achieved so far. Therefore, other parameters to reduce the costs of gas turbine engines become important:

- In aircraft propulsion the weight to thrust ratio of the engine is an important parameter with direct influence on the specific fuel consumption and air pollution, which enforces the design of lighter and more compact engines. This involves both the use of new materials and composite structures and the minimisation of the structural integrity margins of the components. For example a necessary thickening of rotor trailing edges by 0.1 mm (to ensure an endurance limit) leads to 0.1 % specific fuel consumption penalty [ADTurB 2, 2000]. Other constructive measures to reduce weight are the decrease of the number of stages and the number of blades in a blade row, leading to increased loads of the individual blades. Also axial distances between engine components are minimised, which on the other hand leads to increased levels of dangerous aerodynamic interactions.

- In stationary applications competition drives the turbine designers to increase load and performance of the engines and to optimise material use to be cost efficient.

- The lifetime of engine components is an important cost factor and reducing maintenance efforts for the engine is a major goal for gas-turbine manufacturers to be competitive. For aircraft engines the guaranteed lifetime of engine components is of special importance because of the safety requirement of such engines.

- The development costs of new gas turbines are enormous. Major savings can be made when replacing extensive tests with reliable “table design methods”. Prototypes of the largest stationary gas turbines are usually tested first when installed in the power plant. A failure detected at this stage is very expensive.

- The development and validation of numerical tools to calculate structural and aerodynamic behaviour is a key factor to replace semi-empirical methods in the design process, so that new and unconventional designs can be proved fast and cheap without the need of testing.

The present research work is motivated by the needs for improved designs for turbine engines, some of the major actual driving forces for new developments have been listed in this chapter.

1.1.2 Gas turbine engine vibration problems

Most components in a gas turbine engine are exposed to vibrations caused by unsteady forces due to relative motions of rotating and non-rotating parts. Currently, related research work focuses on four broad, sometimes overlapping, areas: vibrations related to combustion instability, acoustically relevant vibrations, rotor instability (whirl) and vibrations of blades, the latter one is subject of the present thesis.

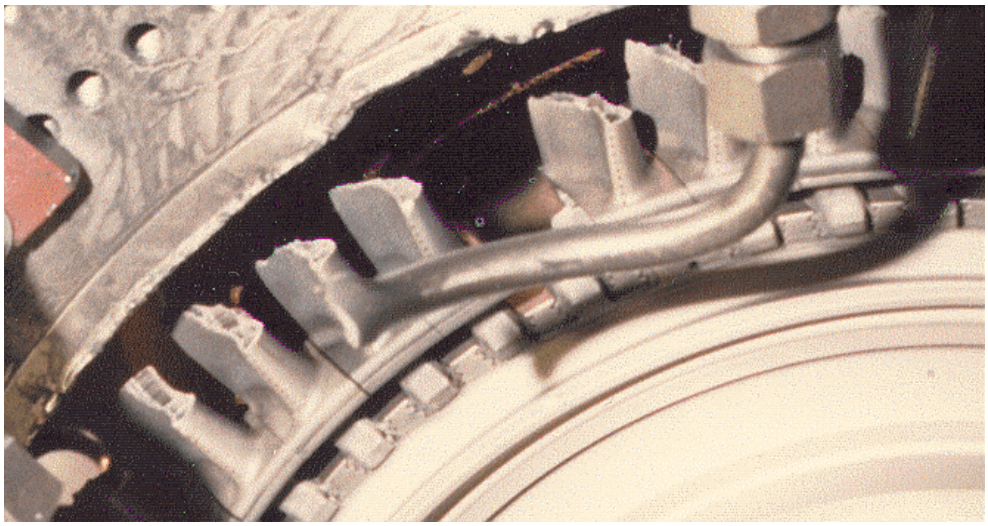

Figure 1: *Photograf of a broken blade in a turbine test rig, the purpose of the experiment was to fail the blade (by courtesy of Rolls-Royce plc)*

Beside other impacts the vibrations of gas-turbine-engine parts can cause High-Cycle Fatigue (HCF) failures, which are characterised by fractures due to large numbers of alternating stress cycles. Such failures are sudden events, because the cracks caused by HCF usually propagate very rapidly and can in extreme cases lead to blade release. A photograph of a HCF damaged blade is shown in Figure 1. In difference to Low-Cycle Fatigue (LCF) the stress level is so small that no plastic deformation of the part occurs. A typical number of cycles until a HCF failure is of the order 10'000 – 1'000'000. In [Wisler 1998a] one can read that "*HCF problems account for between 10 and 40 percent of the total development problems in gas turbine engines … The average developmental program has about 2.5 serious HCF problems to resolve*". These problems tend not to diminish in future having in mind the developmental trends towards higher performance and optimised material use, which will lead to more vibration sensitive structures.

The HCF risk of a vibrating machinery part is usually assessed with help of a "Goodman Diagram", an example of such a diagram is given in Figure 2. For a certain guaranteed lifetime of a material expressed as a number of vibration cycles (10^7 in the example) before failure an experimentally obtained line can be drawn indicating the maximum allowable steady and alternating stresses. Obviously, the allowable alternating stress level, also named endurance limit, decreases with increasing steady stresses. When the steady stress in the blade is known the allowable alternating stress, which still ensures the specified material lifetime can be read from the diagram. The steady load of the blade, which is the steady aerodynamic load and the centrifugal force in rotating parts, causes a static displacement and the steady stress whereas the unsteady load can lead to blade vibrations and thereby cause the alternating stress. In the present example the steady and alternating stresses are given at various locations on the sketched blade surface, the connection of these points describes the stress envelope. It shows that various parts of a blade experience different loads, with the critical load in the present example in point C.

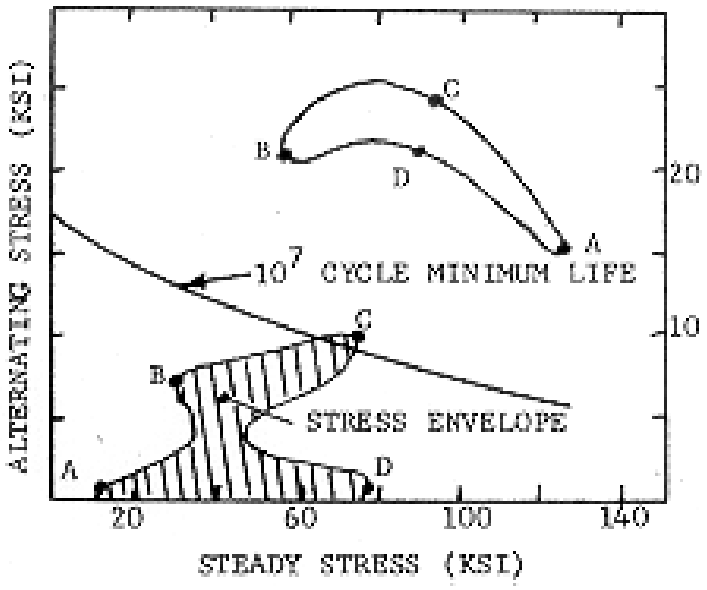

Figure 2: *Example of a Goodman Diagram for a turbine blade [Abell et al. 1977]*

The vibration behaviour of a blade is described by the blade mode shapes, which are a result of a modal analysis of the vibrating system. These are flexing (bending) modes, torsion modes, edgewise bending modes and plate modes and describe the deformation of the structure under free vibration. Typical mode shape figures are illustrated in Figure 3 showing a fist torsion mode (1T), a second flex mode (2F) and the second edge mode (2E). Under the assumption of cyclic symmetry (i.e. a tuned blade row) the circumferentially periodic vibration pattern along the annulus of a bladed disk is described with the “Nodal Diameter” (ND) of the mode or the “Interblade Phase Angle” (IBPA). This is described in more detail in Chapter 4.1.

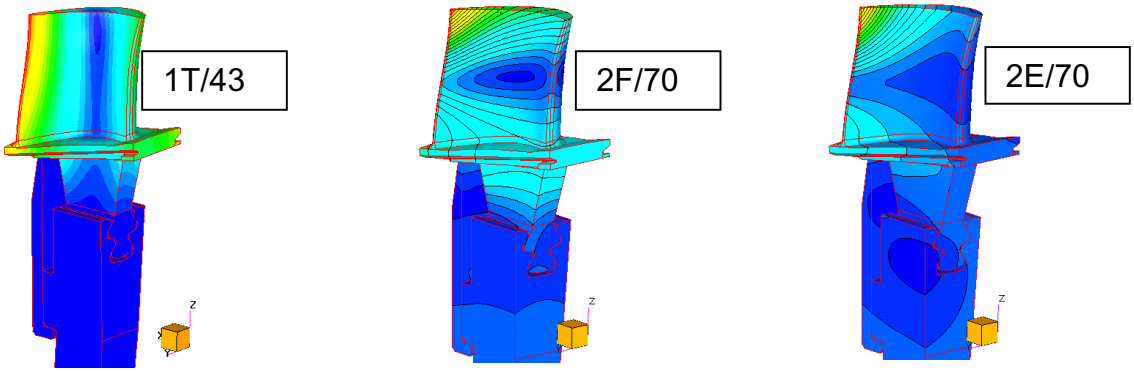

Figure 3: *Displacement contours of typical blade mode shapes [Green, 2001]*

Various mechanisms are commonly defined describing the vibrations of turbomachinery blades, usually classified according to the origin of the excitation. These can be of mechanical thermal or aerodynamic nature. Mechanical excitations include blade tip casing contact or foreign object damage; aerodynamic excitations include blade row interaction (forced response), self excitation (flutter), impact of cooling jets, compressor surge and rotating stall as well as turbulence [Murthy et al. 1993]. Figure 4 exemplifies the main unsteady flow effects present in a turbine stage, the blade row interaction is split into wake/rotor interaction and potential interaction (detailed definitions follow in Chapter 1.1.3, “Flow Defects”).

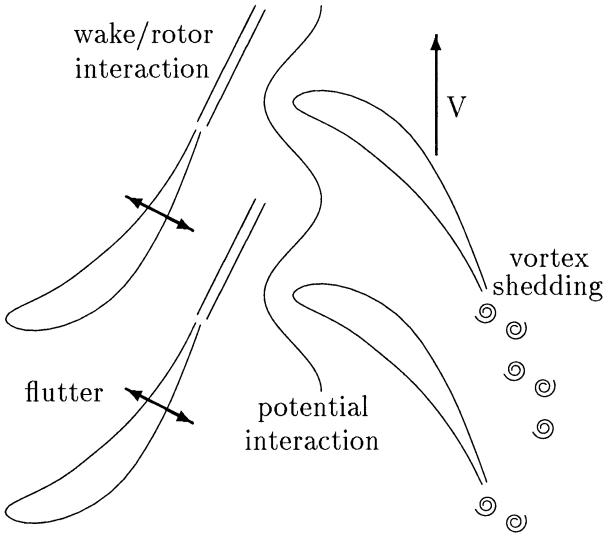

Figure 4: *Illustration of unsteadiness in a turbine stage [Giles 1991]*

Self excited vibrations

When the vibrations are self excited (flutter) the vibration motion of the blade itself causes an unsteady pressure field around the blade sustaining the vibration. Such behaviour is usually started by small aerodynamic or mechanical disturbances above a critical flow speed. It can lead to drastically increasing blade vibration amplitudes and rapid blade failure, if the mechanical damping is too low to dissipate the aerodynamic energy put on the blade. Long and slender structures are more prone to flutter, i.e. the fan blades and 1st stage compressor blades, but also low pressure turbine blades. Flutter is not a problem in the high pressure turbine.

Forced Vibrations

Forced vibrations (forced response) are characterised by aerodynamic excitation sources, which are flow disturbances acting periodically on the blades and originate from upstream and/or downstream obstacles. The most common forced vibrations are due to inlet distortions originating at the air intake (inlet struts, cross winds), blade row interactions and hot streaks originating from the burners. Also the burner cans themselves cause circumferential variations in the burner exit flow. The time-periodic excitation is in all cases caused by the relative rotational motion of excitation source and the excited structure, which leads to excitation frequencies multiples of the rotation frequency. A common way to illustrate forced response regions of a blade row is the “Campbell Diagram”, an example shown in Figure 5, which is a key plot in the unsteady design process. It shows the eigenfrequencies of the structure as it varies with its rotational speed, in the figure various torsion and bending mode frequencies are shown. Furthermore, excitation frequency lines for various numbers of excitations per revolution (usually called the excitation order, EO) are plotted with constant slope versus rotational speed, in the example excitation orders due to burner cans as well as due to upstream and downstream vanes are shown. When an eigenfrequency line crosses an excitation line, the risk of resonant excitation of the structure exists. Practically, in high pressure turbines vane passing does not excite the 1st flex mode because of its low eigenfrequency (typical frequencies correspond to 8 to 10 excitations per revolution in the operating range, compare also Figure 5). Modes at such low frequency may vibrate due to low engine order excitation, which can be caused by non-uniformities due to manufacturing variations and wear (for example vane erosion, burnout). Only the higher blade modes (1T, 2F, 2E, …) are prone to vane passing excitation, where the majority of problems occur at the 1st harmonic vane passing frequency.

But not only the excitation frequency must coincide with the blade eigenfrequency, also the excited mode shape of the structure must fall together with the circumferential and local blade excitation pattern to result in a dangerous excitation. The circumferential consistency requirement is expressed in Equation 4-2, with which the interblade phase angle due to the excitation order can be estimated. If only the blades participate in the vibration, which is the case at high frequency with relatively stiff disks, this requirement will give the interblade phase angle of the blade vibration. If the disk is involved in the vibration the nodal diameter of the disk mode must meet the excitation order to be receptive for the excitation (see further [Ewins, 1988]). Therefore, not all crossings in the Campbell Diagram are marked as resonance conditions. The receptiveness of the local blade mode shape to

the excitation pattern is part of the present work. Even though several conditions must coincide for a forced response occurrence it is not trivial to avoid it because of the amount of engine order excitation sources present in an engine. Typically, the designer avoids the empirically most critical resonant excitations, but he is not able to eliminate all resonance conditions in the operating range of the engine.

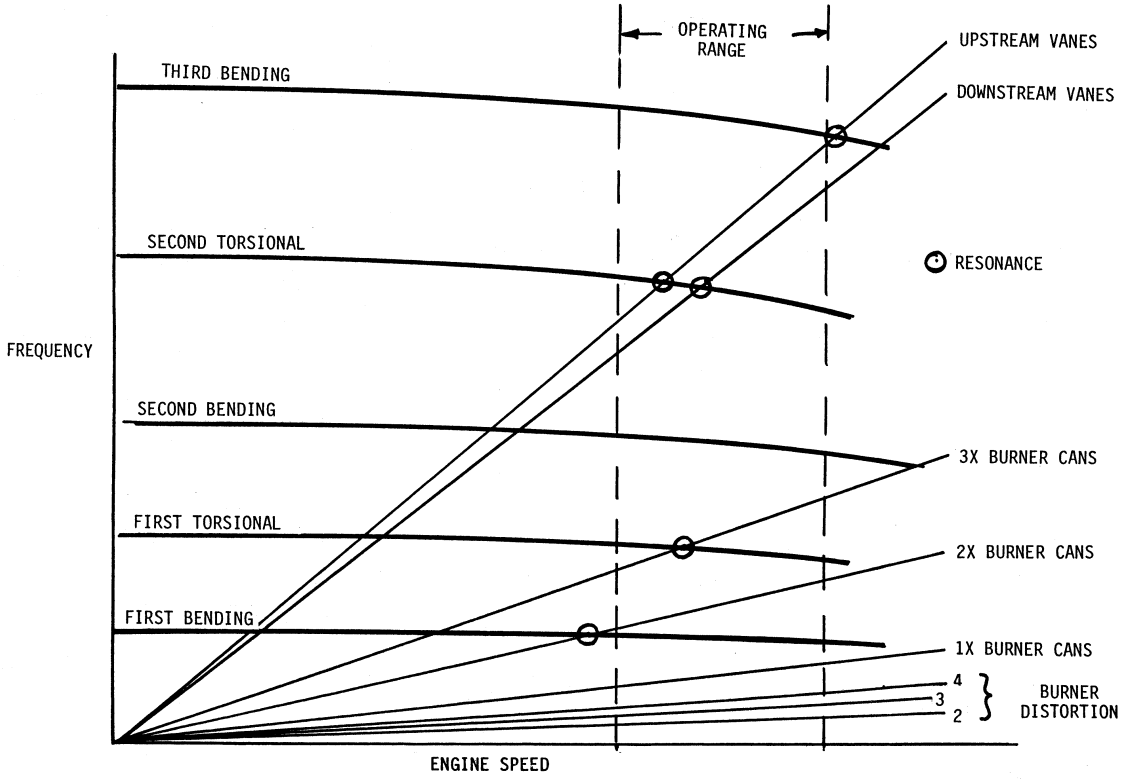

Figure 5: *Example of a Campbell diagram [Jay et al. 1988]*

Dynamic aeroelasticity of turbomachinery blades

If turbomachinery blades are aerodynamically excited to vibrate, no matter if self- or externally excited, a complex interaction between the unsteady flow around the blades and the involved solid structures takes place: The unsteady flow causes the blades to vibrate, whereas the blade motion itself modifies the unsteady flow. Hence, a coupling exists between the structural behaviour of the blades (mass, stiffness, damping, friction, fixation) defining the blade motion and the unsteady flow defining the excitation. This is classically shown by “Collar’s Triangle of Forces” [Collar 1946], which illustrates the interaction between inertia forces, elastic forces and aerodynamic forces. This triangle is sometimes extended by a vertex for thermal forces and a vertex for control forces, two additional parameters increasing the complexity of the problem.

1.1.3 What controls blade vibrations of turbomachinery blades?

As vibrations in turbo engines have been a problem since the early beginning of their development, there exist numerous empirical and semi-empirical methods to suppress vibrations. These are usually devices to modify the mechanical behaviour of the structure to avoid resonance. Also the adaptation and control of aerodynamic parameters has become a possibility to optimise the vibration behaviour of engine components, which in turn requires the knowledge of the unsteady flow phenomena in the machine. The following section will summarise the most important measures to control the blade vibration behaviour with help of constructive measures, mechanical and damping measures, mistuning and unsteady aerodynamic measures.

Constructive measures

Figure 6 shows a 2D blade section of a turbine stage and some main constructive measures influencing the aerodynamic excitation explained below. Also the wake and the pressure wave emanating from the stator are illustrated in the figure.

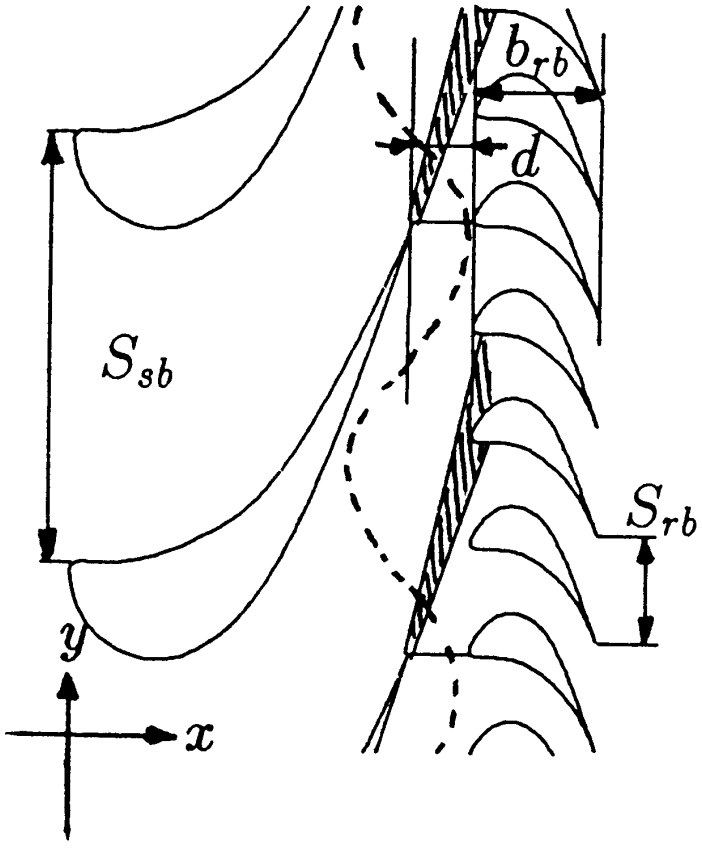

Figure 6: Illustration of potential and wake excitation sources and constructive parameters in a turbine stage [Korakianitis 1992a]

- Axial distances between blade rows (“d” in Figure 6) have a direct impact on the unsteady aerodynamic interaction, the potential excitation decreases exponentially with

axial distance, whereas the wake excitation diminishes only slowly with axial distance. Changing the axial gap means also changing the length of the whole engine, which has implications on the complete engine design. Smaller axial gaps would reduce the weight of the engine, which is to consider in aero engines.

- The pitches of the blade rows (S_{sb} and S_{rb} in Figure 6) do not only change the excitation frequency in stator-rotor interactions but also the strength of pressure wave interactions (potential excitations). The solidity (pitch to chord ratio) has also an optimum regarding the stage losses. Furthermore, a reduction of vanes or blades would give weight savings without impact on other part designs (as a change in axial gap would have), which is to consider for aero engines.
- The stagger angle influences both the steady and the unsteady load and is therefore not straightforward to modify to reduce the aerodynamic excitation.
- Low aspect ratio blades are more exposed to resonance [Murthy et al.1993].
- When disk and blades are manufactured from one piece ("blisks") reduced mechanical damping is present compared to conventional bladed disks [Murthy et al. 1993] because of the lack of friction contacts between blades and disk.
- The circumferential alignment of stator blade rows or rotor blade rows in a multistage engine, known as "clocking" or "indexing", can be beneficial for reducing losses and maybe also to reduce excitation impact. Determination of the optimum clocking positions is a presently very active research area (e.g. [Arnone et al. 2001]).

Mechanical modifications and damping devices

The classical method to tackle vibration problems of turbomachine blades, once they are detected, is to change the vibration characteristics of the structure by modification of damping and stiffness of the system. Damping is inherent to the aeroelastic system in form of friction damping, material inherent damping (usually small) and aerodynamic damping. It decreases the vibration amplitude whereas a stiffness modification shifts the resonance frequency. However, stiffness modification may not be sufficient for engines with varying operating conditions, i.e. aero-engines. One straightforward and classical approach of mechanical modification is to connect the blades within a blade row with wires or laces. Beside the added weight another drawback of this method is the weakening of the blades due to the necessary holes to fasten the wire or lace. More advanced is the use of part span shrouds, which is common practice to stabilise fan blades and long compressor blades. Part span shrouds establish a friction contact between the blades at a certain blade height. Also this measure adds weight to the engine and can be problematic as it disturbs the main flow introducing increased risk of flow separation. The design of the shrouds is an active research area (see for example [Sextro 2000]). In turbine designs the use of tip shrouds is possible.

The vibration characteristics of turbine blades can be modified with "under platform dampers". These dampers do not disturb the flow, but modify the vibration characteristic of the blades by changing the friction contact between neighbouring blades. Currently, considerable research work is done regarding the design of these dampers [Jareland et al. 2000], [Panning et al. 2000]. Future developments of damping devices include magneto-mechanical blade surface coatings [Yen et al. 2000] or the inclusion of friction material in hollow blades [Griffin et al. 1996]. These methods are interesting for "blisks", where no blade to blade damping can be established.

Mistuning

Recent research work (for example [Silkowski et al. 2001]) points out that the beneficial effect of mistuning on flutter can be applied to suppress self-excited blade vibrations of compressor blades or low pressure turbine blades (high pressure turbine blades do not flutter). There are approaches towards using intended mistuning for optimising the vibration behaviour of blade rows in turbomachines. However, in the case of forced response blade vibrations mistuning effects can cause mode localisation leading to amplified vibrations of singular blades in a blade row. Such effects are obviously in conflict with the beneficial one of mistuning to suppress flutter. Mistuning as a possibility of passive forced response control is proposed in [Chiang et al. 1992], where incompressible operating turbine rotors were detuned both structurally and aerodynamically by circumferentially varying rotor spacing. Also the distortion of the excitation periodicity can be regarded as an aerodynamic mistuning, for example the excitation due to an upstream stator can be mistuned by introducing vane to vane geometry differences in the stator. Clark et al. [2002] have demonstrated the potential to reduce vibratory response of a high-pressure turbine rotor by such a modification of the upstream stator.

Unsteady aerodynamics

The flow in turbomachines is highly unsteady, and indeed without unsteadiness it would not be possible to convert aerodynamic work to mechanical work and vice versa. Beside this unsteadiness brings several benefits and drawbacks regarding the performance (time averaged flow aspects), flow stability (surge and stall in compressors) and blade mechanical integrity (time resolved flow aspects). The following part will give a short introduction to the unsteady aerodynamics present in turbine stages (and partly also in compressor stages) with focus on the impact on blade vibration risks.

Flow Defects

In case of forced response blade vibrations the aerodynamic excitation mechanism is due to flow defects, which are spatial non-uniformities in the flow field upstream or downstream of the observed blade row. These flow defects are usually regarded as steady in the reference frame of the generating obstacles. They become unsteady when moving relative to the observed blade row. Flow defects can be related to different physical phenomena, the most relevant are listed below [Kielb et al. 1992].

- Wakes are generated due to the development of a boundary layer on the blade surfaces, which separate from the blade at its trailing edge. The wakes are characterised by a velocity deficit of a certain magnitude, a spatial width and a (negligible) small static pressure deficit. The low momentum fluid inside the wake has increased vorticity and entropy and is convected with the local flow velocity. It is clear that the wake is a completely viscous phenomenon. Many empirical and semi-empirical models exist to describe the wakes behind turbomachine blades.

- Vortex shedding behind a vane or blade (see Figure 4) is another flow defect related to the detachment of the boundary layer at the trailing edge. In case of occurrence left and right rotating vortices are shed at a Reynolds number dependent frequency, which

is usually much higher than typical wake passing frequencies. The related disturbance on the downstream rotor is hence a superposition of wake passing and vortex shedding. Due to the high frequency and small velocity variations (see also [Hummel 2001] the vortex shedding related excitation is usually not regarded in forced response problems. However, it has a significant impact on performance.

- The static pressure field upstream and downstream of a blade row is varying circumferentially (and radially) due to the blade load. This causes a flow defect, which is felt as unsteady pressure waves by the relative moving blade rows. It is an inviscid phenomenon commonly modelled with potential flow theory. A simplified analysis of the problem (i.e., [Hodson 1998]) expresses that the upstream and downstream potential field is proportional to a term of type $e^{-2\cdot\pi\cdot\sqrt{1-M^2}\frac{d}{S}}$. Here, d is the distance from the blade, S is the pitch. The potential wave induces also a relatively small velocity deficit, which can be assessed with help of linear potential flow theory (Chapter 4.2).

- Shock waves are a special category of pressure waves, which occur due to the strong pressure gradient over a shock. This gradient is experienced as unsteady pressure wave by relative moving blades. The shock excitation in transonic turbine stages is probably the main contributor to blade vibration excitations (see for example [Chiang and Kielb 1992]). A typical shock structure at the stator trailing edge of a transonic high pressure turbine stage is illustrated in Figure 7. Pressure gradients due to shocks do not decay exponentially in axial direction.

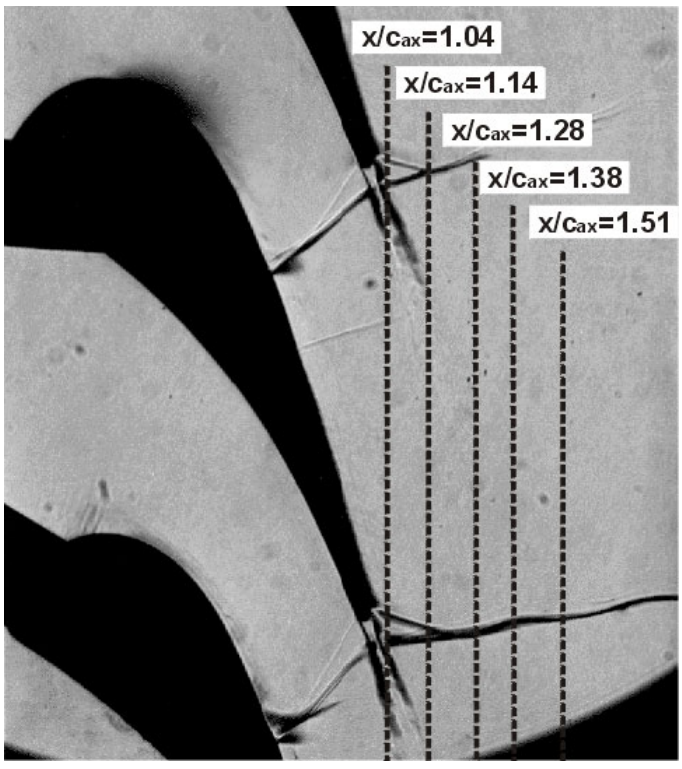

Figure 7: *Schlieren picture of turbine cascade measured by Kapteijn, see Colantuoni et al. [1995], at M_{2is}=1.05, illustrating the shock structure at the stator trailing edge, also shown are the evaluation positions of present stator only investigations*

- Inlet distortions are related to all effects at the machine's inlet, which cause a deviation of axisymmetry of the inlet flow, such as the inlet support structure itself, crosswinds during ground running and severe manoeuvres during flight for aero-engines, partial admission for steam turbines. Partial admission is a method to control steam turbine power output by blocking one or several circumferential inlet segments to reduce the mass flow. This causes large circumferential pressure distortions (see for example [He 2001]).

- Hot streaks are caused by variations in combustor outlet temperature, which can lead to severe unsteady temperature loads in the first high pressure turbine stage.

- Several passage vortices are present in the blade rows of turbines and compressors, which are summarised as secondary flow effects (see Figure 8). These are inherently three-dimensional and are generated by the local pressure gradients in the passages. (tip clearance leakage, end wall boundary layer induced vortices at hub and tip). Recent three dimensional investigations (e.g., [Fan and Lakshimanarayana 1996]) have pointed out that these can significantly influence the unsteady blade surface pressures, even if the steady flow can be considered as two-dimensional.

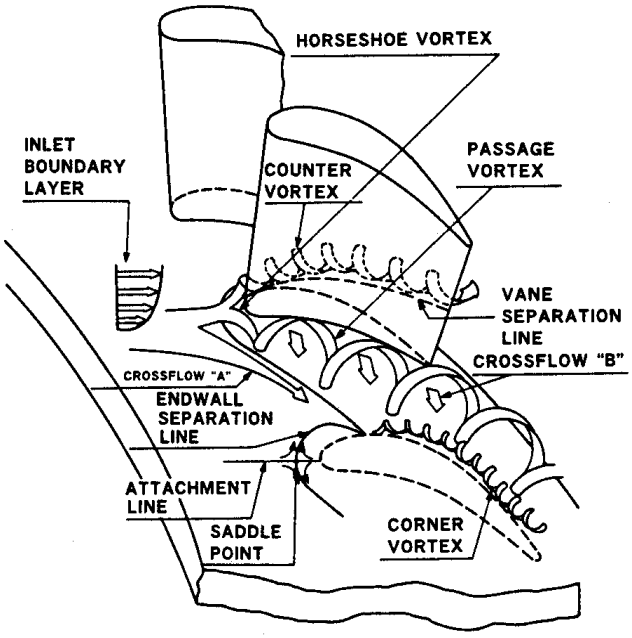

Figure 8: *Secondary flow phenomena in a turbine blade cascade [Takeshi et al. 1989]*

- The gust is defined as "... rapid increase in wind speed relative to the mean strength at a time ..." [AGARD 1980]. The gust is a common way to describe flow defects at the inlet or outlet of a blade row in terms of the flow velocity defect. The gust due to pressure non-uniformity is called potential gust, the gust due to the wake is called vortical gust and an entropy gust related to entropy variations is used additionally in transonic flow descriptions. This distinction of gust types originates from the linear flow analysis based on the Euler equations (see also Chapter 4.2).

It is obvious that the control of the flow defect has the potential to control the blade excitation and hence the blade vibration. In particular, the various flow defects can interact with each other (i.e. wakes and pressure waves, shock – wake interaction) and by that either amplify or diminish blade excitation. The present work is aimed at identifying the relative influence of flow defects and of their interaction on high pressure turbine blade excitation with regard to constructive measures. The active aerodynamic modification of flow defects is a further way to aerodynamically control blade vibration. This is for example the wake modification by blowing air out of the wake generating trailing edge of blades [Ubaldi et al. 2001]. Such measures are not subject of the present work.

Aerodynamic damping

The unsteady aerodynamic damping is a beneficial unsteady flow effect regarding the blade vibration in turbomachines as long as it is positive. If it is negative flutter occurs, which by all means must be avoided in the operating range of the engine. The beneficial positive aerodynamic damping to the forced response of blades is mostly neglected in design considerations, because it is regarded low compared to mechanical damping. This disregard of aerodynamic damping gives an additional (unknown) safety margin towards HCF failure. Recent work by Kielb et al. [2001] came to the conclusion that the aerodynamic damping can be a significant distributor relative to typical structural damping in turbine blades. The central parameters controlling the aerodynamic damping are listed below. These parameters are mainly evaluated regarding their influence on flutter stability because of its historical importance.

- The reduced frequency expresses physically the ratio of flow velocity to blade vibration velocity. Empirical limiting values state that flutter occurs mainly at low frequencies i.e 1^{st} flap mode $k<0.2$, 1^{st} torsion mode: $k<0.6$ [He 2001]. At very low frequencies the vibration is regarded as quasi steady, i.e. at each instant of time the steady flow condition corresponding to the current blade positions establishes.

- The interblade phase angle measures the circumferential wave length, which is fixed to the flow defect periodicity for forced response (see Equation 4-2). In the flutter case blade vibrations do mostly not have to follow a certain circumferential periodicity, instead a worst case interblade phase angle is often applied to judge the flutter risk. However, the interblade phase angle has a significant influence on the aerodynamic damping, for example He [2001] shows its influence on the shock oscillation on a compressor profile.

- The influence coefficients describe physically the influence of a vibrating blade on the aerodynamic damping on itself and on each other in a blade row. This concept is completely consistent with the concept of interblade phase angles [Bölcs 1989] but gives a different physical approach to the problem. Understanding the damping influence of vibrating blades on each other can give insight to stabilise blades or increase the damping.

- Shocks and all other large flow gradients (i.e. separations) can contribute significantly to vibration excitation once they are oscillating due to the blade motion.

- Recent research has pointed out the significant dependency of the aerodynamic stability on the blade mode shape ([Panovsky and Kielb 1998], [Tchernycheva et al.

2001]. Stability maps showed very similar trends of stability in dependence of the torsion axis location for several subsonic low-pressure turbine vanes and blades.

The control of these parameters beyond the avoidance of flutter could enhance the stability of forced vibrations.

1.1.4 Why is the high-pressure turbine stage of interest?

The present work focuses on the aerodynamic excitation mechanisms due to the unsteady flow in the high-pressure turbine part of axial gas-turbine engines with respect to the design of the turbine vanes and blades. The unsteady flow in the high-pressure turbine attracts large attention presently because

- The high-pressure turbine stage performance has a large impact on the overall engine efficiency (e.g. [Michelassi et al. 1998]).
- It operates in an extremely hostile environment, which puts extreme requirements on material and cooling technique to ensure structural integrity. Friedrichs [2001] states illustrative these conditions: "…a gas temperature of 1600°C, which is 200 °C above the melting point of the blade material, 10000 rpm result in a steady load equivalent to a lorry hanging at each blade, the energy transfer is about 750 horse powers per blade…".
- High cycle fatigue problems are likely to occur due to the large steady and unsteady mechanical and thermal loads.

1.2 Problem Formulation

"*The basic problem in the aerodynamic design of an axial flow turbine is obtaining the maximum overall efficiency within the limitations imposed by stress, turbine matching, and other considerations, such as efficiency trade-off versus the number of stages*", [Fielding 2000].

The designer of future gas turbine engines is asked to develop reliable, safe and cost efficient engines and must at the same time meet the aggravated constraints due to performance, structural integrity and maintenance requirements as well as environmental restrictions. In particular, one difficult problem to solve is to ensure a guaranteed lifetime of the components, which is strongly related to the vibration behaviour of the structure. Performance improvements implicate often higher vibration risks of the turbomachine blades. The high-pressure turbine is in a key position both regarding the influence on the engine efficiency and the thermal and aerodynamic load, so the blades are prone to high cycle fatigue due to forced response. In order to incorporate vibration risk assessment of the blades in an early design phase, which in turn reduces design iterations and development costs, the designer needs suitable tools, which are as simple as possible and as accurate as necessary. The knowledge of fundamental design rules based on the understanding of the physics to avoid blade vibration problems would be very beneficial. As the primary cause of blade vibrations must be found in the unsteady aerodynamics the present work concentrates on the unsteady flow in turbines to assess and understand the relevant unsteady aerodynamic excitation mechanisms.

1.3 Structure of the present work

Chapter 2 gives a state-of-the-art review regarding unsteady numerical tools and performed design studies in the open literature. Chapter 3 states the objectives of the present work and the approach to achieve them. Chapter 4 provides the theoretical background to the performed evaluations and Chapter 5 introduces the two turbine stages and the vibrating blade cascade on which the computations were performed. In Chapter 6 the results are summarised and discussed with reference to the publications 1-6 in the Appendix. That part of the thesis comprises rather a critical completion of the published work than a pure repetition of the results in the publications. It is split into the sections “Validations”, “Excitation Mechanisms”, “Parametric Studies” and finally “Potential for Unsteady Design Improvements”, and each of these aspects is discussed based on the main findings in the investigated turbines. The thesis is completed with a conclusions section and statements on the future work from the author’s perspective. Some aspects of the applied numerical tools are given in the Appendix with reference to the original developmental work published in the open literature.

2 STATE-OF-THE-ART

The present review of the state-of-the-art focuses on the design process of gas turbine stages with emphasis on the available unsteady aerodynamic methods and generic unsteady flow design studies. Prefacing the general design process is described as is common practice in industry to the knowledge of the author.

2.1 Sketch of the general turbine design process

In Figure 9 the principle design steps necessary to develop blades for axial turbine engines are summarised from [Wilson and Korakianitis 1998].

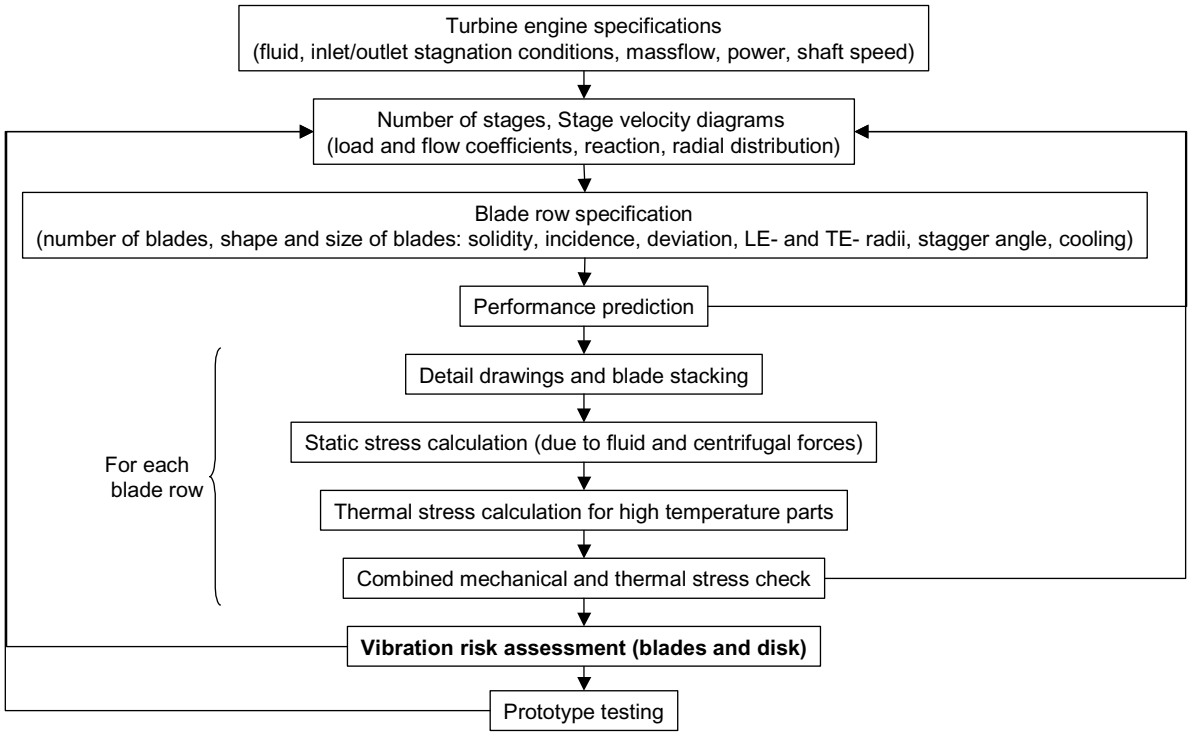

Figure 9: *Principle design steps for turbomachinery blades*

It shows the highly iterative character of the design process with involvement of aerodynamic design and the structural scrutiny, which often have conflicting optima. Typical turbine cascade design parameters are shown in Figure 10. For most of the design steps computerised methods are at hand, like through flow methods to estimate the velocity triangles, inverse design methods to find the optimum blade shape, CFD and CSD methods to perform the flow and structure analyses. At present effort is put into combining these methods, which is not trivial because of the differences in nomenclatures, co-ordinate systems, computational meshes and other conventions in the often independently developed tools. Moreover, the subject is highly interdisciplinary, so that only a few experienced specialists have the potential to promote the integration of the disciplines.

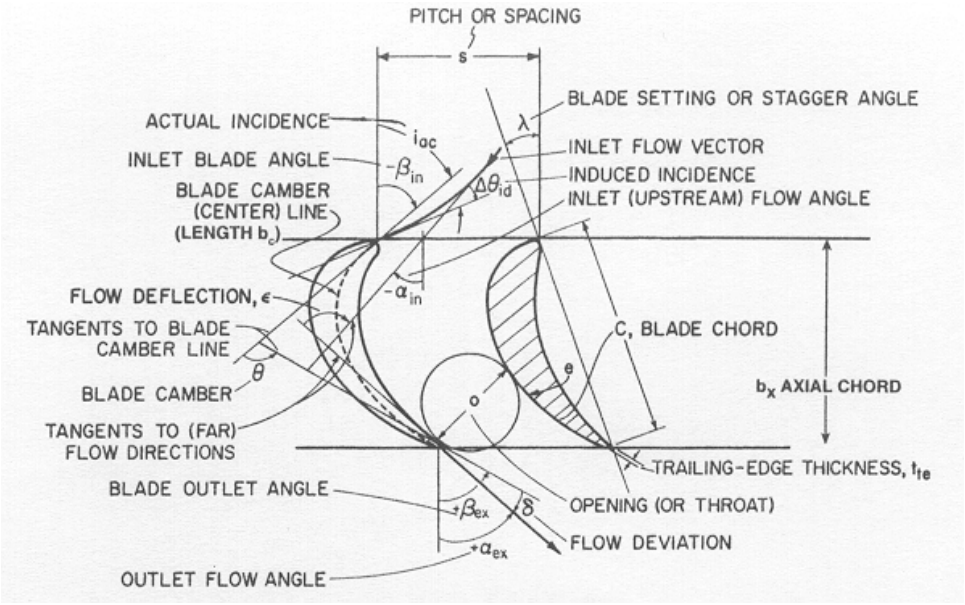

Figure 10: *Cascade design parameters [Wilson and Korakianitis 1998]*

Industrial design practice is to perform the aerodynamic throughflow and blading design first on 2D stream sheets before the 3D flow behaviour is investigated. Present design system improvements aim to invoke fully 3D flow predictions into design routines with help of correlation, databases, artificial neural networks and 3D inverse methods (see for example [Shahpar 2001] and [Van den Braembussche 2001]). Promising is the development of “adjoint methods” for unsteady design parameters allowing the search for optimum design regarding unsteady performance parameters [Campobasso et al. 2001], [Florea and Hall 2001]).

Figure 9 also points out that vibration assessment is very late in the process and can require the re-design of the stages. To enhance the design process it is aimed at finding design criteria which can be applied in an earlier design phase as well as accelerating the vibration assessment approaches. The following section will give the state-of-the-art of prediction methods to assess the vibration risk of turbomachinery blades with focus on the unsteady aerodynamics.

2.2 Predictive methods to assess the vibration risk with focus on the unsteady aerodynamics

The assessment of vibration risk of turbine blades consists of the proof that the design is flutter free and that the vibration levels at unavoidable crossings in the Campbell diagram (Figure 5) are acceptable so that maximum stresses fall well below the endurance limit. To achieve that numerical tools and prediction systems of varying complexity exist. Wisler [1998a] stated concerning the state-of-the-art in forced response predictions: *“The current state-of-the-art shows a comparison of analysis and measurement ranging from good agreement to more than a factor of ten difference. A typical absolute prediction is within a factor of three. Relative predictions are used regularly to compare designs for different engine conditions.”*

Forced response prediction is obviously a difficult task, because several parameters are involved, which are hard to assess:

- The exact geometry under operating conditions, which is dependent on the rotational speed and influences the steady aerodynamics
- The excitation itself due to the complex unsteady aerodynamics (details see below)
- The coupling between aerodynamic excitation and blade vibration (see below)
- The mode shapes of the blades, because stiffness and mechanical damping values change during engine operation
- The vibration modes of the bladed disk, where single blade modes can be coupled through the disk or the fluid
- The non-linear mechanical damping, which might be introduced by dampers and shrouds or simply is present due to friction in the blade fixations
- Circumferential variations of mass, stiffness, damping, frequency, mode shape or geometry parameters due to manufacturing tolerances introduce mistuning and complicate the problem even more having a significant influence on the forced response behaviour

To tackle the complexity of the problem the analysis is with good engineering practice split into several smaller analyses, an example illustrated in Figure 11, which shows an analysis system commonly used to estimate the stress level due to the forced response of blades in turbine engines. Principally similar representations of analysis systems have been reviewed in Kielb and Chiang [1992], Chiang and Kielb [1992], Murthy and Morel [1993], which can be regarded as the present state-of-the-art.

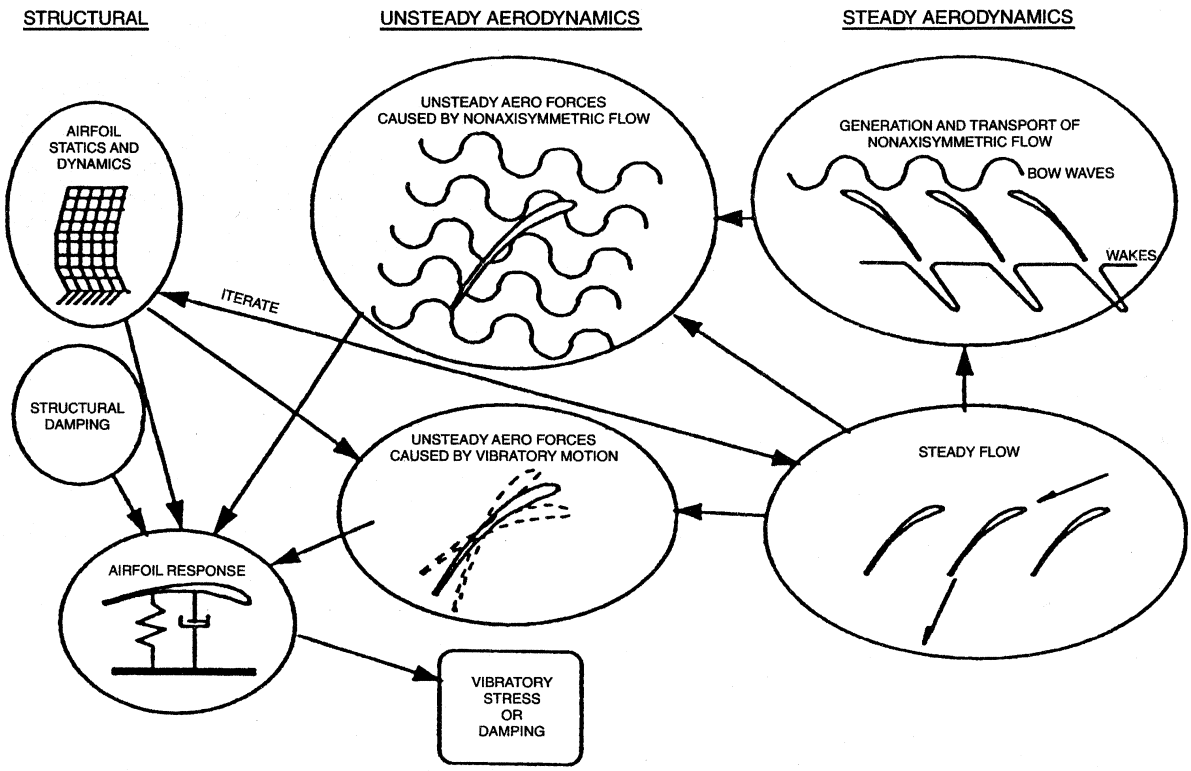

Figure 11: *Schematic of forced response prediction system [Hilbert et al. 1997]*

A structural analysis provides the mode shapes and eigenfrequencies of the blades. In iteration with the steady aerodynamic analysis, which gives the steady blade load, it also provides the static displacement at operating conditions. Once the steady conditions and geometry are established flow disturbances might be estimated, which are all non-axis-symmetric flow structures causing unsteady flows in relative moving blade rows. With help of these or by performing unsteady stage analyses the forcing function, i.e. the unsteady blade forces due to flow disturbances can be calculated. The steady flow solution is also basis for the estimation of the unsteady blade forces and aerodynamic damping due to blade vibration, where the blade motion is obtained from the structural analysis. Having the forcing function and the aerodynamic damping the blade response can be calculated. Structural damping is often regarded by empirical damping models.

Applied design systems differ in the tools used for the various analyses as well as in the degree of interaction allowed between them. Tools for structural analyses are well established and commercial software packages are routinely used. On the CFD side the steady flow analysis seems to be sufficiently developed for engineering purposes, even though many flow aspects like boundary layer details and transition as well as turbulence prediction are only weakly captured by state-of-the-art methods. For the sake of computational efficiency simple models are still regularly applied (algebraic turbulence models and transition prescription are mainly used in industry, for research purpose two-equation turbulence models are often applied) even though boundary layer and turbulence prediction might have significant impact on the unsteady flow prediction, especially in the interaction with shocks [Kielb and Chiang 1992].

In the field of unsteady aerodynamics numerous code developments and computational results have been presented. The main development trends in computational methods were to switch from 2D approaches to 3D approaches, improvements of farfield boundary conditions as well as periodicity treatment, development of linearised methods including linearisation of the viscous flow equations. As the main subject of this work is the prediction of unsteady flows a more detailed review will be given below regarding both methods development and applications.

Another research field is the study and implementation of integrating the structural and unsteady aerodynamic solutions. The application of an integrated method to solve a fluid-structure coupled problem means that a tight interaction between the aerodynamic field and the structure field is allowed in the solution process, i.e. the fluid can modify the structural motion and vice versa. Integrated methods get increased attention also in industry due to the recognised need to permit coupling and the possibility to perform coupled analyses with increased computational resources. However, they are not yet introduced into common practice of unsteady design. Some reasons for that might be 1. The analysis is more complex and needs interdisciplinary knowledge of the user and 2. Many problems can be solved sufficiently with a de-coupled approach. Several approaches are documented in the open literature and Marshall and Imregun [1996] published a review recently. They distinguish between “Classical Methods” (uncoupled), “Partially Integrated Methods” and “Fully Integrated Methods”, the latter ones using the same equation solver for both the structural and aerodynamic equations. The approaches are usually documented for flutter analyses but apply as well for forced response analyses. This is due to the practice of forced response analyses as described above, where a separate calculation gives the aerodynamic damping due to the blade vibration. Such forced response analyses do not allow for interactions between the forcing effects and

vibration effects on the flow. Only recent research ([Vahdati et al. 1998], [Breard et al. 2000], [Schmitt et al. 2001]) has investigated the effect of these interactions on the forced response using a coupled analysis approach.

The need of coupled methods for flutter and forced response predictions is difficult to answer due to the lack of experimental evidence. As blade vibrations occur at resonant conditions it is very difficult to obtain measured data of the flow and the blade motion at these conditions. Actual research programs (e.g., [Hennings and Elliott 2002]) aim to provide the necessary experimental data to validate prediction methods. From physical reasoning it seems sufficient to apply classical methods in cases where no non-linear effects are expected (i.e. small vibrations of the structure and continuous changes in the flow). Furthermore, the frequencies and mode shapes should not be modified by the aerodynamics. The lighter the blades are in comparison to the surrounding air mass the stronger is the vibration modification by the presence of the flow. This is presently not expected in high-pressure turbines due to the high mass ratio of these blades. For flutter analyses the question arises if a prediction of flutter onset is sufficient, which usually happens at small amplitudes, or if a prediction of limit cycle flutter and its amplitude is needed (see Figure 12). For the latter case a coupled approach is necessary, if non-linearity of both the flow and the structure cause the limit cycle behaviour.

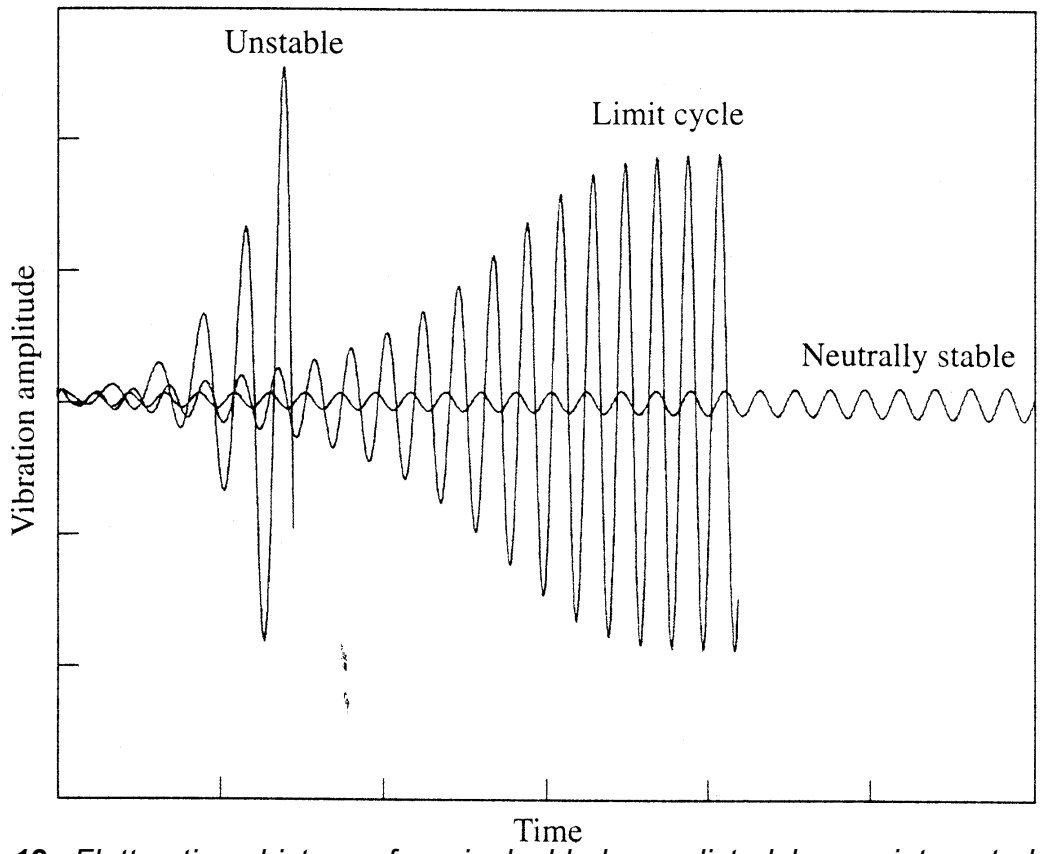

Figure 12: *Flutter time history of a single blade predicted by an integrated nonlinear aeroelasticity method, Marshall and Imregun [1996]*

Unsteady Aerodynamics – Methods

Great progress has been achieved in the development of numerical tools suited for the investigation of the unsteady aerodynamic effects due to blade row interaction and blade vibration. The following summary is not complete but covers the main milestones achieved during the last two decades.

Single blade row models:
An important step from analytical analyses of unsteady cascade flows on flat plate models (LINSUB [Smith 1972; Whitehead 1987] was the development of unsteady time-linearised potential flow solvers, mainly to name FINSUP [Whitehead et al. 1985, 1987, 1990] and subsequent modifications for gust response by [Suddhoo and Stow 1990] and by Verdon and his colleagues (LINFLO [Verdon and Caspar 1984]). These models were two-dimensional (2D) on blade to blade planes considering radial effects with source terms in the 2D flow equations (quasi-three-dimensional (Q3D) approach). Their advantage over the analytic methods was that they consider the influence of the non-uniform steady blade load on the unsteady pressure response. The limitation of these methods to irrotational and isentropic flows was most relevant for transonic and supersonic flows, for which difficulties in the shock prediction enforced the development of time-linearised Euler solvers (for example [Hall and Crawley 1987], [Kahl and Klose 1991]). These were later extended to three-dimensional models (e.g., [Hall and Lorence 1992], [Marshall and Giles 1997], [Kahl 1997] [Montgomery and Verdon 1997]). Recently, also time-linearised Navier Stokes solvers were presented (e.g., [Holmes et al 1997]). All linearised methods were based on the assumption that the unsteady flow is a small disturbance to the steady flow. For most flutter cases this assumption is justified because the prediction of flutter onset at small blade vibration amplitudes inducing small flow perturbations is the desired result. The validity of linearity of forced response predictions is not so clear, but several validations demonstrated a good agreement of the results by linearised methods and by non-linear time marching methods even for transonic flows ([Marshall and Giles 1997], [Sudhoo and Stow 1990]). In the vicinity of shocks or for large blade vibration amplitudes or in case of flow separations the validity of the linearised methods is not clear today.

Also non-linear time marching methods were developed and applied to solve both flutter and forced response aerodynamics. The solution of the Euler equations (for example by [Pandolfi 1980], [Hodson 1985], [Fransson and Pandolfi 1986], [Carstens 1993]) was extended to also regard viscous effects. Either the efficient hybrid invscid/viscous approach were used, where the Reynolds averaged Navier-Stokes equations are only solved in thin layers around the blades (e.g., [Giles 1991], [Hwang and Liu 1993]) or fully viscous approaches were applied (for example [Siden 1991]). Subsequent 3D methods were developed (beside others by [Gerolymos 1993], [Groth 1996], [Grüber and Carstens 1996]). The non-linear methods came along with complications to treat the far-field boundaries of the steady and unsteady computations: inlet and outlet boundary conditions should be non-reflecting for waves leaving the computational domain, but incoming waves (gust) as specified for blade excitation calculations must be allowed. A two dimensional treatment was introduced for turbomachinery applications by [Giles 1988, 1989], a steady quasi three dimensional approach by Saxer and Giles [1993] and also an unsteady three dimensional approach was presented [Fan and Lakshminarayana 1996]. An important extension of the inlet/outlet boundary conditions treatment was given by Sillkowski and

Hall [1997], who demonstrated the importance of partly reflecting boundary conditions to model wave reflections from upstream and downstream blade rows on blade flutter stability.

The described single blade row approaches differ for blade vibration and blade excitation applications mainly in the specification of the boundary conditions. Whereas the first kind of simulation needs a treatment of moving blades in the computational domain, blade excitation calculations need, as named above, a specification of (empirical, semi-empirical or computed) unsteady inlet and outlet boundary conditions, which requires assumptions on the relative flow distortion at these boundaries. On the other hand single blade row methods to calculate the forcing function allow the isolated study for different distortion types, which are described as potential, vortical and entropical type. A comprehensive comparison of state-of-the-art gust method results to experimentally obtained unsteady blade surface pressures has been shown by Manwaring and Wisler [1993]. By comparing linear to non-linear method results they concluded that for the investigated subsonic turbine and compressor cases non-linear effects were not significant. They also pointed out the importance to correctly specify the gust to obtain a good agreement to measurements, especially the potential gust specification for the turbine computation is essential. Chen [1994] compared his frequency domain potential method using empirical wake models to predict unsteady blade pressures to experimental data and viscous predictions. Good agreement was found for the investigated low speed turbine both on the stator and on the rotor.

Multi-blade row models:
To account for the details of complex blade row interactions, as they can occur when shocks interact between the blade rows or when the axial gap is so narrow that potential waves interact bi-directionally, computations on single blade rows were coupled to multi-blade row computations. These time accurate computations work with relative moving grids fixed to the respective stator model and rotor model. Time accurate transfer of the flow variables between the relatively moving grids accounts for the interaction of the two flow fields. Also time averaged transfer of these variables is documented (“mixing plane approach”, a comprehensive review is provided in [Adamczyk, 1999]) but this has more importance for the performance computations and is less applicable to predict the forcing function [von Hoyningen-Huehne et al 1999a]. Early works of unsteady full stage turbine stator-rotor computations appearing in open literature are by Koya and Kotake [1985] (inviscid 3D), Fourmaux [1986] (inviscid 2D), Lewis et al. [1987] and by Rai [1989] (3D viscous). The introduction of time inclination for stage calculations by Giles [1988b, 1990] was an important development step and removed blade count restrictions, which otherwise have been treated by scaling of blade rows to handle the circumferential periodicity with phase lagged boundary conditions (see below). Clark et al. [2000] demonstrated recently that the scaling of blade rows can significantly change the unsteady flow simulation result compared to the correct (non-scaled geometry) result. An implementation of the time inclined method to a 3D-Navier-Stokes solver was reported by Jung et al. [1996], Laumert et al. [2002] included time inclination in a 3D Euler method. Comparisons of full stage computations to single blade row computations by Barter et al. [2000] suggest that even for transonic flows with shock interaction in a high pressure turbine stage the single blade row approach captures the primary rotor excitation effects. But the vane excitation due to the passing downstream rotor needs a stage computation approach to capture the

important excitation features. Recent code developments are presented among others by Dawes [1993], Liamis [1994], Michelassi et al. [1998], Eulitz et al. [1998] and He [1999].

Note on 3D methods:
Either 3D methods or Q3D methods applied on stream sheets at several radii can provide the complete forcing function and aerodynamic damping for a blade. Hilditch [1998] demonstrated the importance to correctly specify the stream height evolution in Q3D methods to match the blocking effects, which is crucial for an acceptable steady and unsteady flow prediction, especially in transonic flows. As the required stream height evolution is often not the geometrical one its specification needs an a-priori steady 3D calculation or empirical data. Investigation of the flow at several stream sheets may give the complete forcing function, but mixing processes between stream sheets are present at least in low aspect ratio turbines. Furthermore, hub and tip casing as well as tip leakage flow do induce secondary flows, which may influence the 3D blade excitation. Fan and Lakshminarayana [1996] studied a subsonic turbine stage with a 3D inviscid single blade row approach, specifying the secondary flow and wake at the rotor inlet with 3D non-reflecting boundary conditions. It has been stressed that the 3D secondary flow field has significant influence on the unsteady blade pressure, even at midspan where the steady flow can be regarded as two dimensional. Busby et al. [1999] and Vanable et al. [1999], Weaver et al. [2000] and Haldeman et al. [2000] compared numerical results obtained with various models to experimental data. The first two publications evaluated the results at midspan of a transonic turbine stage and concluded good agreement between 2D and 3D methods. The latter two publications investigated a counter-rotating transonic turbine stage. The comparisons suggested that both 2D and 3D codes are capable to predict the unsteady flow features of the investigated turbines at midspan, but at other blade heights 3D effects are significant for the unsteady flow features. The above named complications in using 2D methods and the today non-significantly larger effort to perform 3D analyses suggest 3D methods for use in design applications (see also [Kielb 2000]), whereas 2D methods have their main justification in phenomenological and parametric studies.

Note on periodicity treatment:
To treat circumferential periodicity the direct store method by Erdos [1977] was regularly applied both for linearised and non-linear solvers. It stores the solution history of a complete computational period on the periodic boundaries in order to apply the correctly phase lagged boundary conditions according to the interblade phase angle of the problem. Thus the computation can be limited to one blade passage for arbitrary interblade phase angles for flutter predictions. Also for forced response predictions this method is applied, but then it requires that the circumferential extensions of the excitation domain (i.e. the inlet boundary condition, or in full stage simulations the exciting blade row domain) and the excited blade domain are equal. For unequal counts of excitations and excited blades on the circumference this was achieved by modelling several passages in combination with a geometric scaling of one of the domains. Giles [1988b, 1990] introduced the concept of the “Time Inclined Method”, which circumvent Erdos’ storage procedure by introduction of a time inclination in the computational space. The grade of inclination is physically limited and cannot be applied for large interblade phase angles but is very useful to take into account unequal counts of wakes and blades in the computation model without scaling of blades. The method is however generally limited to two blade rows moving relative to each other. He [1992] developed another approach to treat the periodic boundaries named

"Shape Correction Method", which has the advantage to allow multiple disturbances in the flow (e.g., blade vibrations and gust excitation).

Note on turbulence modelling:
Even though turbulence modelling itself is presently an important and active research area the application of turbulence models to turbomachinery flows is limited. The simplest algebraic closures of the Reynolds averaged Navier Stokes equations [Cebeci and Smith 1974] [Baldwin and Lomax 1978] are still mostly used in all applications. Other models based on the eddy viscosity hypothesis [Boussinesq 1877] are realised with one-equation transport models (e.g. [Birch, 1987] [Spallart and Allmaras 1992]) and two-equation transport models [e.g., the k-e models by [Launder and Spalding 1974], [Chien 1982]). The application of non-linear eddy viscosity models is rarely found for predicting turbomachinery flows, mainly due to computational costs of these methods and often for engineering purposes satisfactory results by the simpler models.

Unsteady Aerodynamics – Applications to forced response predictions

A large amount of applied research work has been published during the last two decades and the following summary will focus on the main achievements of phenomenological studies of unsteady aerodynamic flow predictions in turbine stages and blade rows. It appears that phenomena are significantly different in subsonic and transonic flows and therefore the following review is accordingly split.

Subsonic investigations:
The numerical investigations in [Hodson 1985] and [Giles 1988b] focused on the detailed analysis of the unsteady wake effect in a low pressure turbine stage. The incoming wake was prescribed at the rotor inlet boundary. The "negative jet" effect of the wake was well predicted and also the successive cutting roll up and shearing of the wake when passing through the rotor passage. However, these works did not investigate the effect of the wake on the unsteady blade surface pressure, but focused on its influence on boundary layer status and related heat transfer characteristics.

Korakianitis [1991, 1992a, b, and 1993a, b] also used a single blade row approach to investigate in detail the influences of axial gap and stator blade count and blade size on the excitations of a rotor blade row in a subsonic turbine stage. He found an optimum axial gap, where vortical and potential excitation effects cancel out partly. Furthermore, he demonstrated the increased potential and decreased wake influence on the blade excitation level with enlarged stator-rotor pitch ratios: high ratios (>3) resulted in mainly potential excitation and very low ratios (<1) resulted in mainly vortical excitations. He also found that an optimum axial gap exists at which vortical and potential excitation mechanisms partly cancel so that the forcing function showed a minimum.

Singh and Hall [1996] investigated axial gap and rotational speed influence on the unsteady blade forces in a test turbine, where the stator was rotating to obtain more easily test data on the stationary rotor blades. Viscous and inviscid 2D predictions gave significantly different excitation forces. The experiments showed a rapid increase of

excitation for the smallest axial gap. An analysis of the flow related to the unsteady blade forces is however not given.

Lakshminarayana et al. [2000] and Chernobrovkin et al. [2000] studied in their two part paper a subsonic turbine stage describing the influence of numerical parameters, turbulence model and operating conditions on the blade excitation in comparison to experimental data. Potential excitation was found to be very weak and only present near the leading edge of the rotor blade, whereas the other parts of the blade excitation were due to the wake. The counter rotating vortices generated by the wake chopping mechanism were comparable in predictions and flow field measurements. The wake caused a high pressure region upstream of the wake centre and a low pressure region downstream of the wake centre on suction side, which was directly related to the wake induced velocity variations. The influence of the wake on the rotor pressure side was significantly weaker.

Von Hoyningen-Huene et al. [1999b] studied the influence of axial gap on a subsonic high-pressure turbine stage using a commercial 2D method and succeeded to derive a geometrical design rule for the axial gap with regard to rotor incidence angle variation. Potential and wake excitations were of same order of magnitude, the excitation decreased significantly with increased axial gap, mainly due to the declination of potential interaction.

Transonic investigations:
Several studies, numerically as well as experimentally, document the dominant excitation influence of vane trailing edge shocks on the downstream blade row in transonic turbine stages with up to 53% in lift variation (e.g., Koya and Kotake [1985], Doorly and Oldfield [1985], Sharma et al. [1992] Rao et al. [1994], Saxer and Giles [1994]).

Experiments in the Oxford Turbomachinery Group on a linear cascade with unsteady shock and wake passing induced by rotating bars is well documented by Johnson et al. [1989]. These fundamental experiments in subsonic and transonic flow described in detail the unsteady phenomena, which would be expected in real turbine stages. The work gives experimental evidence in both the wake induced unsteady pressures on the rotor as well as the complex sequence of refraction, reflection and re-reflection of the moving shock waves.

Giles [1990] presented the capability of his Q3D method UNSFLO to predict stator-rotor interaction in a transonic turbine stage with a dominant shock excitation. The unsteady shock movement was described in detail giving a comprehensive understanding of the excitation mechanism. The unsteady lift variation has been estimated to 40% and its significance for both vibration excitation and loss production has been pointed out.

Rangwalla [1992] showed a two-dimensional investigation of three axial gap configurations to study a new turbine design. The importance of time accurate stage calculations to obtain a shock in the flow solution is pointed out as well as the strong impact of the shock at close stator rotor spacing. Increasing the axial gap resulted in a shock free stage.

Abhari [1992] analysed the temporal development of the shock system in a transonic turbine stage with help of a Q3D method (UNSFLO) and validated the results against experimental heat transfer data. The importance of correct prediction of shock strength

was stressed. Hwang and Liu [1993] demonstrated the importance of shock –boundary layer interaction for the prediction of a low-pressure turbine forcing function due to an incoming wake. Moss [1997] and Hilditch [1998] used UNSFLO to analyse the blade excitation and heat transfer in transonic turbine stages in comparison to experiments. In detailed space and time resolved comparisons they tracked various excitation mechanisms, i.e. shock excitation and wake excitation. Especially, the shock sweeping over the rotor blade leading edge has been demonstrated causing an “upstream travelling“ pressure fluctuation. Busby et al. [1999] and Vanable et al. [1999] presented a very comprehensive experimental and numerical study of the shock blade interaction in a turbine stage with varying axial gap. Beside the assessment of prediction capability of various computational tools conclusions were mainly related to the influence of axial gap and the analysed unsteady flow features on performance. Also the forcing function variation with changed axial gap is shown.

In the second part of a two part paper by Von Hoyningen Huehne et al. [2000a, b] the authors analysed in detail the 3D computed time resolved vane and blade unsteady pressures in a highly subsonic and in a transonic turbine stage. Conclusions are drawn on the excitation mechanisms present in the stages, which were identified by analysis of the propagation characteristics of disturbances. Wake induced unsteady pressures are found on suction side whereas the leading edge region and the pressure side are mainly exposed to potential excitations. Also radial variations are discussed.

Denos et al. [1999, 2000] presented a comprehensive study in the VKI turbine stage operated at subsonic and transonic flow conditions with variations of rotational speed and axial gap. The work pointed out the relatively small wake influence on the unsteady pressure and the non-significant influence of cooling flow blown into the wake at the vane trailing edge. The often in transonic turbines observed temporal double peak of pressure excitation at the rotor leading edge was related to local shock or pressure wave reflections.

The same turbine was investigated by Laumert et al. [2000, 2001a and b] regarding the three dimensional aspects of the blade forcing. Detailed descriptions of the excitation mechanisms were given. The identification of the excitation mechanisms was enhanced by comparison of the original transonic case to a subsonic and a highly transonic case, which pointed out the dominant excitation due to the shock and a minor wake influence on the unsteady pressure, only clearly identified in the subsonic case. Significant radial variations of the unsteady pressures were found. The translation of the excitation mechanisms into excitation forces on chosen mode shapes has been analysed.

Summary:
Many investigations have studied the excitation mechanisms present in subsonic and transonic turbine stages. With varying detail the effects of wake, potential field and stator trailing edge shock on the unsteady rotor blade pressure have been described. A translation of the detailed flow phenomena in unsteady blade forces was discussed in [Laumert et al. 2001a, b]. Other studies have focused on the effect of design parameters, mainly the axial gap, on the unsteady pressure magnitude. To the knowledge of the author only the work by Korakianitis [1991, 1992a, b, and 1993a, b] related variations of the design parameters axial gap and stator count to the magnitude of unsteady blade forces with valuable conclusions on the choice of these parameters to minimise excitation forces. His work is however limited to subsonic turbine flow and the stator-rotor interaction is

assessed with a simplified gust model not taking into account the possible complex flow interactions in the stator rotor gap. The method did not allow a clear relation of the propagation characteristics of wake-, potential- and shock effects to the changed parameters, which would give additional insight in their physical impact.

3 OBJECTIVES AND APPROACH OF PRESENT WORK

3.1 Objective

The objective of the present work is to evaluate the design parameters axial gap and stator count of high pressure turbine stages towards their influence on the unsteady aerodynamic excitation of the rotor with help of numerical flow solvers. Of particular interest is if and how unsteady aerodynamic considerations in the design can reduce the risk of high cycle fatigue failures of the turbine rotor. This objective has been split into the following tasks:

- Evaluate the limits of the applied state-of-the-art numerical flow solvers and validate the method to be used for further calculations.

- Determine the aerodynamic mechanisms causing the perturbation pressures on the turbine rotor blade with regard to operating conditions.

- Quantify the influence of the chosen design parameters axial gap and stator count on the aerodynamic excitation and rotor blade vibration risk with consideration of the excitation mechanisms.

- Investigate the potentiality to improve the high pressure turbine stage design in order to reduce the high cycle fatigue risk of the rotor by unsteady aerodynamic means.

3.2 Approach

When this work was initiated the available computer power and the state-of-the-art numerical tools to calculate unsteady flows in turbines suggested to use a two-dimensional (2D) approach towards the above objectives. The validated and well documented 2D/Q3D code UNSFLO [Giles 1991] is chosen to perform the core of the studies. Some reasons for this choice are the code's capability to treat arbitrary stator-rotor pitch ratios, the efficient construction of the hybrid inviscid/viscous numerical method, the flexibility to solve both flutter and forced response problems and the included mesh generation tools. However, during the course of this work development has not stood still and efficient 3D numerical tools have been developed, which deliver results in reasonable times on high-end supercomputers with up-to-date acceleration techniques (parallel computing, vectorisation). Therefore, the present work includes comparisons to results obtained with various tools and approaches, both for aerodynamic damping and forcing function calculations, in order to prove the validity and the limitations of the applied method UNSFLO compared to other methods. The results are validated against experimental data. The perturbation pressure on the rotor blade surfaces is the measure of highest interest in the present study of blade excitations and is therefore the main validation parameter. The sensitivity to some chosen boundary conditions (stream tube definition, back-pressure, rotational speed, axial gap) are also studied to quantify their influence on the solution accuracy. All two-dimensional results are interpreted as aerodynamic excitation mechanisms on stream sheets neglecting all three-dimensional effects.

Literature suggests the forcing function of the rotor blades to be strongly influenced by the design parameters stator count and axial gap. Previous studies on these design

parameters by Korakianitis [1991, 1992a,b and 1993a,b] have been pursued in order to gain physical understanding of the parameter influence on the forcing function for the investigated high pressure turbine stages. The turbine stage configurations investigated in this thesis are taken from two different applications:

- First, a typical aero-engine high pressure turbine stage is studied at subsonic and transonic flow conditions, with two axial gaps and two stator configurations. This is chosen because it is subject of an extensive research study including valuable measurements [Freudenreich 2001a, b], [Hennings et al. 2002] to validate the numerical results. Operating conditions (rotor speed) are according to the resonant conditions of the blades used in the experiments.

- Secondly, a subsonic high pressure turbine intended to drive the turbopump of a rocket engine is investigated in the frame of a design pre-study including four axial gap variations, and three stator geometry variations. This configuration is chosen because it allows independently of any experimental program the systematic study of the parameters in order to extend and generalise the findings made on the first study.

Beside the different turbine geometry the major difference to the investigations by Korakianitis [1992a, b, 1993a, b] is that in the present study transonic flows are included and smaller axial gaps are regarded. Furthermore, a full stage analysis is mainly used instead of a gust approach to capture more complete the bi-directional stator-rotor interaction as well as shock excitations. This extended computational effort seems especially justified to respect the more complex stator-rotor interaction mechanisms in transonic flow and at very small axial gaps.

To enhance the physical understanding of the aerodynamic excitation mechanisms a parametric analysis of the vortical and potential excitation effects and their interaction is performed. Therefore, the turbopump turbine stage is chosen offering a highly loaded turbine stage still operating in the subsonic flow range, so that the effects are not superposed by shock excitations.

To complete the studies towards a vibration risk assessment the results are extended by a blade mode shape consideration. Therefore, mode shape sensitivity analyses in two-dimensional planes assuming bending and torsion rigid body motions of a blade section are performed to assess the excitation risk in a stream sheet fashion.

Out of the results obtained in the various studies conclusions have been drawn towards the incorporation of unsteady aerodynamic considerations in the design of high-pressure turbine stages.

4 EVALUATION TECHNIQUES APPLIED IN THIS WORK

The numerical solution provided from an unsteady flow solver gives a large amount of data and its physical interpretation needs intensive post-processing. The present section will describe the applied physical models and underlying theory to analyse the unsteady results obtained in this work.

4.1 Blade vibration, concept of IBPA and aerodynamic damping

In order to consider the aerodynamic damping in forced response analyses separate blade vibration computations are performed as outlined in the state-of-the-art section. Due to circumferential periodicity of the tuned rotor blade row (which is an assumption) the blades vibrate with discrete phase angles to each other, the interblade phase angle σ, as introduced by Lane [1956].

$$\sigma = \frac{2 \cdot \pi \cdot n}{N_{rotor}},\ n = -\frac{N_{rotor}}{2},\ldots\frac{N_{rotor}}{2} \qquad \text{Eq. 4-1}$$

Whereas in flutter cases all interblade phase angles may have to be checked for flutter stability, tuned forced response vibrations can only take certain interblade phase angles due to periodicity conditions of both the vibration mode and the excitation. The excitation due to a stator with N_{stator} vanes would cause excitation orders of $n_e = h \cdot N_{stator}$, the rotor can respond to periodic excitations of the orders $n_e = k \cdot N_{rotor} \pm n$, which leads to the following formula for the possible travelling wave orders n:

$$h \cdot N_{stator} = k \cdot N_{rotor} \pm n \qquad \text{Eq. 4-2}$$

The factors h and k are arbitrary integers. The frequency of vibration is the frequency of excitation in the case of resonance. For turbine blades the vibration frequency is usually expressed as reduced frequency k defined herein by:

$$k = \frac{\omega \cdot c}{2 \cdot |\vec{w}_{exit}|} \qquad \text{Eq. 4-3}$$

Blade vibration computations are performed with prescribed amplitude, frequency and interblade phase angle of blade motion. The resulting unsteady pressures on the blade surface are evaluated in terms of a pressure coefficient, the aerodynamic work and the aerodynamic damping.

The pressure coefficient is defined as

$$\tilde{c}_p(x,t) = \frac{\tilde{p}(x,t)}{A \cdot (p_{t1} - p_1)} \qquad \text{Eq. 4-4}$$

where A is the non-dimensional amplitude of vibration.

During each cycle of vibration aerodynamic work might be exchanged with the blade motion, the direction of net exchange is the criterion for aerodynamic stability. This aerodynamic work per cycle from fluid on blade can be integrated from the time periodic surface pressure variations ($\tilde{p}$) on the blade and the local displacement velocity ($\vec{u}$), the normal surface vector $\vec{n}$ is pointing outwards:

$$W = \int_0^T \left[\int_{Rhub}^{Rtip} \oint_S \left(-\tilde{p} \cdot (\vec{u} \cdot \vec{n}) \right) \cdot ds \cdot dr \right] dt \qquad \text{Eq. 4-5}$$

A local expression of aerodynamic work per cycle from fluid on blade might be given by

$$W_{local} = \int_0^T \left(-\tilde{p} \cdot (\vec{u} \cdot \vec{n}) \right) dt \qquad \text{Eq. 4-6}$$

The aerodynamic work as defined above will be positive in case of destabilising flow, i.e. the flow will put work into the blade motion during each period of vibration, which in turn will increase the amplitude of vibration. It is convenient to non-dimensionalise the aerodynamic work to formulate the aerodynamic damping coefficient, positive for stabilising unsteady aerodynamics:

$$\Xi = \frac{-W}{(p_{t1} - p_1) \cdot c \cdot A} \qquad \text{Eq. 4-7}$$

The vibration amplitude can only be specified in the case of harmonic rigid body motions. Otherwise, the aerodynamic damping may be obtained with a local displacement vector:

$$\Xi = \frac{1}{(p_{t1} - p_1) \cdot c \cdot H} \cdot \int_{Rhub}^{Rtip} \oint_S \frac{-W_{local}}{\left| \vec{\delta}_{local} \right|} \cdot ds \cdot dr \qquad \text{Eq. 4-8}$$

To relate the aerodynamic damping to the damping used in structural calculations the concept of logarithmic decrement is useful, which describes the amplitude ratio of two successive damped vibration cycles [e.g., Wölfel 1991]:

$$\Lambda = \ln \frac{A^i}{A^{i+1}} = \frac{2 \cdot \pi \cdot D}{\sqrt{1 - D^2}} \qquad \text{Eq. 4-9}$$

A^i is the amplitude of the ith vibration period, D is the damping ratio (damping to critical damping). The aerodynamic part of this decrement can be derived from a simple linear system to (see [Carta 1988])

$$\Lambda_{aerodynamic} = \frac{-W}{4 \cdot K} \qquad \text{Eq. 4-10}$$

K is the mean kinetic energy of the vibrating blade.

In a structural forced response analysis the so obtained damping might be input to a structural code with the aerodynamic damping term as additional damping in the system. Alternatively, the forcing function due to excitation (f_e) on the right hand side might be extended by motion induced aerodynamic damping forces (f_m), as indicated in the following single degree of freedom vibration equation with mass m, damping d and stiffness k:

$$m\ddot{x} + d\dot{x} + kx = f_e(t) + f_m(t) \qquad \text{Eq. 4-11}$$

Both f_e and f_m are periodic and can be expressed in terms of Fourier coefficients based on the excitation frequency. The temporal relation of the damping forces to the blade motion is a solution of the blade vibration calculation, but the temporal relation between the forcing function and the blade motion is generally a solution of the dynamic forced response analysis. For simplified analyses however the temporal relation might be derived from the observation of a single degree of freedom vibration system, the equations below are found in basic structural dynamics text books (for example [Wölfel, 2001]). The rigid body vibration of a blade, where no blade deformation is present and all motion is induced at the blade fixation, is such a simplified system. Its transfer function, which relates the excitation forces to the displacement, is

$$\frac{f_m}{x} = \frac{1}{k + i \cdot d \cdot \omega - \omega^2 \cdot m} \qquad \text{Eq. 4-12}$$

with the eigenfrequency $\omega = \sqrt{\frac{k}{m}}$. This transfer function is complex, such describing amplitude amplification and phase relation ε between the forcing function and the blade motion. This phase is given by

$$\tan\varepsilon = \frac{d \cdot \Omega}{k - m \cdot \Omega^2} = \frac{d \cdot \Omega}{k \cdot (1 - \frac{\Omega^2}{\omega^2})} \qquad \text{Eq. 4-13}$$

where Ω is the excitation frequency. This equation makes clear that in general the phase between the excitation and the response is dependent on the system properties damping stiffness and eigenfrequency, but in case of resonance ($\Omega=\omega$) the phase ε is always 90°. This phase describes the case, where maximum work is done on the blade by the excitation forces. The relation is fundamental in [Jöcker et al. 2002b] (publication 6 in the Appendix) to estimate generalised forces for a given mode without the knowledge of the phase relation between blade motion and excitation forces.

4.2 Potential and vortical interactions

Flow disturbances can be split in 4 parts based on a mathematical analysis of the boundary conditions upstream and downstream of the blade row assuming the validity of the linearized Euler equations. Thus, the disturbances can be separated in:

1. Potential disturbances propagating downstream;
2. Potential disturbances propagating upstream;
3. Vortical disturbances propagating downstream;
4. Entropical disturbances propagating downstream.

This approach of separating the disturbances is completely documented in the open literature and is here summarised for convenience. The principle concept was used by Giles [1988a] to formulate 2D non-reflecting boundary conditions for the Euler equations and thereafter used by many researchers in the field to describe the unsteady boundary conditions of a turbomachinery blade row (e.g., [Henderson and Fleeter 1993a, b], [Manwaring and Wisler 1993], [Feiereisen et al. 1993], [Johnston et al. 1998]. The aim in these publications was always to separate measured data at the inlet and/or outlet of a turbomachine blade row into these different contributions, mostly limited to the potential and vortical contributions. In [Chung and Wo 1997] this approach was applied to a Navier-Stokes solution in order to separate the numerically obtained disturbance into a vortical and potential part. In the present work a similar splitting is performed to study the vortical and potential excitation sources in the subsonic turbopump turbine stage.

Splitting into vortical and potential effects builds on the following fundamental splitting theorem by Goldstein [1978] which states that the velocity disturbance is composed of a vortical part and a potential part, each related to different physical phenomena.

$$\partial\vec{w} = \partial\vec{w}_w + \partial\vec{w}_p \qquad \text{Eq. 4-14}$$

where $\partial\vec{w}$ is the velocity perturbation vector in the wake frame of reference. The vortical perturbation (rotational velocity) results from the wake of the upstream blade row and the potential perturbation (irrotational velocity) results from the pressure field of the upstream and downstream blade rows.

The assumptions on these perturbation parts are:

a) vortical perturbation:

$$\nabla \cdot \partial\vec{w}_w = 0 \quad \text{(divergence free (solenoidal), incompressible)} \qquad \text{Eq. 4-15}$$

$$\frac{D(\partial\vec{w}_w)}{Dt} = 0 \quad \text{(convective, non-dissipative)} \qquad \text{Eq. 4-16}$$

with a convection velocity $\vec{w}_{Fw}$ of the mean flow field.

b) potential perturbation:

$$\partial \vec{w}_p = \nabla \Phi_p \qquad \text{Eq. 4-17}$$

$$\nabla \times \partial \vec{w}_p = 0 \text{ (rotational free)} \qquad \text{Eq. 4-18}$$

It follows a description of the vortical and potential wave model as used in UNSFLO and for the analysis in this work. The details of the UNSFLO code specific nomenclature are given in the Appendix, to which the reader is referred to for an illustration of the describing parameters.

4.2.1 Vortical velocity perturbation

The vortical perturbation velocity field is transported only by convection, which can be expressed in a complex wave equation of n harmonics of type:

$$\partial \vec{w}_{w,n} = \Delta \vec{w}_{w,n} \cdot e^{-i \cdot \vec{k}_n \cdot \vec{x}} \qquad n = 1,2,3 \ldots \qquad \text{Eq. 4-19}$$

$\vec{k}_n$ is the wave propagation vector. Periodicity dictates the tangential component of this vector:

$$k_{yn} = \frac{2 \cdot \pi \cdot n}{P_S} \qquad \text{Eq. 4-20}$$

With a gust propagation vector perpendicular to the convection vector,

$$\vec{k} \cdot \vec{w}_{Fw} = 0 \qquad \text{Eq. 4- 21}$$

the axial component follows to

$$k_{xn} = -k_{yn} \cdot \frac{v_{Fw}}{u_{Fw}} = -k_{yn} \cdot \tan \alpha_w \qquad \text{Eq. 4- 22}$$

In common nomenclature the negative of the gust propagation vector is called the wave number vector [Feiereisen 1998].

The application of the condition of divergence free vortical perturbations onto equation 4-19 shows that also the perturbation amplitude is perpendicular to the wave propagation vector and hence that mean and vortical perturbation vectors are parallel. The proportionality of these vectors is expressed as

$$\partial \vec{w}_{w,n} = D_n \cdot \vec{w}_{Fw} e^{-i \cdot \vec{k}_n \cdot \vec{x}} \qquad \text{Eq. 4- 23}$$

where D_n is the proportionality constant of the nth harmonic. This is identical to the definition of the vortical sinusoidal perturbation used in UNSFLO, if only the first harmonic of the real part is regarded.

4.2.2 Potential velocity perturbation

Solutions to the potential disturbance equation [Liepmann and Roshko 1957] of the form

$$\left(1-M_x{}^2\right)\cdot\frac{\partial^2\phi}{\partial x^2}+\left(1-M_y^2\right)\cdot\frac{\partial^2\phi}{\partial y^2}-2\cdot M_x\cdot M_y\cdot\left(\frac{\partial^2\phi}{\partial y\cdot\partial x}\right)=0 \qquad \text{Eq. 4-24}$$

are given by a wave equation with exponentially decaying amplitude in axial direction:

$$\Phi_n(x,y)=A_n\cdot e^{\left(-i\cdot k_{yn}\cdot y+\lambda_n\cdot x\right)} \qquad \text{Eq. 4-25}$$

The axial wave number λ_n can be calculated to

$$\lambda_n=\frac{-i\cdot k_{yn}\cdot M_x\cdot M_y\pm k_{yn}\cdot\sqrt{1-M^2}}{1-M_x^2} \qquad \text{Eq. 4-26}$$

which is sometimes represented as

$$\lambda_n=-i\cdot\chi\cdot k_{yn},\qquad \chi=\frac{M_x\cdot M_y\pm\sqrt{M^2-1}}{1-M_x^2} \qquad \text{Eq. 4-27}$$

where χ is the axial decay factor. This factor characterises the wave:

- For M<1 the axial wave number λ is complex and the wave is decaying in positive or negative x direction, depending on the sign of the root. These waves are called sub-resonant.
- For M>1 the axial wave number λ has a real part and hence the waves travel non-attenuated in spatial direction. These waves are called super-resonant.

The application to the present work is limited to the case of sub-resonant waves decaying in positive axial direction. Hence, the potential perturbation velocity vector is

$$\begin{aligned}\partial\vec{w}_{p,n}=\nabla\cdot\Phi_n(x,y)&=\nabla\cdot\left(A_n\cdot e^{\left(-i\cdot k_{yn}\cdot y+\lambda_n\cdot x\right)}\right)\\&=\begin{bmatrix}A_n\cdot\lambda_n\\-A_n\cdot i\cdot k_{yn}\end{bmatrix}\cdot e^{\left(-i\cdot k_{yn}\cdot y+\lambda_n\cdot x\right)}\\&=\begin{bmatrix}\chi\\1\end{bmatrix}\cdot A_n\cdot i\cdot(-k_{yn})\cdot e^{\left(-i\cdot k_{yn}\cdot y+\lambda_n\cdot x\right)}\end{aligned} \qquad \text{Eq. 4-28}$$

This equation is also basis for the specification of the potential disturbance in UNSFLO. The input parameter for the code is based only on the first harmonic and instead of the

amplitude of the velocity potential (A) the amplitude of the pressure disturbance (P) is input to the code.

4.2.3 Combined vortical and potential velocity perturbation

The complete velocity perturbation field can be reassembled with equation 4-14. When the evaluation is done at x =0 (trailing edge position or measurement position) the following set of complex equations for the velocity perturbations is obtained:

$$\begin{aligned} \partial u_n &= \partial u_{w,n} + \partial u_{p,n} = (u_{Fw} \cdot D_n + \lambda_n \cdot A_n) \cdot e^{-i \cdot k_{yn} \cdot y} = \Delta u_n \cdot e^{-i \cdot k_{yn} \cdot y} \\ \partial v_n &= \partial v_{w,n} + \partial v_{p,n} = (v_{Fw} \cdot D_n - i \cdot k_{yn} \cdot A_n) \cdot e^{-i \cdot k_{yn} \cdot y} = \Delta v_n \cdot e^{-i \cdot k_{yn} \cdot y} \end{aligned} \qquad \text{Eq. 4-29}$$

Δu_n and Δv_n are the amplitudes of the combined perturbation velocity vectors in axial and tangential direction. This leads to

$$\begin{aligned} (u_{Fw} \cdot D_n + \lambda_n \cdot A_n) &= \Delta u_n \\ (v_{Fw} \cdot D_n - i \cdot k_{yn} \cdot A_n) &= \Delta v_n \end{aligned} \qquad \text{Eq. 4-30}$$

which can be resolved for the complex amplitudes D_n and A_n of the vortical and potential perturbation parts in dependency of the usually experimentally obtained combined amplitudes Δu_n and Δv_n.

4.2.4 Potential pressure perturbation

The potential disturbance leads also to a pressure variation, which is not regarded so far. The relation of the potential velocity perturbations to these pressure perturbations is expressed in

$$\partial p = -\rho_{Fw} \cdot (u \cdot \partial u_p + v \cdot \partial v_p) \qquad \text{Eq. 4-31}$$

This equation is obtained from the assumptions of constant entropy and constant total enthalpy.

4.3 Flow field evaluations

The evaluation of the flow field is a very sensitive procedure to validate computational results. It requires much care to ensure the correctness of the comparison. In the present work CFD results have been compared to flow field measurements obtained with Laser Two Focus (L2F) anemometry by Freudenreich [2001b]. A comprehensive way to analyse the unsteady flow field is to view the temporal development of the flow with help of animations. But, this does not allow the qualitative comparison of measured and calculated results. Therefore, time averaged values as well as time resolved flow field data were compared at selected positions in the flow field ([Freudenreich et al. 2001a], Publication 4 in the Appendix).

Contour plots of perturbation pressures of stator-rotor interaction are used. A jump at the interface occurs in these plots (see for example Figure 25), even though the pressure is expected to be independent of the chosen frame of reference. Indeed it is, only the time averages in stator respectively rotor frame are different, accordingly causing the observed discontinuity at the interface between these domains.

4.4 The forcing function

In this work the forcing function represents the unsteady load of a blade due to an aerodynamic excitation source. Hence it does not include the unsteady load due to blade vibration, the aerodynamic damping force. The analysis of the forcing function is the key evaluation in this thesis to judge the aerodynamic predictions of rotor excitation.

4.4.1 Fourier decomposition

A common way to look at the unsteady pressure distribution is to Fourier transform the time dependent blade surface pressures and analyse them in terms of amplitudes and phases of harmonics based on the excitation frequency. Main attention is given to the 1st harmonic, because forced response is most likely governed by it. However, as found during this work some excitations have significant contributions of higher harmonics, which in principle have the potential to excite other blade vibration modes beside the one identified in the underlying Campbell diagram. Fourier decomposition is performed throughout the work based on

$$U(t) = \mathrm{Re}\left(\sum_{k=0}^{K} \hat{U}_k \exp\left(2\pi i \frac{kt}{T}\right)\right)$$
$$= \hat{U}_k + \frac{1}{2}\sum_{k=1}^{K}\left\{\hat{U}_k \exp\left(2\pi i \frac{kt}{T}\right) + \hat{U}_k^* \exp\left(-2\pi i \frac{kt}{T}\right)\right\} \qquad \text{Eq. 4-32}$$

where *Re(z)* and *Im(z)* denote the real and imaginary part of the complex variable *z*. z^* is the complex conjugate of *z*. T is the period of the signal *U(t)*. For the presentation of the unsteady pressure on the rotor, the variable *U(t)* is thus the static pressure, $\hat{U}_k$ the associated Fourier coefficients and *T (=T_r=P_s/V)* is the period of the signal *U(t)=p(t)*. From these Fourier coefficients, the amplitude and the phase are defined as it follows:

$$\left|\hat{U}_k\right| = \sqrt{\mathrm{Re}\left(\hat{U}_k\right)^2 + \mathrm{Im}\left(\hat{U}_k\right)^2} \qquad \text{Eq. 4-33}$$

$$\varphi = \tan^{-1}\left(\frac{\mathrm{Im}\left(\hat{U}_k\right)}{\mathrm{Re}\left(\hat{U}_k\right)}\right) \qquad \text{Eq. 4-34}$$

To avoid a phase shift in the comparison of the phase of unsteady pressure coefficients the rotor has its leading edge always aligned with the stator leading edge at the time t=0. This aligned rotor blade is referred to as the reference blade.

4.4.2 Time –space presentation

Fourier decomposition of the forcing function is useful to judge the magnitude of an excitation but gives very limited insight in the flow physics causing the excitations. Beside the analysis of the unsteady flow field (Chapter 4.3) the time resolved presentation of the unsteady blade pressure is very useful to study aerodynamic excitation mechanisms. Two ways of presentation have been established in the open literature, either the time development of the blade surface pressure is presented at selected points of the blade surface for one excitation period, or contour plots of the perturbation pressures are shown as function of time and space. In the latter one the time axis comprises one excitation period, the space axis spans one surface line around the blade, in the present investigations at the blade midspan. These plots are very informative as they contain the complete time and space resolved forcing function at one particular blade section and is preferably used in the present work.

4.4.3 Forces

Integrating the 2D blade surface pressure of the blade surface leads to the blade force and moment. In the time domain this is expressed as follows:

Force vector: $$\vec{f}(t) = -\int_S p(t) \cdot \vec{n} \cdot ds$$ Eq. 4-35

Out of plane moment: $$m(t) = -\int_S p(t) \cdot \vec{n} \cdot \begin{pmatrix} -\Delta y \\ \Delta x \end{pmatrix} \cdot ds$$ Eq. 4-36

Δx and Δy are the axial and tangential distances of the pressure location on the blade from the axis location about which the moment is computed.

The forces might also be expressed as Fourier components, to be obtained from the time signal as outlined in Chapter 4.4.1. The amplitudes of up to four harmonics of the Fourier transformed forces and the moment about a fixed point are used and compared in the work (for example in [Jöcker et al. 2000b], Publication 3 in the Appendix).

4.4.4 Mode shape consideration: Definition of generalised forces

In order to evaluate how relevant a certain forcing function is to excite a blade mode shape the concept of generalised forces as a measure of excitability of a mode shape is applied. The generalised force of harmonic h is the blade surface integrated scalar product of the local excitation force vector with the local blade displacement vector:

$$f_{g,h} = \left| \sum_{i=1}^{N} (\vec{q}_{t,i} \cdot \vec{f}_{h,i}) \right|$$ Eq. 4-37

Index t indicates a torsion mode shape pointing out that in the presented approach blade displacements are defined in terms of a torsion axis location in the 2D plane of the blade

section. Only the part of excitation force acting in direction of the blade displacement will contribute to the generalized force so that the integral of the scalar product over the blade surface will give a value of the mode excitation risk. The applied local displacement vectors are real valued assuming a rigid body motion without phase shift. However, the unsteady force harmonics include an imaginary part. The relative phase of the force or pressure harmonic defines the time shift relative to the excitation period, at which the related excitation events (amplitudes) on the blade surface take place. The start and end of an excitation period is given by the relative position of stator to rotor at the beginning of the CFD computation. Eq. 4-37 shows that the local phase differences between excitation and blade motion is regarded by using the complex force vector, but the overall phase shift between blade motion and excitation is not specified. Instead, by evaluating the amplitude of the complex sum of scalar products the worst case phase between blade motion and blade excitation is chosen, so that the phase lag is resulting in the maximum generalised force (which is equivalent to the maximum work). For the presented simplified approach, where rigid body motion is prescribed, the worst case phase assumption as applied is justified. This becomes clear when recalling the forced vibration of a single degree of freedom system, to which the rigid body motion is reduced. The phase lag between displacement and excitation force of such a system at resonance is always 90°, independent of the damping. This corresponds to the worst case phase lag of such a system, at which the work of the blade is maximal (see further Chapter 4.1, Eq. 4-13). Hence, independent of the damping in the system the proposed worst case phase lag describes well the work done by the forcing function under the considered rigid blade motion.

The complete approach is documented in [Jöcker et al. 2002b] (publication 6 in the Appendix), where generalised forces are non-dimenionalised and plotted against a torsion axis location to describe the mode shape.

5 TEST CASES

Three different turbines have been investigated in this thesis. Table 1 presents some geometric and aerodynamic key parameters of these test cases. The ADTurB turbine is a transonic turbine applied in a European research project, the turbopump turbine is a subsonic high pressure turbine investigated at Volvo Aero Corporation in a pre-design study. The International Standard Configuration 11 (STCF 11) is a low pressure turbine rotor investigated experimentally towards flutter stability at the Swiss Federal Institute of Technology (EPFL). Details of each test case will be presented in the subsequent Chapters.

	Blade /Vane count N	Approx. Solidity c/S	Approx. aspect ratio H/c_{ax}	Approx. stagger angle γ [°]	Axial gap g_{ax}/S_s	Approx. stator exit Mach number $M_{exit,design}$	Reduced frequency* k
ADTurB stator1	43	1.3	1.2	52	0.28 0.39	0.85 (subs) 1.05 (trans)	-
ADTurB stator 2	70	1.6	1.7	54	0.45 0.63	0.85 (subs) 1.05 (trans)	-
ADTurB rotor	64	1.3	1.3	-33	-	0.6 (subs) 1.0 (trans)	1.86 (OP2) 5.11 (OP9)
Turbopump stators	12,16 , 32	1.6 1.2	0.8	48	0.05 –0.3	0.73	-
Turbopump rotor	33	1.8	1.2	-34	-	0.83	1.2 – 3.2**
STCF 11	20	1.4	0.7	-41	-	0.69 0.99	0.213 0.155

* based on experimental exit velocity

** based on computed exit flow velocity

Table 1: *Overview of design and flow parameter ranges of the investigated turbines at midspan*

5.1 Aero-engine turbine stages (ADTurB)

The investigated ADTurB turbine stages were designed within the course of two successive European community programs [Santoriello et al. 1993] [Colantuoni et al. 1995] and [Colella and Solazzo 1996]. They comprise state-of-the-art, full size, transonic aero-engine high pressure turbine stages. A 64 blades rotor was run with two different sized but aerodynamically similar stators, 43 nozzle guide vanes (NGV) for stator 1 and 70 NGVs for stator 2. The rotor speed was varied as well, around the design speed n_{design} = 7894 RPM. Both stators have the same design exit Mach number $M_{2\ Stator}$ = 1.05 and exit flow angle $\alpha_{2\ Stator}$ = 73°. The rotor blades have slight 3D shape, while both stators are of similar cylindrical vane shape. Figure 13 shows a meridional view of the test rig with the 43NGV stator mounted. A view of the midspan geometry of the stage with both stators superposed is given in Figure 14.

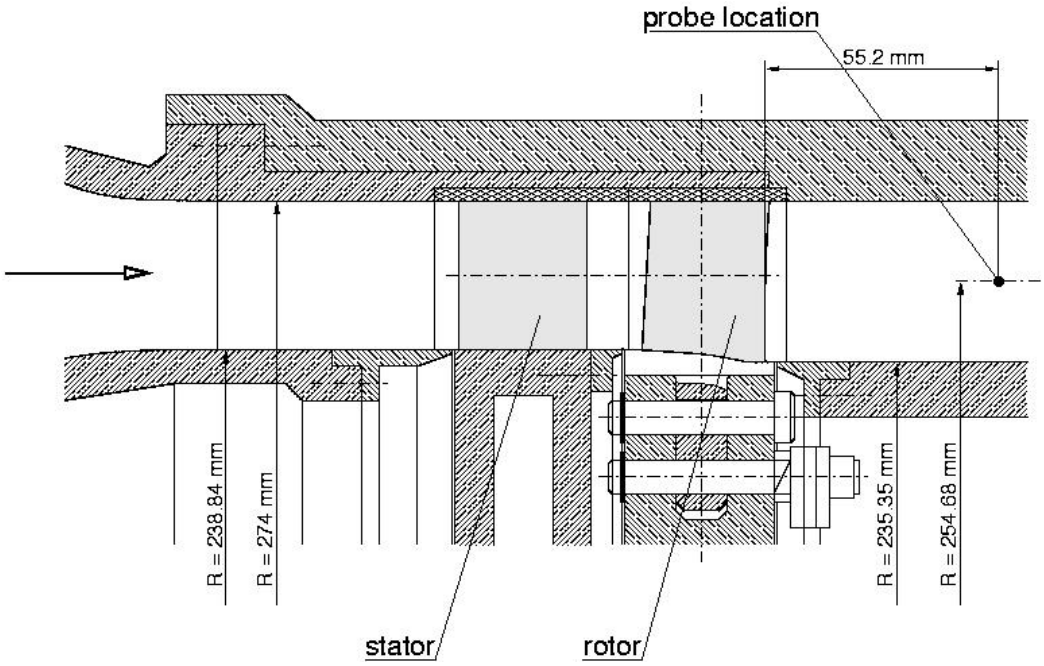

Figure 13: *Meridional view of annular test section (taken from Green [2001])*

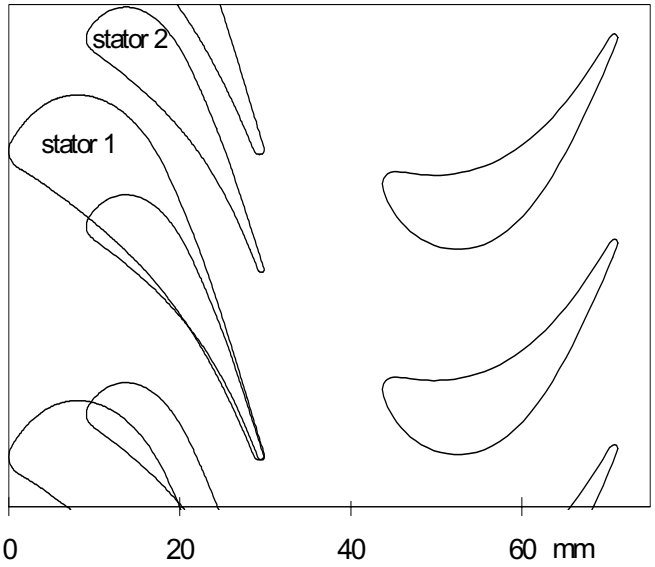

Figure 14: *Stages at 50% span large gap (taken from [Jöcker et al. 2000b], publication 3 in the Appendix)*

The tests comprised measurements of inlet and outlet flow conditions with wedge type probes at three radii including midspan. Extensive flow field measurements were performed with laser two focus anemometry (L2F), which allows the time resolved measurement of velocities, flow angles and turbulence levels without introducing a flow disturbance [Freudenreich et al. 2001a, 2001b]. During transient operation conditions the unsteady pressures on the rotor were measured with fast response pressure transducers. Simultaneously, the rotor blade vibration amplitude was logged with help of strain gauges mounted on various blades. More details on the vibration experiments are found in [Hennings et al. 2002]. It should be noted that for the latter experiments the rotor blades were designed such that resonance conditions fell into the testing range of rotational speed, a sketch of the Campbell diagram is shown in Figure 15.

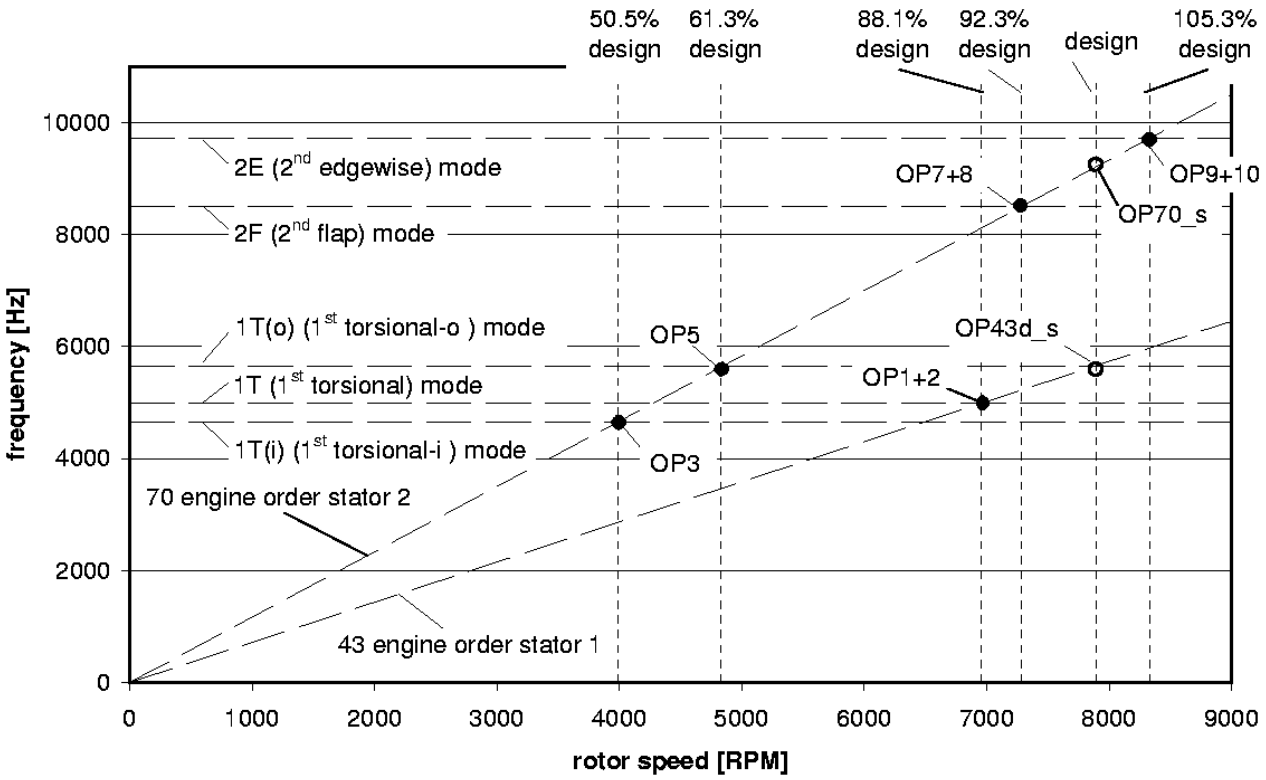

Figure 15: *Principle sketch of Campbell diagram of the investigated turbine stages, taken from Freudenreich [2001b]*

		Basic numerical cases				Experiments		
OP	**# NGV**	**% Ω_{design}**	**$M_{2\ stator}$***	**g_{ax} [mm]**	**p_3/p_{t1}****	**% Ω_{design}**	**$M_{2\ stator}$**	**g_{ax} [mm]**
1	43	88.6	0.80	14.6	0.521	88.1	0.81	13.8
2	43	88.6	0.94	14.6	0.32	88.1	0.99	13.8
1-s	43	88.6	0.81	10.4	0.521	88.1	0.80	9.7
2-s	43	88.6	0.94	10.4	0.32	88.1	0.96	9.6
3	70	-	-	-		50.5	0.85	13.9
5	70	61.5	0.91	14.6	0.5065	61.3	0.83	13.8
5-s	70	61.5	0.92	10.4	0.5065	-	-	-
6	70	61.5	1.03	14.6	0.233	-	-	-
6-s	70	61.5	0.98	10.4	0.233	-	-	-
7	70	-	-	-	-	92.3	0.80	13.8
8	70	-	-	-	-	92.3	0.96	13.8
9	70	105.6	0.76	14.6	0.528	105.3	0.79	13.7
9-s	70	105.6	0.76	10.4	0.528	-	-	-
10	70	105.6	0.92	14.6	0.32	105.3	0.93	13.7
10-s	70	105.6	0.91	10.4	0.32	-	-	-

* from steady stage computation, **prescribed boundary condition in steady computation

Table 2: *Basic operation conditions at theoretical resonance (taken from [Jöcker et al. 2000b], publication 3 in the Appendix)*

The main numerical studies in this thesis are concerned with the operating points OP1 and OP2, which represent a subsonic and a transonic case with the 43 NGV stator (stator 1) close to design speed. But also the majority of the remaining operating points have been investigated numerically and the results are discussed. An overview of the basic numerical and experimental cases is given in Table 2. The experimental and numerical boundary conditions are not identical, because these computations were real predictions, i.e. they were performed before the experiments. Additional studies not listed in the table are made to meet exact experimental boundary conditions for validation purposes after the test results were available.

5.2 Turbopump turbine stages

The investigated turbopump turbine is a one-stage subsonic turbine designed to operate at pressure levels corresponding to the levels to be considered in an extreme closed cycle rocket engine. The stator is of cylindrical type, i.e. the vanes are designed with a profile not varying in radial direction. The stator exit flow is of high subsonic outlet Mach number. The rotor is designed with radial variation in the blade profiles taking into account the variation of the stator outlet condition and with a small outlet swirl angle, the blades are therefore twisted. They are also shrouded. No outlet guide vane is used in the design. Flow design design data are given in Figure 16.

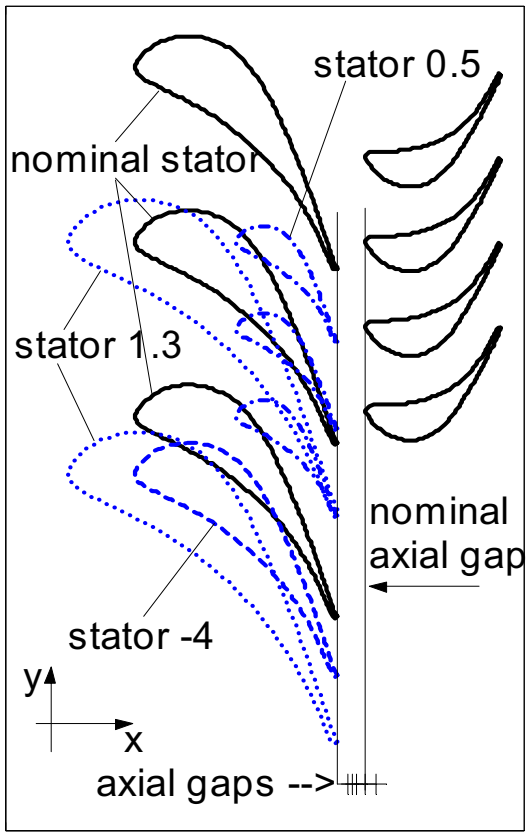

Design point data:

Total inlet pressure	54 Mpa
Total inlet temperature	760 K
Rotational speed	14 000 rpm
Power level	190 MW
Mass flow	1700 kg/s

Through flow data at midspan:

Position	1_{stator}	2_{stator}	2_{rotor}	3_{rotor}
M	0.17	0.732	0.274	0.83
α [°]	0	-72.01	-30.66	66.23
p [kPa]	52540	36498	36498	24275

Figure 16: *Midspan view of investigated turbopump turbine and flow boundary conditions, taken from [Jöcker et al. 2001], publication 5 in the Appendix*

Starting from nominal design parameter studies have been performed investigating the axial gap influence and the stator influence on the unsteady rotor excitation level. Figure 16 shows the stage configuration with the nominal axial gap, the range of investigated axial gaps and the various stator-rotor configurations investigated. Table 3 gives an overview of the presented cases. The axial gap was varied between 8% and 29% of rotor axial chord. The stator count was varied such that the pitch ratio R is between 1 and 3. To achieve a pitch ratio of 2.75 two methods of modification were applied: in case (–4), the stator pitch was increased by removing 4 vanes from the annulus, in case (1.3) the stator was additionally scaled by a factor 1.3 to maintain the steady aerodynamics (see Figure 16).

Name	**g_{ax} [%]**	**# vanes**	**# blades**	**R**	**g_{ax}/S**
Nominal	21.4	16	33	2.063	0.1513
Axial gap study:					
8	8.0	16	33	2.063	0.056
10	9.9	16	33	2.063	0.070
12	11.8	16	33	2.063	0.084
16	15.6	16	33	2.063	0.111
29	28.6	16	33	2.063	0.203
Stator study:					
0.5	21.4	32	33	1.0313	0.303
1.3	21.4	12	33	2.75	0.114
-4	21.4	12	33	2.75	0.114

Table 3: *Turbopump investigated cases overview, taken from [Jöcker et al. 2001], publication 5 in the Appendix*

5.3 STCF 11 – blade vibration test case

In Fransson et al. [1999] (publication 1 in the Appendix) a new International Standard Configuration has been added to the already existing set of 10 Standard Configurations [Fransson and Verdon, 1991, 1992]. It is called the International Standard Configuration 11 (STCF 11). The experimental data has been obtained in the annular test cascade at the Swiss Federal Institute of Technology (EPFL) in Lausanne, Switzerland, which is schematically drawn in Figure 17.

The test facility was supplied with air by a four stage radial compressor with a maximum mass flow rate of 10 kg/s and a maximum pressure ratio of 3.5. An additional compressor was used to suck off the wall boundary layers. In order to simulate unsteady flow conditions in the test cascade, all 20 blades were electromagnetically excited and controlled to vibrate in travelling wave mode. This included the control of vibration amplitude, vibration frequency and the interblade phase angle. The suspensions of the blades were designed to reproduce the eigenfrequency and bending direction of the first bending mode of the blade performing a solid blade motion. Measurements of static and total pressures as well as the flow angles were done in the planes e_1 and e_2 before and behind the cascade. The blade surface distributions of steady and unsteady pressures were measured with pressure taps for the steady state and miniaturized piezo-resistive pressure transducers for the time dependent data measurements, all embedded at

midspan on different blades. The measured flow cases on this configuration varied in incidence flow angles from 6° to 48° and in isentropic outlet Mach number from 0.64 to 1.46. The blade was designed for nominal flow conditions with an incidence angle of 16.8° and M_{2is}=1.0.

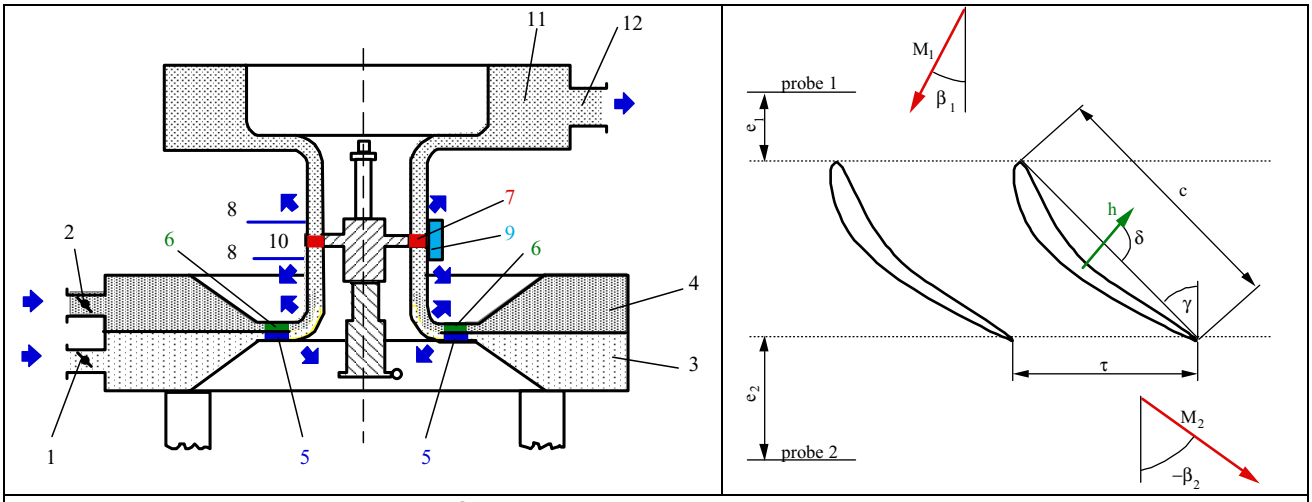

1.2 Inlet valves	9 Cylindrical optic
3.4 Settling cambers	10 Wall pressure taps
5,6 Inlet guide vanes	11 Outlet flow collector
7 Test cascade	12 Outlet vanes
8 Aerodynamic probes	➡ Boundary layer suction

Figure 17: *STCF11: Schematic view of the test facility at LTT/EPFL, taken from Fransson et al. [1999], publication 1 in the Appendix*

Out of the measured data two test cases have been made available in [Fransson et al. 1999] (Publication 1 in the Appendix) to provide turbine blade vibration test data comprising transonic flow conditions and unsteady viscous flow effects. A subsonic attached flow case and an off-design case have been chosen. The latter one is characterised by a separation zone at suction side close to the leading edge and a moving shock on the aft part of the suction side. Several 2D and Q3D codes have been applied to compute the measured unsteady pressures. For the present thesis the cases are relevant to validate UNSFLO towards the prediction of aerodynamic damping and the influence of separations on the unsteady flow.

6 RESULTS AND DISCUSSIONS

In this chapter the main results obtained in various computations of the unsteady flow in the investigated test cases (Chapter 5) are discussed with reference to the publications 1 to 6, which are listed in the Appendix. This is structured as follows: In Chapter 6.1 the results obtained with the code UNSFLO are validated. Therefore, mesh sensitivities and the influence of boundary conditions on the results in comparison to available experimental data are discussed. The gust method and the full stage method are regarded for excitation computations, blade vibration computations are validated against the STCF 11 test case. Chapter 6.2 describes the excitation mechanisms found in the nominal cases of the ADTurB turbine stage and the turbopump turbine stage, which is basis for the discussion of parametric studies in Chapter 6.3. There, operating conditions, axial gap variations and stator size variations are discussed for the two investigated turbine stages. Finally, Chapter 6.4 attempts to derive potentials to improve the turbine stage design towards the reduction of HCF failure based on the findings elaborated in the previous sub chapters.

The discussions comprise a critical review of the results presented in the publications 1-6 in the Appendix and in such a way complete the published work. The findings in the various chapters are usually derived first for the ADTurB test cases and then completed with and compared to the turbopump turbine results.

6.1 Validations

In order to ensure that the applied numerical tools were used correctly and to estimate the possible errors extensive validation studies have been performed. The following part summarises the findings of these studies starting with mesh sensitivity, discussing then the stator exit flow computational results and their relevance for gust computations before examining the excitation prediction quality compared to experimental and other numerical results.

6.1.1 Mesh sensitivity (UNSFLO)

Stage calculations (stator-rotor interaction):

For all studies with UNSFLO mesh sensitivity was checked to choose a suitable mesh in terms of reasonable resolution and sufficient solution quality. Generally, it was found that complete mesh independence of the unsteady computations could not be achieved, even though the steady blade surface pressure appeared mesh independent. Large mesh dependence was found in some cases of purely inviscid stage calculations with UNSFLO. Stator mesh variations led in one extreme case to significantly different steady stator flow causing large deviation of the unsteady rotor blade surface pressures (the relative course stator mesh resulted in an over prediction of 1^{st} harmonic pressure amplitude level on the rotor by about 60%). This was found on the subsonic turbopump turbine configuration [Jöcker 1998b]. It was concluded to drop all further tries to calculate the stator-rotor interaction with the purely inviscid approach.

UNSFLO allows the inclusion of the viscous terms in the solution of the flow close to the blade surface, where a structured O-mesh must be included for this purpose. This approach is more suitable to compute a wake behind the stator, because the inviscid approach would only predict a wake due to numerical dissipation. Also on these meshes the results are dependent on the mesh resolution, though much less than in the above mentioned purely inviscid computation. An example from the ADTurB stage is shown in Figure 18 and Figure 19, where three different rotor mesh resolutions were applied in combination with the same stator mesh (the stator mesh resolution had only minor influence on the present unsteady blade surface pressure on the rotor).

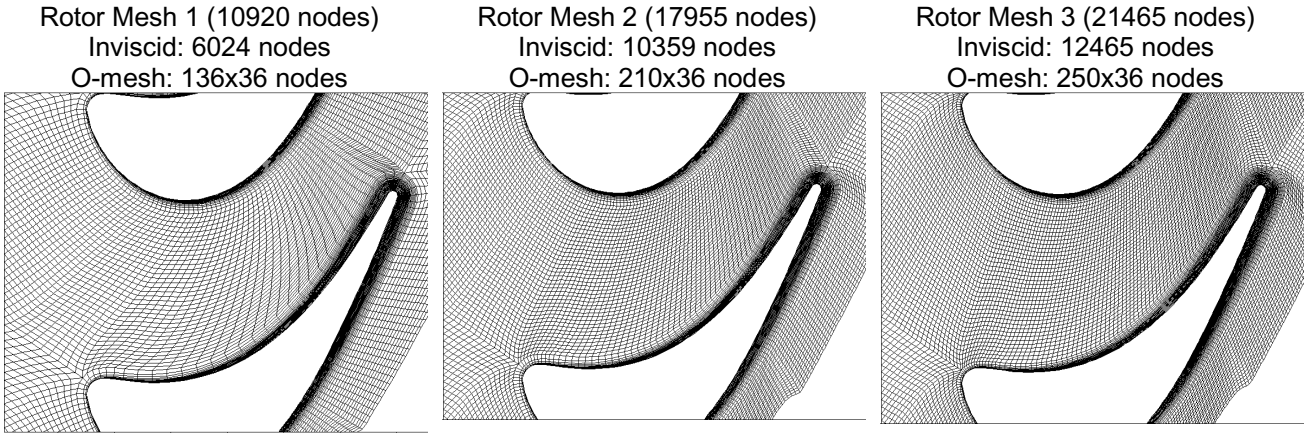

Figure 18: *Rotor meshes for stage calculations, UNSFLO, ADTurB stage*

Obviously, the rotor mesh resolution had an influence both on the spatial resolution of the flow at rotor inlet passage as well as on the unsteady blade surface pressures. The refined mesh resulted in a slightly reduced Mach number level at the rotor inlet, which gave rise to reduced excitation pressures on the rotor blade surface. However, these differences were small compared to the differences to experimental data and other code results, as shown in the following chapters. A medium resolved rotor mesh was used for further studies.

Note on stator-rotor gap
In the turbopump turbine the axial gap study was extended to very small gaps, down to 8% of the rotor axial chord. There, the limit of meshing capabilities with UNSFLO was reached, because the region between stator trailing edge and rotor leading edge became too small to contain sufficient meshing of the vane and blade O-meshes and the stator-rotor interface (the details are documented in Jöcker et al. [2000a]).

Mesh sensitivity of gust calculations (UNSFLO):

Stator mesh:
The quality of a gust calculation result depends on the stator exit flow prediction. Both for the turbopump turbine as well as for the ADTurB turbine the steady stator exit flow (in terms of velocity and pressure on circumference) appeared more smeared out with less pronounced peaks when coarser meshes were applied. When extracting the spatial 1st harmonic gust from such a calculation these differences can be important: Relative vortical amplitude variations of 16% and potential amplitude variations of 8% due to mesh variations were estimated in the turbopump turbine 4% of c_{ax} behind the stator trailing

edge. For comparison, around the same axial position the vortical amplitude varied relatively with 7.6% per mm axial position and the potential amplitude with about 6.2% per mm axial position. More discussions on the stator exit-flow quality follow in Chapter 6.1.2 in comparison to measured data.

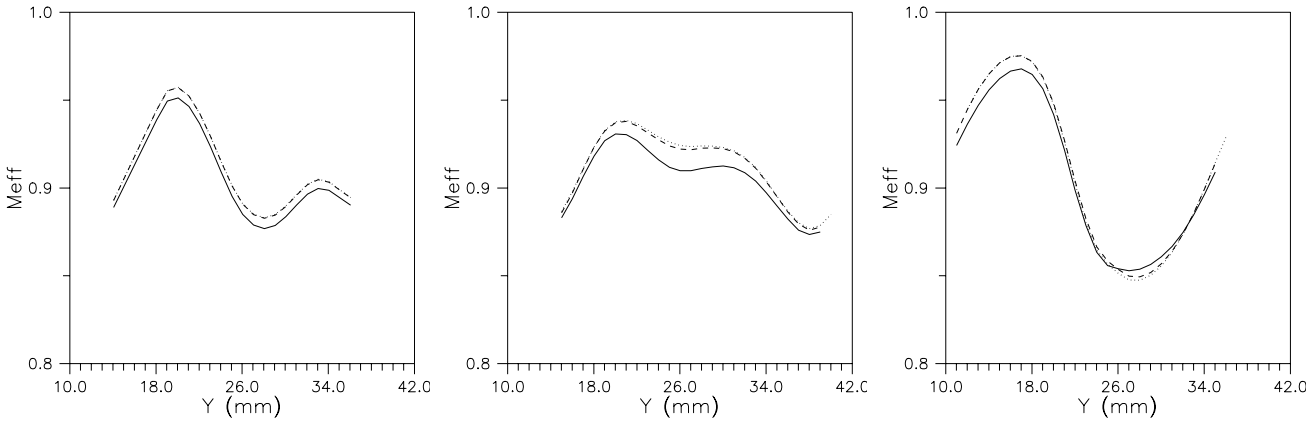

x/c$_{ax}$=1.21 ***x/c$_{ax}$=1.40*** ***x/c$_{ax}$=1.54***

Time averaged effective Mach number in stator frame at various axial locations in the gap

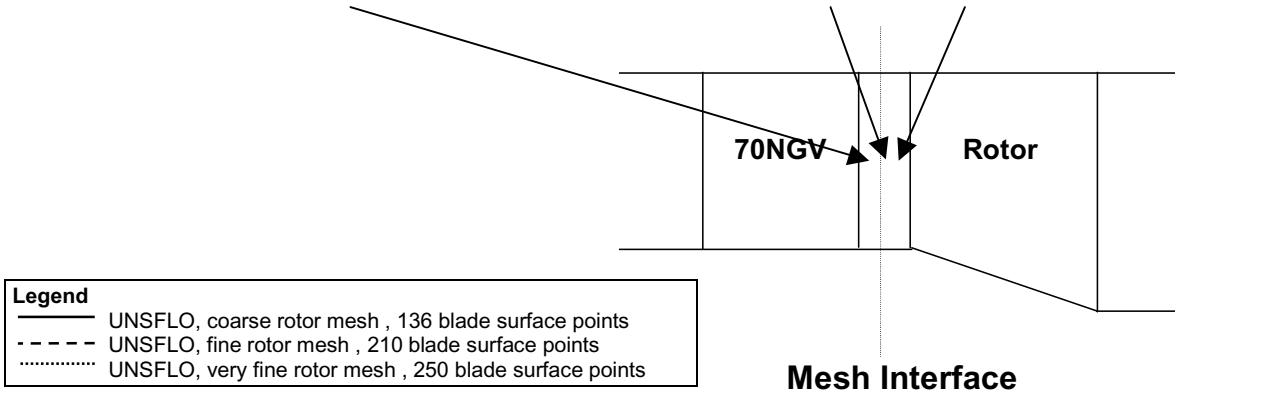

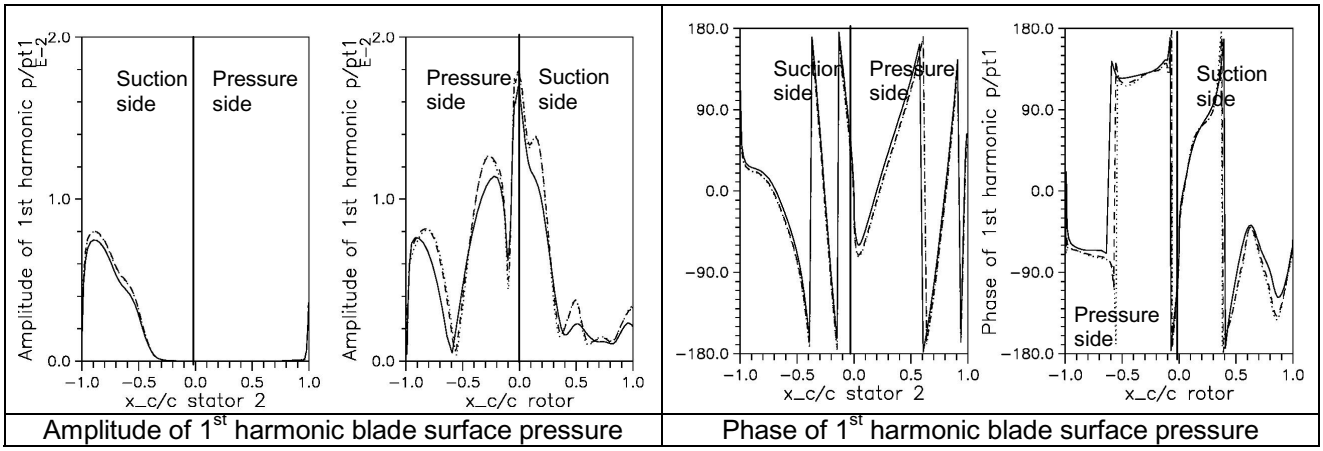

Amplitude of 1st harmonic blade surface pressure | Phase of 1st harmonic blade surface pressure

Figure 19: *Rotor mesh sensitivity of unsteady flow field and blade surface computations with UNSFLO, ADTurB stage (OP10, large axial gap)*

Rotor mesh:

For gust calculations it can be computationally beneficial to model the rotor flow inviscid without computing the blade boundary layer and ensure that the prescribed flow

disturbances at the inlet boundary to the computational domain are sufficient to describe the interactions with the neighbouring stator. For the subsonic turbopump turbine, both inviscid and viscous rotor meshes with varying resolution had only small influence on the blade surface unsteady pressure due to an incoming gust. The variation in 1st harmonic blade pressure due to the viscous or inviscid model of the rotor flow was comparable to the one found in the ADTurB stage computations shown above (Figure 19). So the rotor boundary layer had no significant influence on this result. On the other hand the application of adaptation of the inviscid mesh, i.e. the local rotor mesh refinement according to the local density gradient, resulted in the 1st harmonic pressure amplitudes on the blade surface to be reduced by about 20%. No explanation for this was found and the non-adapted mesh results seemed more reliable, so that this option was not further used. The details of the study on the stator and rotor mesh influence on the turbopump turbine are documented in [Jöcker et al. 2000a].

6.1.2 Stator exit flow prediction quality

It is obvious that the quality of the stator exit flow prediction is important for the gust specification, and it is also the main source for unsteadiness in the stage computed stator-rotor interaction. Validations of predictions against steady probe and laser measurement data in the ADTurB stage were published in [Freudenreich et al. 1999] (publication 2 in the Appendix). The results towards methods validations are summarised below and a few additional aspects are discussed.

Stator exit flows predicted by UNSFLO (Q3D at mid span) and a 3D fully viscous solver (VOLSOL) were compared with L2F traverse measurements at 5 axial mid span positions in terms of effective Mach number. Focus was laid on the cases with transonic flow conditions with a typical trailing edge shock system similar to the one shown in Figure 7. The measurements were performed behind the isolated stator row with the rotor removed, boundary conditions for the computations were specified according to these measurements. The velocity profile in circumferential direction was characterised by two deficits, one due to the wake propagating in approximate exit flow direction (about 73° from axial) and one due to a shock propagating in approximately axial direction from the stator trailing edge. Similar results have been obtained downstream of the 43 NGV stator, which are shown in Figure 21. Depending on the axial distance behind the trailing edge these two velocity deficits were merging into one large deficit or two separate deficits appeared. The locations of the deficits were computed correctly by the codes but the numerical results showed also some differences to the measured data. None of the numerical methods reflected the measured diminution of the wake deficit with axial distance. UNSFLO gave a too small Mach number deficit in the wake shortly behind the vane (x/c_{ax}=1.04), which then did not decay in axial direction as fast as the measured one. VOLSOL predicted the deficit too large close to the stator trailing edge (at x/c_{ax}=1.04), but ended up with a similar wake decay as UNSFLO further downstream (x/c_{ax}=1.74). The main difference in mid span flow between the two predictions was the shock strength (VOLSOL gave a larger change in Mach number over the shock), even though the computations were driven by the same blade pressure ratio (p_2/p_{t1}). This was also indicated by the comparison of blade surface pressure distribution at midspan. On the other hand the Mach number deficit due to the wake was less pronounced in the VOLSOL result than in the measurements and the UNSFLO results.

Discussion:
Shock strength and position prediction are very sensitive not only to the blade pressure ratio but also to the area relation of throat area to flow exit area. The specification of the stream tube expansion in the Q3D method is controlling this area relation, whereas 3D methods have the advantage that these area relations are included in the model. The difficulty to specify a correct stream tube evolution in Q3D methods to match the 3D flow is a known weakness of these methods. But not only shock strength, also wake deficit was predicted differently by the methods. The deviation in the computed wake Mach number deficits could be due to the different turbulence models. UNSFLO was applied with a one-equation turbulence model in the near blade region only whereas VOLSOL was applied with a Baldwin-Lomax type turbulence model in the complete flow field. Also 3D effects may have caused the differences between the predictions. Radial velocity components at mid span were significant in the wake flow but not in the core flow, which could have modified the appearance of the compared 2D Mach number.

The main conclusion from this study with regard to unsteady stator-rotor predictions was that the boundary conditions for a steady stator computation to estimate the gust were difficult to specify correctly in the applied Q3D method. For a stator exit flow of good quality the blade pressure ratio and the stream tube definition are sensitive parameters, especially in the studied transonic flow. The observed difference between 3D computation and experiment was probably caused by an unknown mismatch of such boundary conditions. The results from the presented steady stator only computations showed also that the agreement to the measured gust is furthermore dependent on the axial position at which the gust is extracted. At some “intermediate” axial positions the agreement is better than very close to or far downstream of the stator trailing edge. This might not be general.

6.1.3 Gust specification

An assessment of the relevance of the observed differences in stator exit flow computation for the rotor blade excitation prediction could only be made with knowledge of the separate influence of wake, pressure wave and shock excitation. The generic study of potential and vortical excitation of the turbopump turbine ([Jöcker et al. 2001], publication 5 in the Appendix) indicated that in the type of investigated turbines the wake influence on the excitation is rather small compared to the potential excitation. This suggested that the differences in wake prediction are not so relevant, but that the differences in potential and shock strength prediction had a large influence on the excitation pressure. The excitation mechanisms are discussed further in Chapter 6.2. The same investigation demonstrated also the difficulty to define the UNSFLO input parameters for a gust computation (a description of these parameters is given in the Appendix). Neither the application of a velocity splitting according to the documentation in Wisler et al. [1993] (see Chapter 4.2) nor the extraction of the pressure amplitude from the steady computation revealed the gust input parameters, especially the potential disturbance amplitude, which gave the best agreement to the full stage computation. However, this best agreement solution, which was obtained by variation of the inlet gust amplitudes, showed the relevant rotor blade excitation pressure in the 1^{st} harmonic (no higher harmonics could be resolved with the method without knowing the higher harmonics of the excitation). The gust method was judged to give a good result of the investigated case, when the gust boundary conditions were well specified. Possibilities to obtain the unsteady gust boundary conditions are given

by good quality through flow computations, steady stage computations or experiments. For the 3D gust computation on the ADTurB stage shown in Chapter 6.1.4 a 3D viscous steady stator computation was performed with VOLSOL according to experimental boundary conditions measured in the stage, a comparison of blade surface pressure to experiments is shown in Figure 20. For reference also the Q3D stator only UNSFLO result is included. The 3D computation agrees very well with the experimental data, even though the stator test data was obtained without the rotor, whereas the computation was made with boundary conditions from a full stage measurement. The main differences of these boundary conditions to the stator only boundary conditions used for the UNSFLO computation are a slightly modified hub contour and the blade pressure ratio was by 4.2 % larger, which gave a weaker shock with better agreement to experiments.

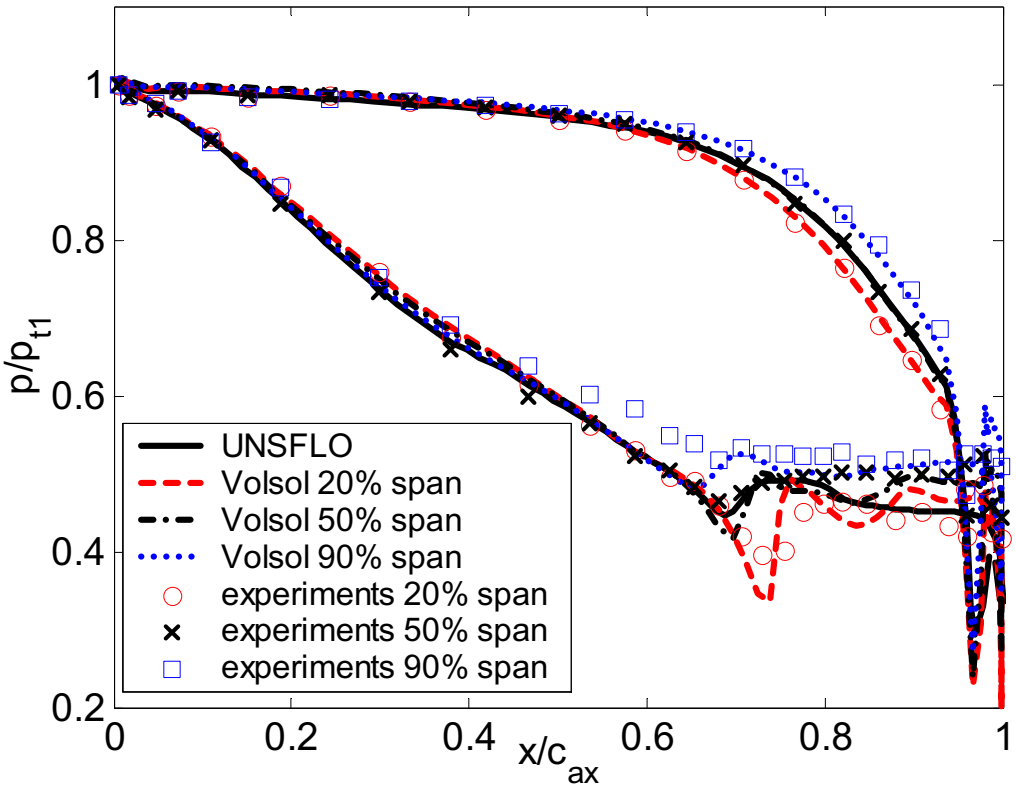

Figure 20: *3D stator only calculation (stator 1, 43 NGV) with VOLSOL for gust definition*

A comparison of the computed gust in terms of Mach number and pressure at midspan behind the stator is shown in Figure 21. The circumferential distribution of Mach number is similar to the one discussed for the 70NGV stator (publication 2 in the Appendix [Freudenreich et al. 1999]), which were also described in the above discussion of stator exit flow predictions (Chapter 6.1.2). Two deficits, one due to the wake and one due to the shock are seen, which merge at some axial distances behind the stator, because they propagate in different directions (see also Figure 32). In the pressure distribution only the flow compression over the shock is seen, the wake deficit is as expected not accompanied by a pressure deficit. Due to the modified boundary conditions the VOLSOL exit flow is now at a lower Mach number level compared to the UNSFLO result leading to a smaller pressure change over the shock. Both VOLSOL and UNSFLO give a fairly good prediction of the stator downstream Mach number distribution. A clear difference between VOLSOL and UNSFLO is seen in the pressure at about the middle of the passage exit flow, where a

pocket of increased pressure appears in the VOLSOL computation. The reason for this is not clear. Both the differences between 2D and 3D flow but also differences in the "reflectivity" of the computational exit boundaries to pressure waves could cause the deviation.

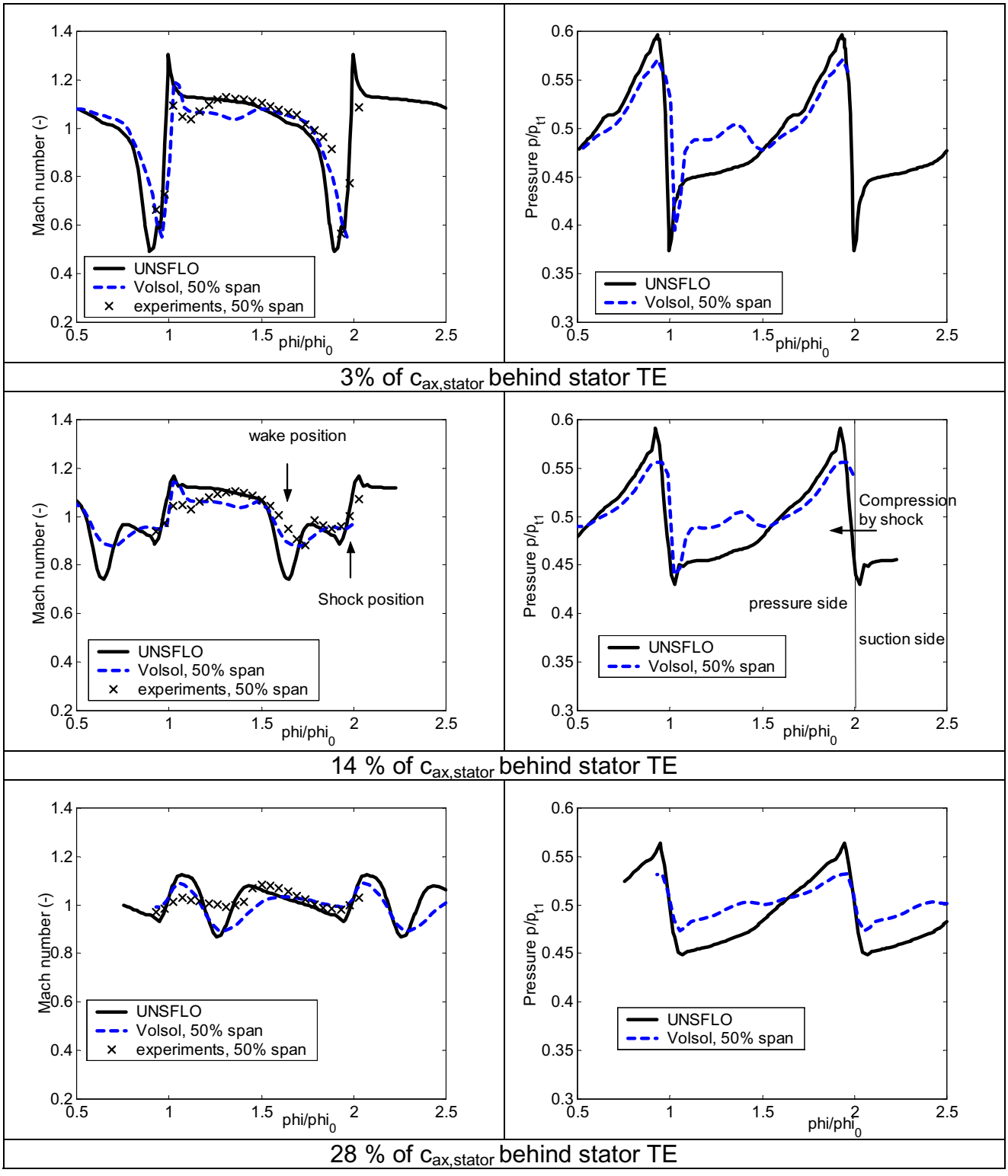

Figure 21: *Comparison of predicted and measured Mach number and predicted pressure behind stator 1 (43 NGV) at three axial positions, stator only data*

6.1.4 Excitation prediction

In this chapter various results of excitation computations in terms of blade surface pressure harmonics are discussed and compared to experimental data. Validations of this kind were published in [Jöcker et al. 2000b] (publication 3 in the Appendix), where the excitation pressures were computed with UNSFLO on a test case similar to the ADTurB case. At that time no experimental data was available for validation on the ADTurB case itself. This test case was measured at the “Von Karman Institute for Fluid Dynamics” (VKI) in Bruessels, Belgium. The test case is named here VKI test case and is described in detail by Denos et al. [1999, 2000] including numerical analyses of the unsteady flow. It differs from the ADTurB case by a geometric scaling and slightly different boundary conditions (rotational speed and blade pressure ratio). Laumert et al. [2000, 2001a, b] provided additional 3D unsteady numerical studies on the VKI case. Taking the scaling and modified boundary conditions into account the present UNSFLO stage calculation results could be compared to the published experimental and numerical work. It was found that UNSFLO predicted the unsteady flow at midspan comparably well. Similar to the numerical results by Denos and Laumert an under-prediction of the shock sweeping excitation at front part suction side was found. This was visible both in the time resolved surface pressure in this region as well as in the 1^{st} harmonic of the blade surface pressure on the complete suction side. The second harmonic amplitude agreed better to the experimental data, also the phases of both 1^{st} and 2^{nd} harmonic compared well. From this study it could already be concluded that the applied UNSFLO method gave acceptable results at midspan. Especially the unsteady pressure on the rotor was reasonably well predicted in comparison to published 3D computations and the overall pattern of the unsteady blade pressure was also in agreement to the measured ones. It was proven that the simplification of the stream tube thickness was not the reason for the under-prediction of shock strength. Also small variations of the stage back pressure (by 0.9 %) and rotational speed (by 0.5%) did not change the predicted rotor excitation.

Later, experimental data of the unsteady blade pressure of the ADTurB rotor became also available both for subsonic and transonic flow conditions. A comparison of the predicted and measured pressure amplitudes is presented in Figure 22. UNSFLO is in good agreement with the subsonic data but over-predicts the 1^{st} harmonic pressure in the transonic case with up to 75% in the leading edge peak. For the transonic case the rotor excitation pressure was also computed with SliQ, a 3D linearised gust computation method, for which the incoming gust boundary condition was specified from the 3D viscous VOLSOL computation discussed above (Chapter 6.1.3). This gust computation gave a fairly good agreement in both 1^{st} and 2^{nd} harmonic of excitation pressure.

Discussion:
The found level of agreement between measurement and prediction of unsteady blade surface pressures is not unusual for such computations. The present comparison shows that the Q3D method UNSFLO did a fairly good job in predicting the unsteady pressures for subsonic flow, in transonic flow the observed over-prediction is probably caused by the too high Mach number computation already in the stator-rotor gap (see Figure 4 in [Jöcker et al. 2000b], publication 3 in the Appendix). The reason for this difference between the UNSFLO computation and experiments could be a mismatch in boundary conditions

induced by the stream tube definition as also discussed in Chapter 6.1.2 for the stator exit flow prediction.

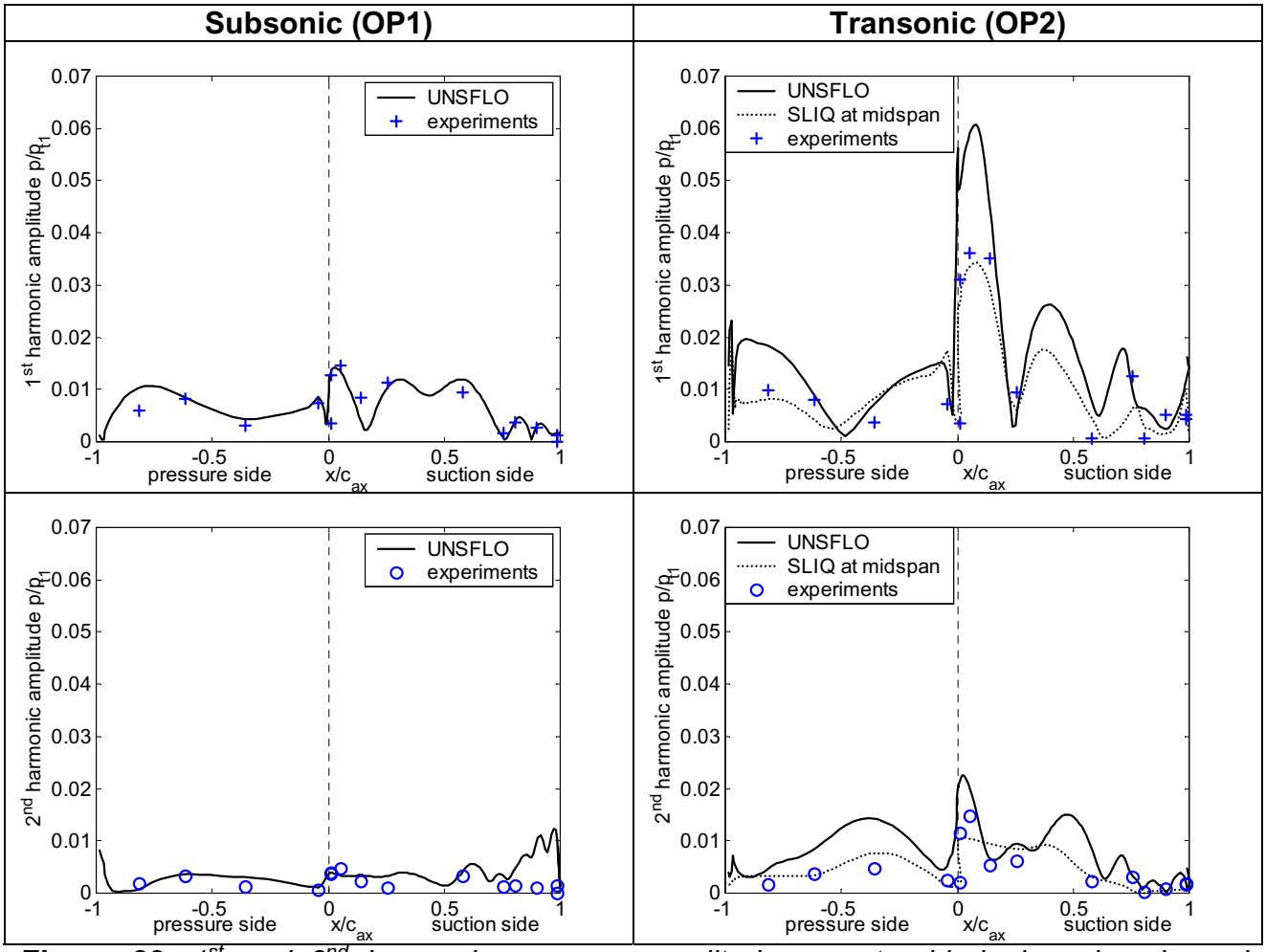

Figure 22: *1st and 2nd harmonic pressure amplitude on rotor blade in subsonic and transonic flow, comparisons to experiments*

In the present case of a choked rotor this mismatch could not be corrected with an adapted rotor outlet pressure. It is most probably the Q3D specification of stream tube expansion, which did not allow the correct stator outlet prediction in the stage. However, a modification of the stream tube definition without a physical basis seemed not to be legitimate for the validation of prediction methods and hence no further studies than to specify the geometrically correct stream tube were performed. This did not remove the mismatch though. The effect of Mach number over-prediction in the gap on the unsteady blade surface pressure reduces at lower stator exit Mach numbers, because the shock excitation disappears. This explains why the over-prediction was less significant in the subsonic case.

The application of the 3D linearised gust method SliQ gave a much better agreement to the measured blade surface pressures. A necessity to obtain this good agreement was of course a reasonable specification of the inlet gust, which is discussed above (Chapter 6.1.3). This gust was for validation reasons obtained with a steady stator computation based on the experimental unsteady time averaged stage conditions in the gap. It is remarkable that also the 2nd harmonic pressure excitation (computed with the 2nd harmonic

of the inlet gust) was predicted well in magnitude, even though the gust computation could not regard any pressure wave reflected back from the stator row. It is concluded that the present 3D linearised gust method can give a good representation of the blade excitation pressure at least at midspan. This depends strongly on the quality of the gust specification, which is assumed to be close to the test conditions, because the boundary conditions were extracted from the unsteady test result itself.

The difference between UNSFLO and SliQ at midspan can not be explained with the presence of 3D flow effects like secondary flows and strong radial flow components. If 3D effects would cause the over-prediction by UNSFLO it could hardly be explained that in the validation against the VKI turbine this code as well as other Q3D and 3D codes under-predicted the rotor excitation. Also here a mismatch in boundary conditions is more likely.

A critical assessment of the above comparison must also point out eventual mismatches in experimental boundary conditions.

- It is possible, even though not experimentally confirmed, that leakage flows in the test rig modified slightly the boundary conditions, especially the Mach number in the stator-rotor gap.

- It has also been found that the axial gap varied during test rig operation due to thermal stresses in the hardware. Even though this was detected early and compensated for in the presented comparisons it introduces a small uncertainty.

- Blade vibrations could have modified the unsteady pressures on the rotor, however the presented unsteady pressure data were measured at computed resonance conditions, which differed from the real resonance conditions and it is confirmed that the blades did not vibrate during the measurement of the data in Figure 22 [Hennings 2002b].

- To model the flow in the turbine stage needs usually some degree of idealisation of the geometry. In the present computations all stator vanes are assumed to be identical as well as all rotor blades, which is normally not the case in reality. It has been found during the ADTurB measurement campaign that the vanes are not perfectly identical, which introduced vane to vane variations in the gust. These can introduce low engine order excitations, which can modify the excitation pressures on individual rotor blades, especially lower harmonics of excitation due to the low engine order might be present. The appearance of lower harmonics in the excitation might reduce the vane passing frequency excitation compared to a perfectly periodic vane excitation. The existence of low engine order excitations during the test is illustrated and discussed in [Hennings et al. 2002].

For the remainder of the present study the above results are most important to show that the Q3D method UNSFLO predicted the excitation effects in terms of blade surface pressure harmonics both compared to experiments and to the 3D calculation with SliQ. The UNSFLO over-prediction of the excitation will not be relevant for the further study, where the effects will be compared relatively due to parameter variations.

6.1.5 Off-Design computations and the role of the available turbulence models in UNSFLO

Low speed case OP5 and OP6:
Some resonance conditions investigated in the ADTurB stage were at off-design with relatively low rotational speeds (see Campbell diagram, Figure 15). As discussed in [Jöcker et al. 2000b] (publication 3 in the Appendix) these cases showed separations predicted with UNSFLO, which were triggered by the unsteady flow on the rotor suction side. Furthermore, they only appeared when the herein usually applied one-equation turbulence model [Birch 1987] was used. The separations were suppressed when the algebraic turbulence model [Cebeci and Smith 1974] was used. Even though separations are likely to occur in these cases due to the high flow incidence, it is doubtful that the predicted unsteady pressures are correct regarding the capability of the numerical method. Viscous terms are only regarded within the O-mesh layer around the blade and the separations partly extend this region. The induced pressure unsteadiness on the blade surface was very large both in magnitude and in harmonic content. If such conditions were likely to occur in engines it would be important to assess the predictive possibilities of such phenomena and validate it against experimental data. That was beyond the frame of this work, mainly because of the lack of experimental evidence.

Subsonic cases OP1, OP5, OP9:
All subsonic cases showed separations on the blade surface, which were triggered by the unsteady flow. In difference to the low speed cases OP5 and OP6, where these separations extended over the major part of the blades with relatively large separation bubbles, they were local and small at the higher rotational speeds. Furthermore, both the one-equation turbulence model and the algebraic turbulence model, predicted the separations on the subsonic cases. These subsonic cases were included in the discussions in this thesis where useful, because the influence of the separations on the main excitation of the rotor blade was regarded as small and the numerical solution as partly useful. However, the separation influenced the time averaged flow field and these results are regarded with care.

6.1.6 Blade vibration computations

From the work published in Fransson et al. [1999] (publication 1 in the Appendix) it was concluded that the quality of the presented 2D and Q3D predictions had to be improved, especially for viscous investigations. The applied codes ranging from potential, via inviscid linear and non-linear codes to non-linear fully viscous codes could at the most predict the trends of unsteady blade pressures in the case of transonic off design flow. The separation bubble in the off-design case and its influence on the unsteady blade pressure were only indicated by the fully viscous method. For the aerodynamic damping however the separation had a negligible influence, because the pressure phase induced by the separation bubble disturbance is nearly 180° so that no work is done by the flow on the vibrating blade.

The test case has been used to verify the prediction quality by UNSFLO. The blade motion during a computation is realised in UNSFLO by deformation of the mesh in the O-mesh surrounding the blade. This required that the motion amplitude was small enough and the

mesh resolution perpendicular to the blade surface was large enough so that the deformation was geometrically possible. All UNSFLO blade vibration computations had to be performed with the Cebeci-Smith turbulence model, transition was specified at the leading edge, the application of the one-equation turbulence model introduced non-physical unsteady flow separations from the blade surface, which destroyed the solution. Strong dependency of the unsteady blade surface pressure on mesh resolution was found for the ADTurB case (torsion motion) both in subsonic and transonic flow. The validation against measured data on STCF 11 (bending motion, subsonic and transonic) did not show this mesh dependency of the unsteady result, when a sufficient temporal resolution (iterations per period) was chosen. Even more uncertainty into the solution quality was introduced by the dependency of the computed unsteady UNSFLO result on the chosen number of iterations.

Figure 23 shows the comparison of predicted pressure coefficient to the measured data with different numbers of iteration per period and different numbers of calculated periods. For reference also the VOLFAP result (non-linear, fully viscous computation) from Fransson et al. [1999] (publication 1 in the Appendix) is included. The chosen case is the off-design condition with a separation bubble at the front part of the suction side and a weak shock impingement on the suction side at about 75% of true chord.

The UNSFLO solution did not change significantly when calculating 20 instead of 10 periods of blade vibration, hence the solutions were judged to be converged. The details of unsteady pressure distribution changed significantly with a smaller time step in the computation. The comparison to the experiments indicated that the solution improved with decreased time step. A reason for that behaviour has not been found and it put some uncertainty on the predicted results. The comparison showed also that UNSFLO predicted the excitation trends due to the separation bubble. But the shock influence at the aft part of the suction side was only seen in the computation with higher temporal resolution.

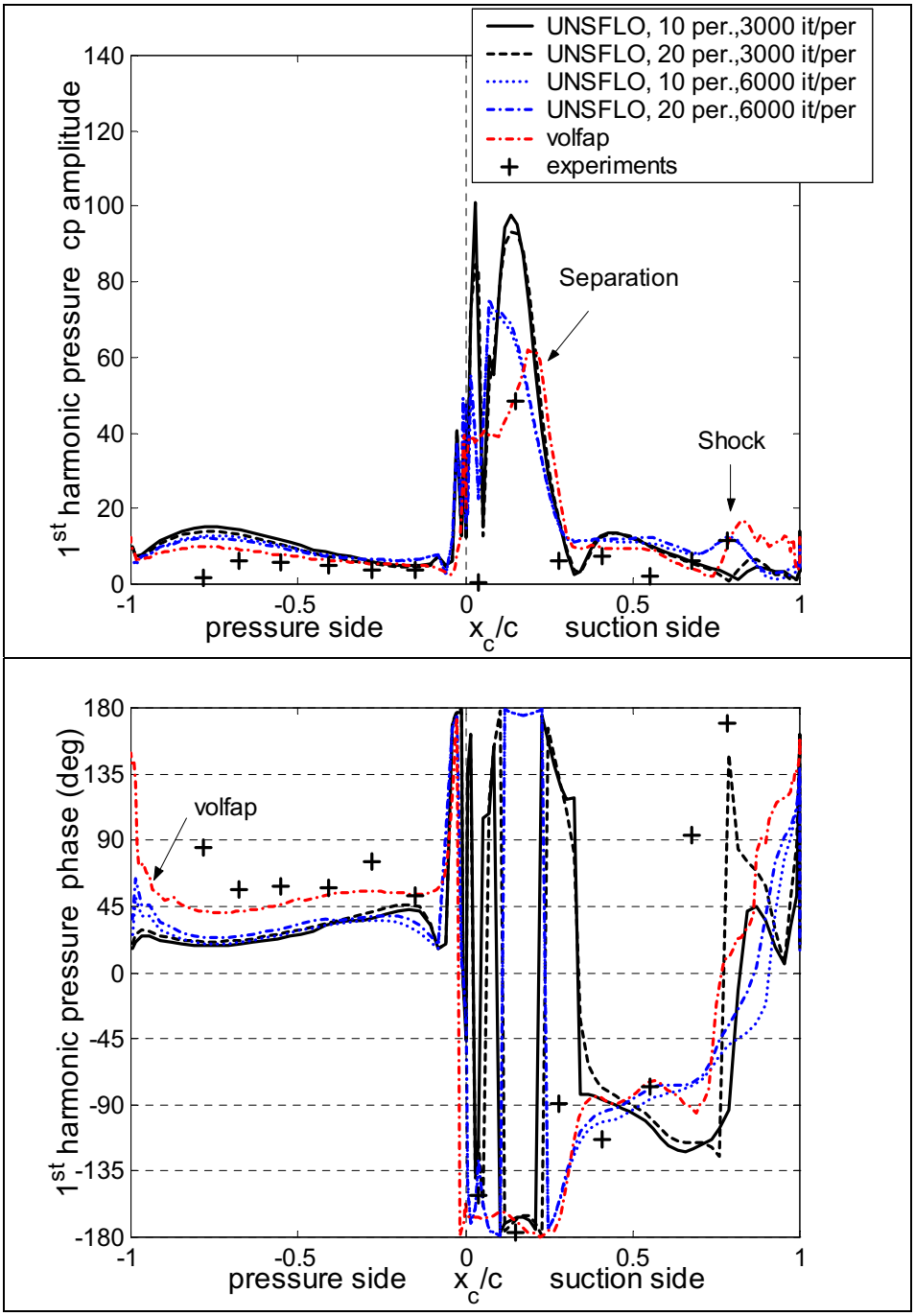

Figure 23: *STCF 11, transonic case, comparison to experiments and volfap*

6.2 Excitation mechanisms

To understand the aerodynamic excitation mechanisms of the rotor blades in the investigated turbine stages the time-resolved study of the flow field and the blade surface pressure is necessary. The main questions are: What are the principle mechanisms observed in the turbines? Can any of the observations be generalised? How relevant are operating conditions and (2D) geometry? The latter question will be more deeply considered in Chapter 6.3, where the parameter studies are discussed. The present chapter focuses on the description of the principally known excitation mechanisms in a high pressure turbine stage, which are due to wake excitation, potential excitation and shock excitation. This is partly supported by the thorough analysis of the unsteady flow in a high pressure turbine stage presented in the work by Laumert et al. [2001a] and the experimental analysis of shock propagation in a linear cascade by Johnson et al. [1989].

In [Freudenreich et al. 2001a], publication 4 in the Appendix, the 1st harmonic excitation peaks of the ADTurB transonic case OP2 (see Figure 22) are discussed by comparison to the time-space presentation of the unsteady blade surface pressures. An attempt has been made to relate the computed blade surface pressure variations to measured Mach number variations in the gust and rotor passage flow field, even though the experiments and the UNSFLO computations were performed at slightly different operating conditions as discussed in the validation part of this thesis (Chapter 6.1.4). This difference caused a stronger stator trailing edge shock in the computations, which enforced the shock and potential excitation effects. A comparison of measured and computed time resolved velocity at distinct positions close to the rotor blade surface demonstrated main differences close to the rotor leading edge, where the stator trailing edge shock has its main influence. The measured flow perturbations in terms of Mach number have been shown to relate in space and time to computed pressure perturbations on the rotor blade surface, so that a positive Mach number perturbation is accompanied with a negative perturbation pressure and vice versa (see also Figure 25). This indicates that the measured and computed unsteady flow field are still comparable in their development. The Mach number however does not allow a conclusion on the excitation mechanism, as both wakes, pressure waves and shocks induce Mach number variations, an identification of the excitation mechanisms needs to track pressure variations regarding their origin and propagation as discussed in the following subchapters.

The study of the turbopump turbine (Chapter 5.2) supported the analysis of excitation mechanisms, as it provided a test case with different geometry and without a shock excitation source. Detailed discussion of this case is published in [Jöcker et al. 2001] (publication 5 in the Appendix) and the findings on excitation mechanisms are included in the descriptions below (Chapters 6.2.2 and 6.2.3).

6.2.1 Excitation due to stator trailing edge shock

The rotor excitation in the ADTurB transonic case (OP2) is characterised by the dominant shock influence. Figure 24 shows to the right the time space representation of the surface perturbation pressure. The shock, which is emanating from the stator trailing edge impinges on the rotor crown at a time t/T_{rotor} =0.8, which is accompanied with a steep

perturbation pressure gradient due to the flow compression over the shock (see arrow in Figure 25 to the right, where the shock is impinging on blade 3).

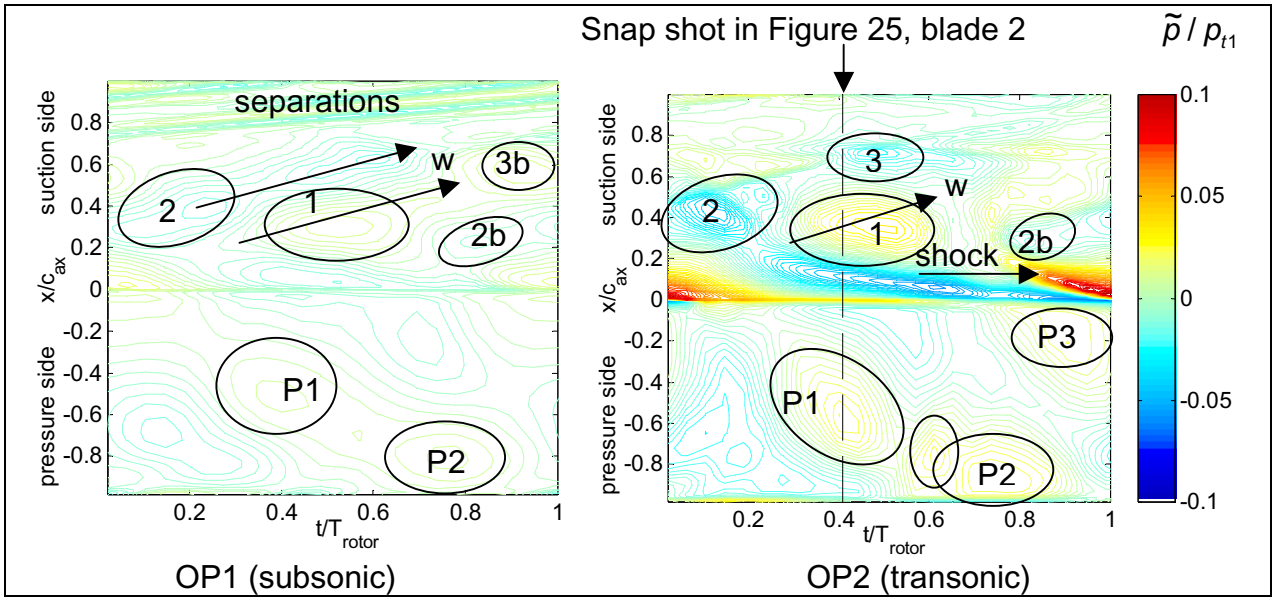

Figure 24: *Time-space plots of computed unsteady blade surface pressures, subsonic and transonic ADTurB case (OP1 and OP2), large axial gap*

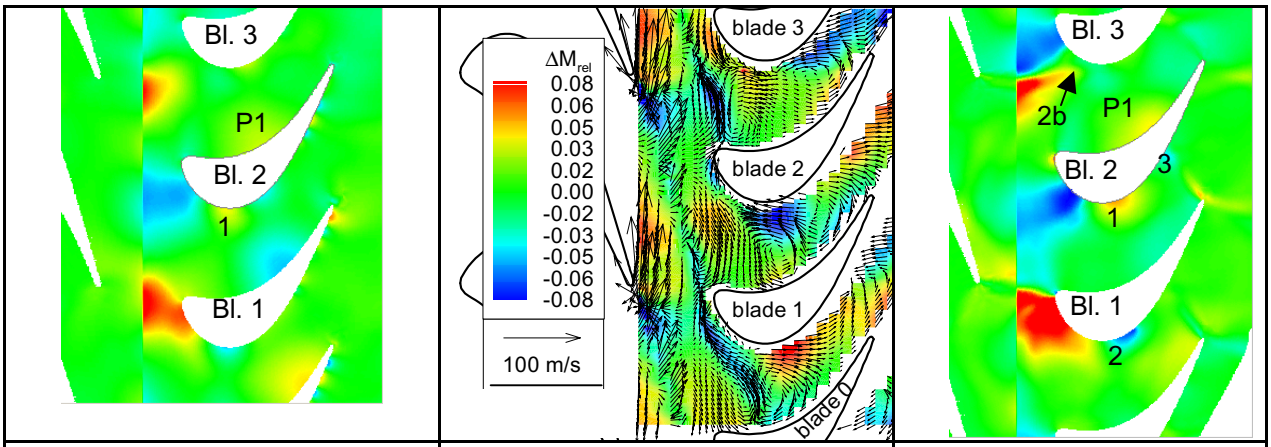

Figure 25: *Snap shot of unsteady flow field and blade surface pressure at t/T_{rotor} =0.41*

This attachment of the shock wave to the blade is usually followed by a shock wave reflection towards the pressure side of the neighbouring blade. This reflection results in the peak P2 on the aft part of the pressure side. The peak P2 is also caused by the potential excitation due to the passing stator (discussed below with potential excitations), therefore, two events are marked with the label P2 in Figure 24, the earlier event related to the shock wave reflection. The pressure gradient induced by the shock sweeps over the blade surface towards the leading edge of the blade and passing it, where it then detaches from the surface. This detachment is, in accordance to published shock wave analyses,

accompanied with a bowed wave reflection travelling upstream towards the stator and the shock end towards the pressure surface of the blade below, where it causes a peak in excitation, labelled P3 in Figure 24. The comparison to literature suggests that the principle mechanism is that both the attachment and the detachment of the shock triggers pressure waves to emanate from these locations, which then travel while being distorted, reflected and diminishing. The strength of these waves and their live time must depend on the strength of the shock. The blade geometry and the mean rotor flow field control the attachment and detachment points and the wave propagation. The pressure gradient of the shock itself causes a strong perturbation while sweeping over the leading edge region, its strength directly related to the pressure gradient over the shock.

6.2.2 Potential excitation

A comparison of the perturbation pressures of the transonic case ($M_{2,stator}$=0.94) to the subsonic case ($M_{2,stator}$=0.81), in Figure 24 to the left, illustrates the large difference in excitation magnitude induced by the shock. Searching for common excitations in both cases possible wake and potential excitations become evident. In the subsonic case the excitation of the rotor leading edge region is also observed but much smaller than the shock induced excitation of the transonic case. Whereas shock induced unsteady pressure peaks in the magnitude ±10% of total inlet pressure were found potentially induced pressure maxima in the leading edge region were typically about ± 3% of total inlet pressure p_{t1}, exceptions are the extremely small gap cases in the turbopump turbine, where a pressure amplitude of about ±9% of p_{t1} were observed. Both the subsonic and transonic case shows the peaks 1,2 and 3 on suction side and the peaks P1 and P2 on pressure side induced by the potential field of the stator, which is cut through by the rotor. The peaks P1, 1 and 3 can be seen in the flow field snap shot of Figure 25, right side (transonic case) on the surface of blade 2. At this time the passage between blade 1 and 2 is approximately between two vanes and the potential stator field has a strong negative pressure influence on the leading edge region of blade 1, which is reflected to also affect the whole pressure side of blade 2. But the rotor has already moved so far that the positive pressure disturbance associated with stator trailing edge of the NGV below reached the rotor blade 2 on suction side initiating peak 1. The very local peak 3 seems to be associated with variations in the rotor passage shock in the throat emanating from the neighbouring blade's trailing edge. This variation is not present in the subsonic case as there is no rotor passage shock.

When the rotor is turning further the positive peak 1 will change to the negative peaks 2b and then 2. On the blade crown, the negative pressure wave 2b appears (see also on Figure 25, blade 3). It diminishes after the shock has attached to the blade and grows again to form peak 2, slightly downstream of the peak 2b location. This is similar in the subsonic case. Whereas the peak 2b is still related to the negative pressure wave sweeping over the same blade's suction side the peak 2 is already induced by the appearance of the negative pressure field of the following NGV. The appearance of this pattern is important because it will have an influence when the axial gap is varied (discussed in Chapter 6.3.2).

On pressure side peak P1 attaches to the blade surface when the positive potential wave passes into the passage. This excitation peak is then travelling downstream while the potential wave approaches the blade above (blade 3 in Figure 25). This excitation is much

weaker in the subsonic case, but still visible. Hence, this is not a purely shock induced phenomenon but also formed by potential wave propagation. The formation of peak P2 on pressure side is different in the subsonic and transonic case due to the involvement of the shocks in the latter one. As explained above this peak is partly due to a pressure wave triggered by the attachment of the stator shock to the rotor blade, which is of course not present in the subsonic case. Furthermore, the passage shock in the rotor seems to modify a wave reflection pattern seen in the subsonic case, where the peak P2 is related to a pressure wave reflection originating from peak 3b on the above suction side. This positive pressure region is also seen in the transonic case just in front of the passage shock and may also participate in the formation of peak P2 on pressure side. In this area it is not possible to make more clear statements on the excitation mechanisms based on the present results, because too many different effects are involved. For further analysis it will be important to see the relative differences in the observed mechanisms related to the parametric variations.

The analysis of the potential excitation mechanisms in the turbopump turbine ([Jöcker et al. 2001], publication 5 in the Appendix) has shown a partly comparable behaviour as observed in the ADTurB stage. Also the excitation level at nominal gap is comparable to the subsonic ADTurB case. The main excitation is associated with the rotor leading edge passing the trailing edges of the stator inducing the large pressure variations on the leading edge region. Also other peaks of excitation distribute similar to the presented ADTurB cases above when relating the time-space resolution of the blade surface unsteady pressures (shown in [Jöcker et al. 2001], publication 5 in the Appendix). When comparing the timely propagation of the unsteady pressure waves it seems that in the turbopump turbine waves are more reflected between pressure and suction side than it appears in the ADTurB cases. This might be due to the relative higher solidity and the specific camber of the blades so that the pressure waves do reflect more often between pressure and suction side before leaving the passage. Figure 26 shows instantaneous plots of the unsteady perturbation pressures at two successive time steps illustrating such a reflection (see arrows).

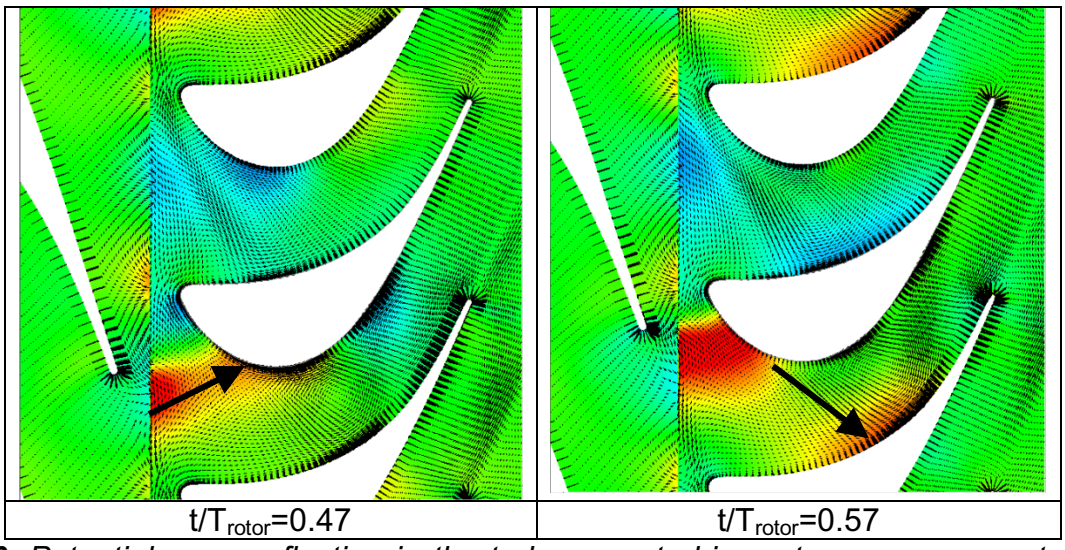

***Figure 26**: Potential wave reflection in the turbopump turbine rotor passage, contours of perturbation pressures and perturbation velocity vectors at two successive times, scale on pressure magnified with factor 5 compared to Figure 24*

The difference in behaviour has the major influence on the exact timing when the pressure peaks appear on the blade surface. It is also obvious from the comparison of the two turbines that the areas affected by the pressure waves are different. The turbopump turbine rotor excitation is characterised by the reflected pressure wave hitting nearly the complete pressure side as indicated in Figure 26 on the right side, whereas the ADTurB turbine shows a more local excitation wave (P1) on pressure side directly induced by the passing stator trailing edge. Reasons for that might be the steady pressure distribution on the rotor blade and the incidence angle of the rotor inlet flow. As discussed in Chapter 6.3.1, where differences due to the operating point are pointed out, these parameters have a significant influence on the wave propagation in the rotor passage.

6.2.3 Wake excitation

The unsteadiness introduced by the wake has generally a large influence on the velocity field, as for example measured in the ADTurB stage by Freudenreich [2001b]. The two counter rotating vortices, which are built due to the cutting of the low momentum flow in the wake by the rotor leading edge is clearly present in measurements and computations. The relative changes in Mach number are also partly seen in variations of static pressure in the flow field. However, the influence of the wake on the unsteady pressure on the rotor blade surface is relative small in the investigated cases, especially when the flow is transonic. The snapshot in Figure 25 is taken at a time, when the wake is expected to have a strong influence on the rotor unsteady pressure, this is when the left turning vortices are attached to the rotor suction side shortly downstream the crown. It is related to a relative strong local velocity deficit, which has been measured and also predicted. Both the wake and the potential field, which induces a relative pressure peak at this time and place, cause this deficit. The peak is seen in the perturbation pressure plot and an indication that it is not due to the wake is given by its short and local appearance, as viewed in the time-space plot (Figure 24). A comparison to the subsonic case OP1 on the left side of Figure 24 shows more clearly the wake influence, its convective character indicated by two arrows (one for the positive pressure change upstream of the wake and a negative pressure change downstream of the wake, see [Chernobrovkin et al. 1999] for the exact description of the mechanism). This is still overlaid by the potential pressure wave indicated here with 1. More confidence in this interpretation of the unsteady pressures was obtained in the study of the turbopump turbine, which demonstrated a similar phenomenon that the wake and potential excitation at the blade suction side crown appear simultaneously. A parametric variation of potential and vortical disturbance strength at the rotor inlet (defined according to Chapter 4.2) led to the same conclusion that the wake influence on the unsteady pressure is very small and local even in that turbine (see also Figure 37). This is discussed in detail in [Jöcker et al. 2001], publication 5 in the Appendix. Figure 26 shows on the left side the situation at which the potential excitation due to the stator overlays the wake excitation influence (middle rotor blade).

A phenomenon seen in the subsonic case OP1 is the appearance of separations on suction side in the trailing edge region (see Figure 24, left side). Due to the larger rotor outlet pressure compared to the transonic case the flow is more sensitive to separations, which are in this case triggered by the unsteady flow, they do not appear in the steady flow solution. The predicted separations induce unsteady pressure variations on the rotor surface of relatively high amplitude and frequency. Due to the lack of confidence these perturbations cannot be further discussed. As pointed out in the validation part it is

doubtful that the numerical methods applied can resolve such phenomena, neither exist experimental evidence of these separations presently. But they are such local and small that in the present case the unsteady pressures solution on other parts on the blades are regarded as useful.

6.2.4 Summary of excitation mechanisms

The excitation mechanisms due to shock, potential waves and wakes have been described at the nominal operating conditions of the investigated turbines. The differences between subsonic and transonic cases pointed out the strength of shock excitation. The shock excitation mechanism was shown to be comparable to other published analyses. Potential excitations have been shown for the two investigated turbines and it was elaborated that the typical wave type excitation is similar, but that differences in the propagation direction of the waves and the wave reflection pattern in the rotor passage lead to differences in the time and space resolved unsteady pressures on the blade surface. The wake influence on the unsteady pressure on the rotor blade was small in the investigated cases. This was explicitly demonstrated on the turbopump turbine, for which wake and potential excitations were varied separately to study their relative excitation influence.

6.3 Parametric studies

6.3.1 Operating point and rotational speed

Figure 27 gives an overview of the computed cases corresponding to theoretical resonance conditions of the ADTurB turbine stages (see Table 2) and additional computations. The calculated unsteady 1st harmonic force magnitude f is shown versus rotational speed. This magnitude gives a first glance of the variation of the forcing function with operating condition. But due to the disregard of phase differences between axial and tangential forces it does not fully reflect the forcing function magnitude. It rather overlays the forcing functions of two special mode shape excitations, a tangential mode and an axial mode excitation. Before the discussion of the changes in excitation mechanism with rotational speed variation, some characteristics of the operating points are presented based on the work in Jöcker et al. [2000b], publication 3 in the Appendix.

Low speed cases
The low rotational speed cases (50% and 61% of rotational speed, 1T crossings due to the 70 NGV stator) gave predicted separations on the rotor suction side due to the large incidence flow. The strong flow acceleration around the leading edge gave also very high local Mach numbers in the rotor passage. A comparison of blade surface isentropic Mach number is shown in Figure 28, where OP6s is characteristic for the low speed cases. The predicted separations are triggered by the unsteady flow (they are not present in steady flow solutions) and induce pressure fluctuations on the rotor suction surface of high amplitude and frequency, but with only little influence on the 1st harmonic force magnitude as seen in Figure 27. As discussed in the validation part the prediction of separations at these operating conditions may be physically sound, but the result of unsteady blade pressures given by the code are questionable and not validated. These operating conditions are not further discussed here.

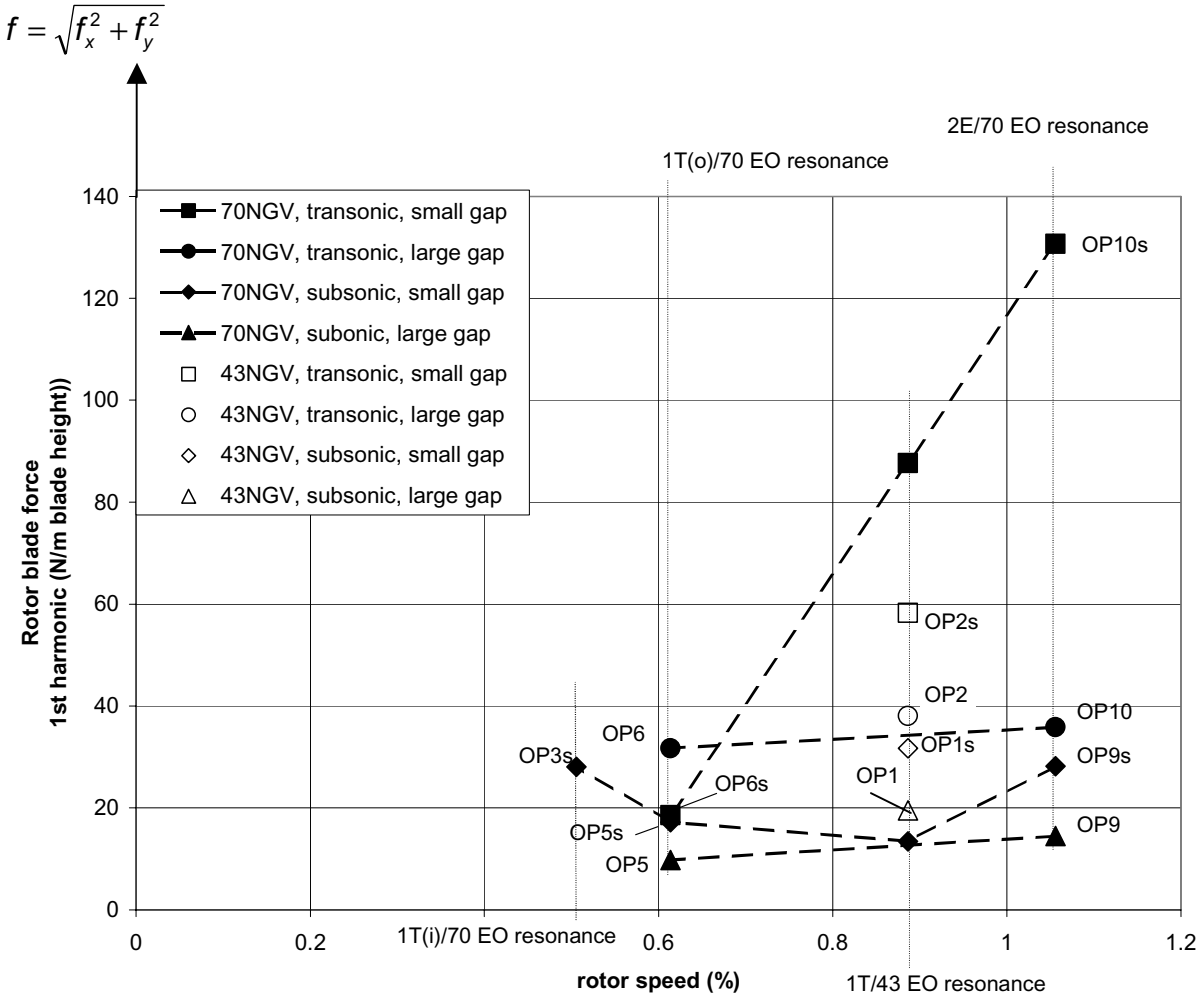

Figure 27: *Calculated operating conditions (OP) of ADTurB configuration and variation of computed 1st harmonic rotor blade force (Campbell Diagram, see Figure 15), s: small axial gap*

43 NGV resonance speed

The only resonance condition due to the 43 NGV stator is at about 88% rotational speed. These cases are discussed in detail both regarding the axial gap influence (Chapter 6.3.2) and the stator influence (Chapter 6.3.3). The axial gap influence on the force magnitude in Figure 27 is as expected in all investigated cases, that the smaller axial gap leads to higher force magnitude. To analyse the stator influence on the excitation two “academic“ cases not corresponding to a resonance condition were computed, which are the excitations due to the 70 NGV stator at this rotational speed. Unfortunately, the two stators do not provide exactly the same steady pressure distribution on the rotor due to the specific design of stator 2. Small differences in the isentropic Mach number distribution are seen on the rotor suction side in Figure 28. This will make it difficult to completely isolate the stator influence on the excitation. Therefore, differences due to stator design are mainly discussed on the turbopump turbine (in Chapter 6.3.3), for which geometrically scaled stators resulted in similar steady and time averaged blade surface pressures on both stator and rotor.

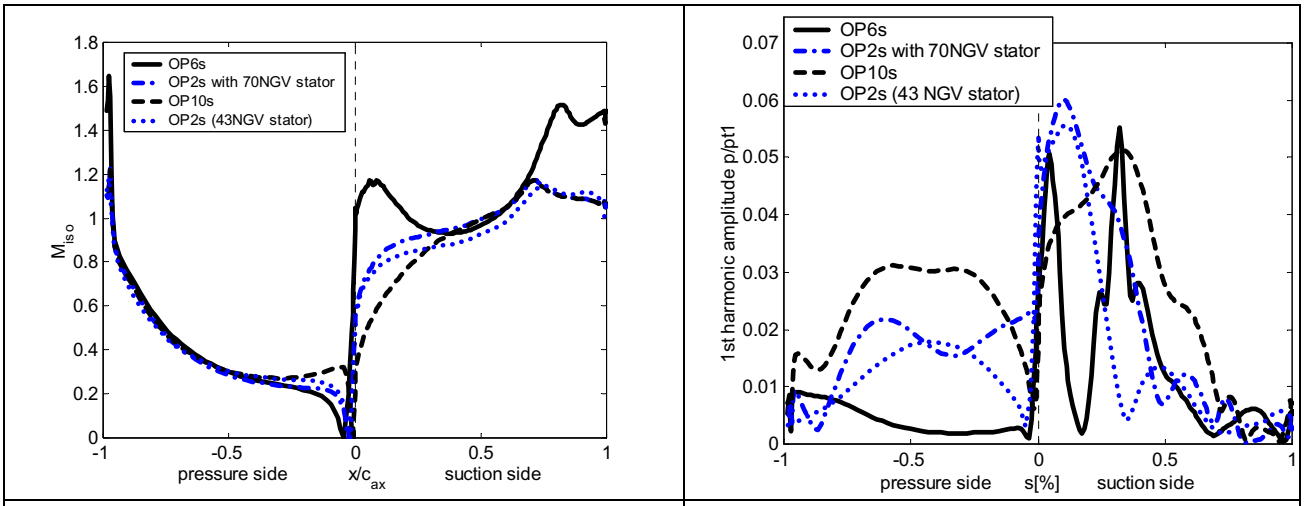

Steady rotor blade isentropic Mach number | Unsteady rotor blade pressure

Figure 28: *Comparison of operating conditions and unsteady rotor blade pressure, transonic cases with small axial gap*

High speed cases

At the high rotational speed of about 105% of design speed the incidence is significantly reduced (the relative flow angle is more axial) leading to a different steady load on the rotor, mainly the suction side leading edge region is affected (see Figure 28, where OP10s represents the high speed cases OP9 and OP10). Obviously, this has a large impact on the excitation forces, most dramatically for the small gap transonic case, and the modification of excitation mechanism due to the high rotational speed is discussed below.

Discussion

It follows a discussion of the influence of the rotational speed on the excitation mechanism by direct comparison of the case OP10 (105% rotor speed, transonic) to the corresponding transonic (academic) case at 88% rotational speed (OP2s-70NGV). Time space plots of the unsteady rotor surface pressures of these cases are compared in Figure 29. The left side shows the OP2 case, which has the same stage pressure ratio and rotor speed as the original OP2, but with the 70 NGV stator instead of the 43 NGV stator. The excitation peaks due to the 70 NGV stator are related to the excitation peaks observed in the study of the 43 NGV excitation in Chapter 6.3.3, where the influence of stator count is discussed.

At high rotational speed the excitation pattern changes drastically. Obviously, the rotor experiences at the higher rotational speed (right side of Figure 29) a strong excitation due to potential excitation, which is emerging further into the rotor passage than at lower rotational speed. The identified peaks 1 and 2 on suction side are not as distinguished from the shock excitation anymore. Instead, potential excitation and shock excitation appear as a continuous process in the time space plot. The situation when the potential excitation hits the rotor suction side is indicated in the snap shot in Figure 30 with an arrow. Also in the subsonic case at high rotational speed (OP9, 105% rotor speed) it has been observed that the potential excitation reaches longer into the rotor passage than at lower rotational speed, but of course the excitation level is much lower according to the discussion of excitation mechanisms above (Chapter 6.2).

The shock reaches also further into the passage before hitting the suction side of the blade. This effect cannot be due to the stator trailing edge shock strength, because the averaged stator exit Mach number is even slightly reduced compared to the OP2 conditions. Furthermore, the magnitude of unsteady pressures is lower than in the case of OP2.

On the pressure side the peaks P1, P2 and P3 are not evident anymore at high rotational speed, they merged into one large excitation region extending over the whole blade length.

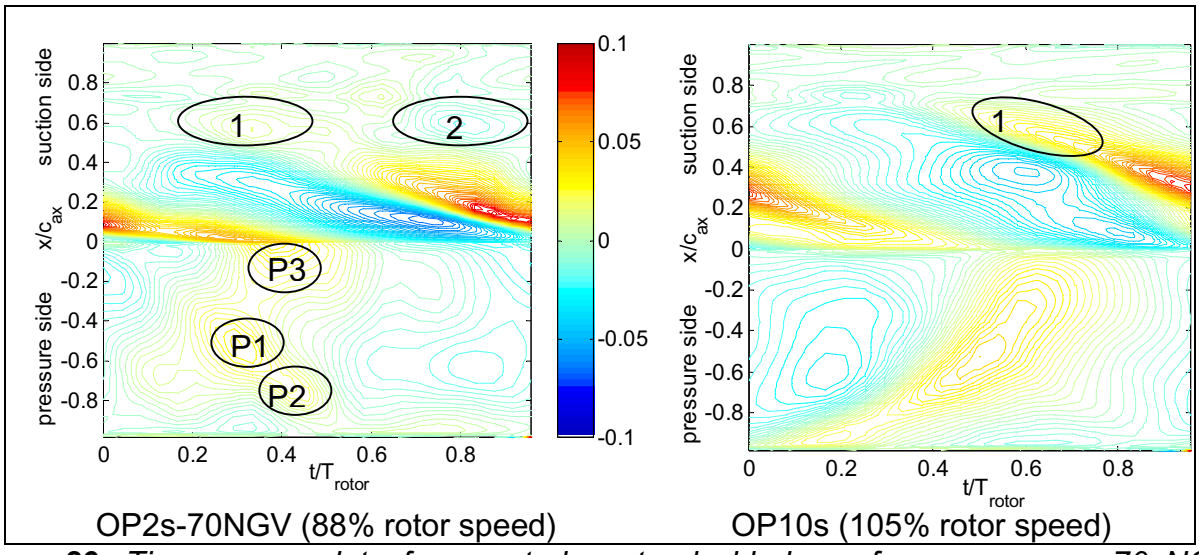

Figure 29: *Time space plot of computed unsteady blade surface pressures, 70 NGV excitation, transonic cases with small axial gap at different rotor speeds*

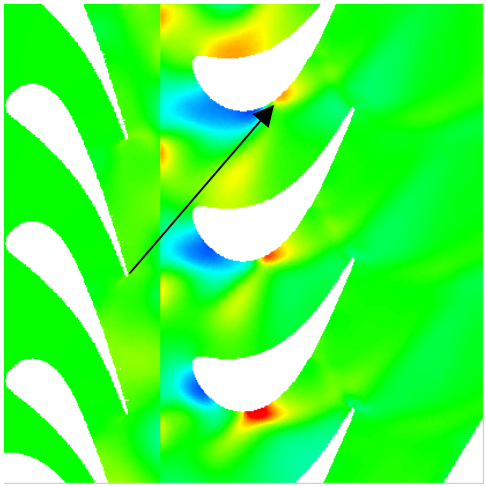

Figure 30: *Snap shot of unsteady flow field and blade surface pressure, case OP10s*

Possible reasons for the different propagation of the shock and potential disturbance are the lower incidence angle as well as the completely different rotor blade load (left side of Figure 28), which gives a different receptiveness of the rotor for the unsteady disturbances emerging from the stator. A key parameter might also be the reduced frequency of excitation, which becomes relatively high (about 5, compared to about 2 for the 43 NGV cases), but a clear relation between reduced frequency and excitation mechanism can not be derived from these two chosen cases. The positive-negative pattern observed in the

temporal appearance of pressure peaks on the blades promotes the excitation by the 1st harmonic. Furthermore, the impact of the pressure waves on the major part of the blade at high rotational speed leads to pronounced 1st harmonic axial and tangential forces as shown and discussed in publication 3 in the Appendix ([Jöcker et al. 2000b]). These forces become also strong because the pressure variations on pressure and suction side are in opposite phase, i.e. a positive pressure perturbation on suction side is accompanied by a negative one in pressure side and vice versa. It explains the large level of 1st harmonic force magnitude of these cases (OP9, OP10) in Figure 27, which is obviously not due to a higher excitation pressure level but only due to the large content of excitation energy in the 1st harmonic over major parts of the blade surface and the specific phase relations of suction and pressure side excitations.

From the operating point analysis it is concluded that excitation mechanisms change drastically with change of operating conditions. Main reasons could be the changed time averaged pressure on the rotor blade surface, which leads to a different receptiveness for the shock and potential excitation waves, and the changes in flow incidence, which could also modify the propagation of these waves. At low speed the unsteady flow is dominated by flow separations from the rotor bade surface. The study demonstrated also how variations in the time and space distribution of the pressure disturbances on the blade modify the harmonic content of blade forces, such that the blade force analysis and blade pressure analysis may not indicate the same trends regarding the level of excitation.

6.3.2 Axial gap

The following effects were observed with variation of axial gap, which contradicted the expected trend that the excitation decreases with increased axial gap:

ADTurB stage:
In the transonic ADTurB case all 1st harmonic pressure peaks inclusive the leading edge excitation peak do not follow the trend to decrease with increased axial gap. Still, axial and tangential forces behave as expected and decrease with increased axial gap (Figure 27). This is outlined in [Jöcker et al. 2000b], publication 3 in the Appendix. The study has been extended with intermediate gap cases, the 1st harmonic unsteady blade surface pressure amplitudes of these cases are compared in Figure 31. A critical discussion follows below.

Turbopump stage:
The high interaction at small gaps in the turbopump turbine led to decreased 1st harmonic force excitations compared to the larger axial gap cases. The decrease is caused by the increased unsteadiness in the gap due to enforcement of the potential excitation, which gives more contributions to higher harmonics and reduces the 1st harmonic content. This is discussed in Jöcker et al. [2001], publication 5 in the Appendix.

Discussion:
It follows a discussion on the influence of the axial gap on the blade surface perturbation pressures on the rotor with regard to the unsteady pressure flow field. The time averaged flow field did not change with axial gap in the investigated cases. First, the ADTurB stage is examined with focus on the transonic case. Then, similarities and differences to the turbopump stage are pointed out.

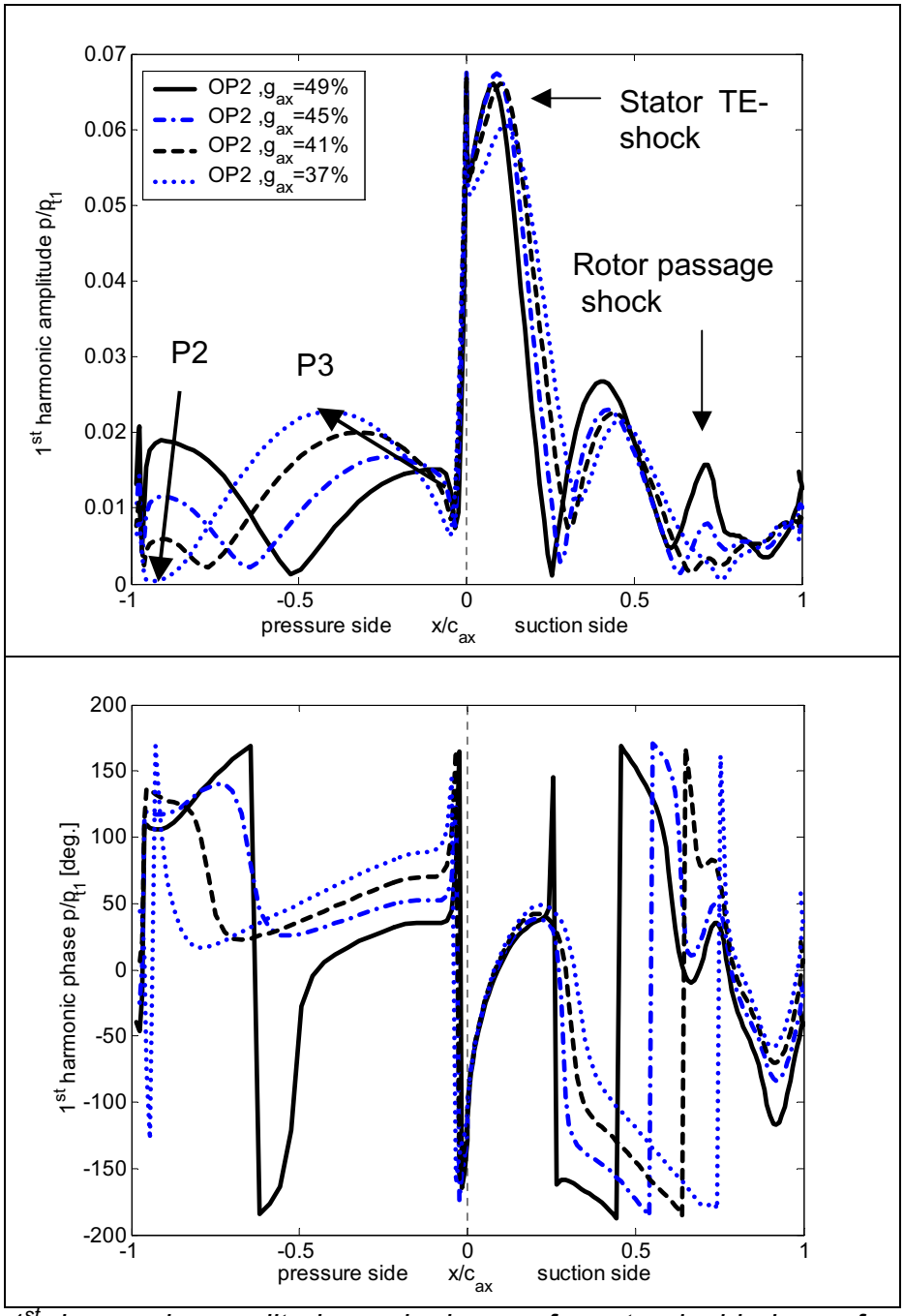

Figure 31: *1st harmonic amplitude and phase of unsteady blade surface pressures, ADTurB case OP2 (transonic), varying axial gap, taken from [Jöcker et al. 2002b], publication 6 in the Appendix*

In the transonic ADTurB cases shock, potential waves and the wake cause the rotor excitation as outlined in the excitation mechanisms chapter (6.2). These stimuli propagate in different directions with different speeds, so that a variation of axial gap will change the interaction between the stimuli and the relative times at which they cause an excitation on the rotor blade. The measured trajectories of the wake and the shock behind the 43 NGV stator are shown in Figure 32. The kink seen in the shock trajectory is explained in [Freudenreich et al. 1999] with the λ– structure of the stator trailing edge shock. For the excitation interaction the leg of the shock pointing towards the rotor is relevant.

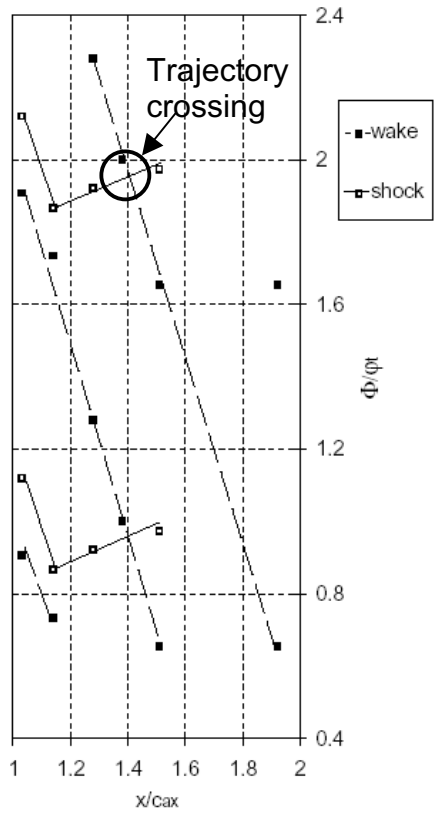

Figure 32: *Measured wake and shock trajectory behind isolated stator 1 [Freudenreich 1999]*

In [Jöcker et al. 2000b] (publication 3 in the Appendix) it has been discussed that unexpected large excitations occurred in the cases, when the wake trajectory crossed the shock trajectory just in front of the rotor leading edge. These are the OP2 large gap case and the OP10 small gap case, for which at these crossing positions also increased gust amplitudes were measured. It is also clear that the crossings are on different axial locations for the 43NGV stator (stator 1) and the 70NGV stator (stator 2) due to the different stator pitches. At other axial positions behind the stator the wake and the shock appear as two distinct events (see also Figure 21), which cause significant second harmonics in the circumferential velocity distributions. It is tempting to conclude that in this special case (OP2) the small axial gap leads to a relative small 1st harmonic excitation compared to the large axial gap because wake and shock excitation have alternating impact on the rotor leading edge during a stator passing period and hence give a stronger 2nd harmonic and a weaker 1st harmonic. However, regarding the discussions on excitation mechanisms above this conclusion should be revised. As it has been identified that the wake has a local (around the blade crown) and relative weak excitation influence in the transonic case it is unlikely that its phase shift to the shock excitation is the main reason for the unexpected small 1st harmonic leading edge excitation of the small gap case. Also small differences in stator exit flow and operation condition may cause the lacking decrease of 1st harmonic excitation by the shock with increased axial gap, which can be due to the uncertainty in the computational model. It follows a discussion: The stream tube definition in the Q3D method (UNSFLO) is a computational parameter with strong influence, especially on the stator trailing edge shock strength, as pointed out in the validation part (Chapter 6.1.4). When varying the axial gap it is optional to keep the stream tube expansion location relative to the stator or relative to the rotor. In the first axial gap study (as documented in [Jöcker et al. 2000b]) the stream tube expansion was located in the same axial position relative to the stator for both axial gap cases. Hence, the stator flow should not see different expansion ratios downstream, which could otherwise modify the strength of the stator trailing edge shock. Still, the time-averaged data in the gap indicates a slightly higher Mach number in the large gap case (0.999) than in the small gap case (0.981) at the same distance behind the stator trailing edge, even though the static to total stage pressure ratio is the same for both cases. Also the average mass flow is by 4% higher than for the small axial gap case result. In the extended study (as shown in Figure 31) the stream tube expansion is fixed axially to the rotor geometry. This is closer to the real geometry, where the hub contour is by construction fixed to the rotor blade geometry (see Figure 13 for a meridional view of the stage). But by decreasing the axial gap the stream tube expansion moves axially closer to the stator, which leads to higher excitation levels on the rotor (the leading edge peak is

increased by 0.5% of p_{t1} compared to the original study, where the expansion location is fixed to the stator). So, the earlier stream tube expansion leads to a stronger effect of the stator trailing edge shock as well as the potential wave. The difference between large and small gap case is hence smaller than in the first axial gap study.

In summary it can be stated that there is some small uncertainty in the prediction of the excitation level with varying axial gap. Still, the 1st harmonic peak at the leading edge is not modified much by the axial gap variation in the investigated range of the case OP2 leading to the conclusion that the axial decay of shock strength is low. It should also be noted that this is not a general conclusion. At the OP10 conditions (high rotational speed cases) the larger axial gap resulted in a significant reduction of the leading edge excitation pressure compared to the small gap case (see [Jöcker et al. 2000b], publication 3 in the Appendix for a comparison of OP10 axial gap cases). A reason for this might be that the 70NGV stator leads to unexpected high excitations with the small axial gap due to the temporal appearance of potential and shock excitations on the rotor blade (see also Chapter 6.3.3).

Important for the vibration excitation is the distribution of amplitude and phase over the surface, because it is related to the receptiveness of a mode shape to be excited (see further Chapter 6.4). In the presented OP2 case it changes significantly with axial gap variation. To analyse this Figure 33 shows the computed perturbation pressures on the rotor blade surface and in a flow field snapshot for the smallest axial gap case at transonic flow conditions, which can directly be compared to the large gap case in Figure 24.

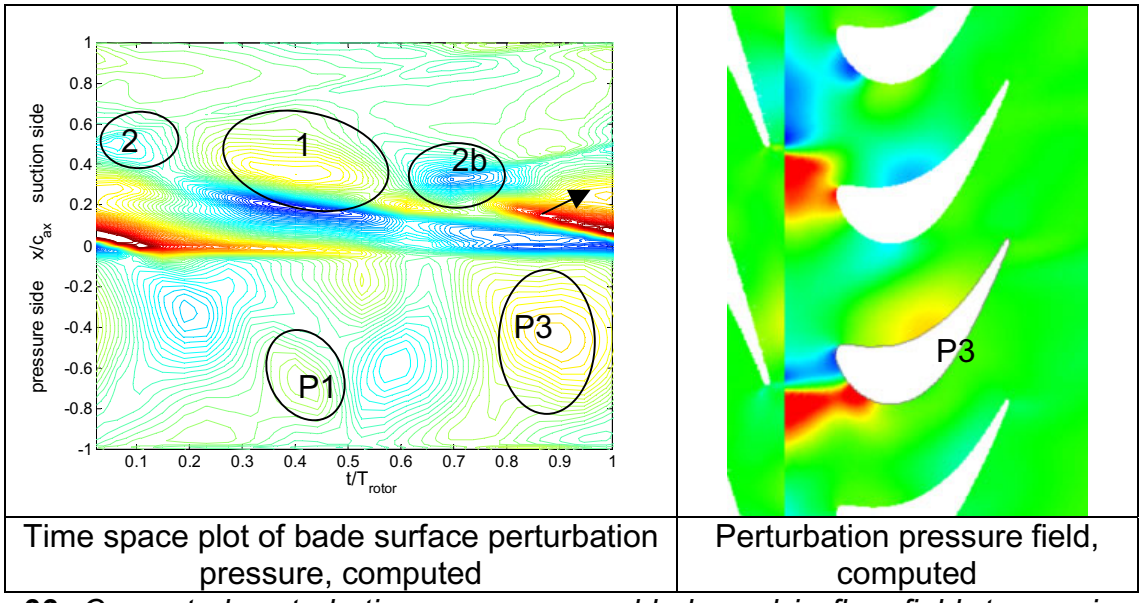

Time space plot of bade surface perturbation pressure, computed	Perturbation pressure field, computed

Figure 33: *Computed perturbation pressures on blade and in flow field, transonic case (OP2), smallest axial gap, scales as in Figure 24*

The observation of the time and space resolved blade surface pressures indicate that the excitation mechanisms are partly modified for the small gap case. The shock impingement and excitation on the rotor leading edge has not changed significantly, it appears on the rotor at about the same time and location due to the approximate axial direction of the shock. The 1st harmonic phase at the leading edge location is accordingly similar for these cases (see Figure 31, right side).

The excitation peak P3 on pressure side, which has been related to the detachment of the shock from the upper blade, (see Chapter 6.2.1) becomes stronger and moves towards the middle of the blade with decreasing axial gap, but the timely occurrence does not change. This effect has a significant influence on the excitation, clearly seen in the 1st harmonic pressure (Figure 31). The modification of the pressure side excitation with axial gap is furthermore due to the disappearance of the potential excitation P2 from the aft part of the blade. Both effects together cause the two-peak excitation to change to one large excitation in the 1st harmonic when decreasing the axial gap.

The most obvious change on suction side is that the excitation 3 due to the passage shock has disappeared in the small axial gap case, which is also clearly seen in the 1st harmonic pressure (Figure 31). This has been observed independently of the chosen stream tube expansion location (see discussion above) so that a modification of the flow acceleration by the Q3D option is not reason for the difference.

Other significant changes are seen in the appearance of the potential waves 2 and 2b on the suction side surface. With decreasing axial gap the peak 2b, which is part of the pressure wave sweeping over the blade leading edge at this time (see further Chapter 6.2.2), becomes stronger and hits the blade earlier, whereas the peak 2 originating from the following NGV pressure field becomes weaker and nearly disappears. This change might be explained with a stronger potential field in the small gap case, which enhances the waves from the closer NGV trailing edge relative to the waves coming from the next NGV, which is further away. Another reason for the weakened peak 2 in the small gap case might be that the pressure wave propagation related to the shock impingement is different in the small axial gap case. It is indicated with an arrow in Figure 33 that this wave is propagating along the suction surface instead of reflecting to the opposite pressure side, where it causes P2 in the large axial gap case. The presence of this positive pressure disturbance on suction side could delay and weaken the negative peak 2. The change of the peaks 2 and 2b is important for the blade excitation because it modifies the harmonic content of the excitation in the middle part of the rotor blade surface. There, the small gap case has now two pressure waves per period giving rise for a stronger 2nd harmonic and a weaker 1st harmonic. The decrease of 1st harmonic is seen in Figure 31, the harmonic content of the excitation is further shown in [Jöcker et al. 2000b] (publication 3 in the Appendix).

Several of the mechanism changes seen in the transonic cases appear also in the subsonic cases, even though at a perturbation level of about a factor 3 smaller than the transonic cases. The 1st harmonic pressure variation with axial gap for the subsonic cases is shown in Figure 34. The leading edge peak clearly increases with decreased axial gap, which is the expected behaviour for this potential excitation. In difference to the transonic case this excitation also changes slightly in phase indicating its different type. On pressure side a similar behaviour as for the transonic case is observed, that the potential peak P2 fades away with decreased axial gap. Also the excitation at the front part of the pressure side around the stagnation point shows a similar but less pronounced trend to increase and move towards the middle of the blade, when the gap is decreased.

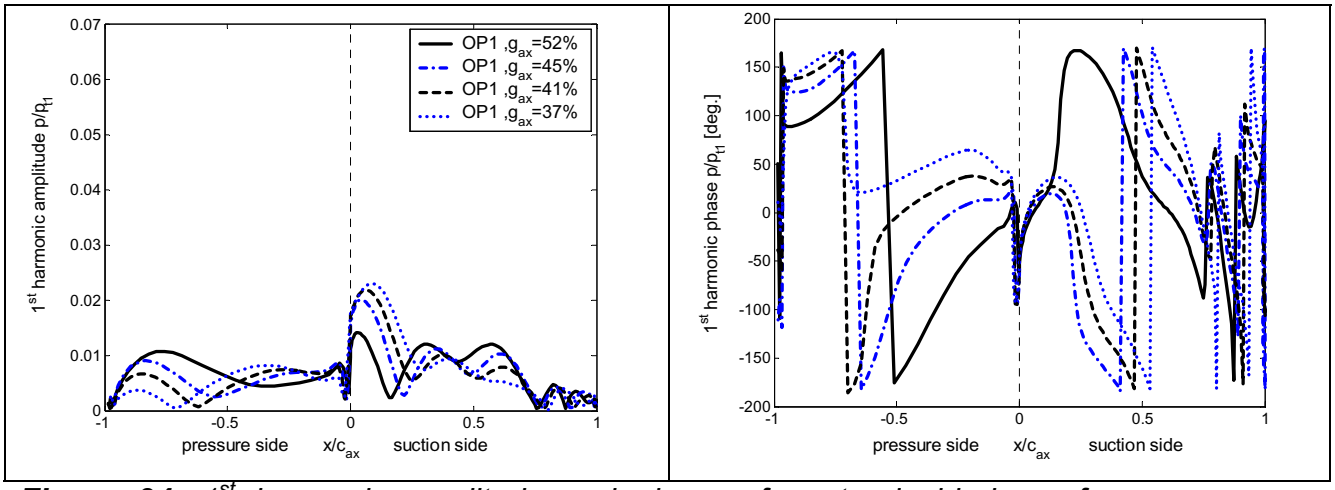

Figure 34: *1st harmonic amplitude and phase of unsteady blade surface pressures, ADTurB case OP1 (subsonic), varying axial gap, taken from [Jöcker et al. 2002b], publication 6 in the Appendix*

The investigation of the turbopump was less difficult, no shock excitations had to be regarded and the complication due to the stream tube expansion was not present in that stage, which has constant radii both at hub and tip. To enhance potential interaction effects the axial gap study was extended to very small gaps, down to 8% of the rotor axial chord. The study showed similar to the ADTurB case that the harmonic content of the excitation increased when the axial gap was reduced, which lead to a decrease of the 1st harmonic excitation. But in difference to the ADTurB case the change of harmonic contribution was on pressure side, where the 1st harmonic trend decreased at smaller axial gaps, see Figure 35.

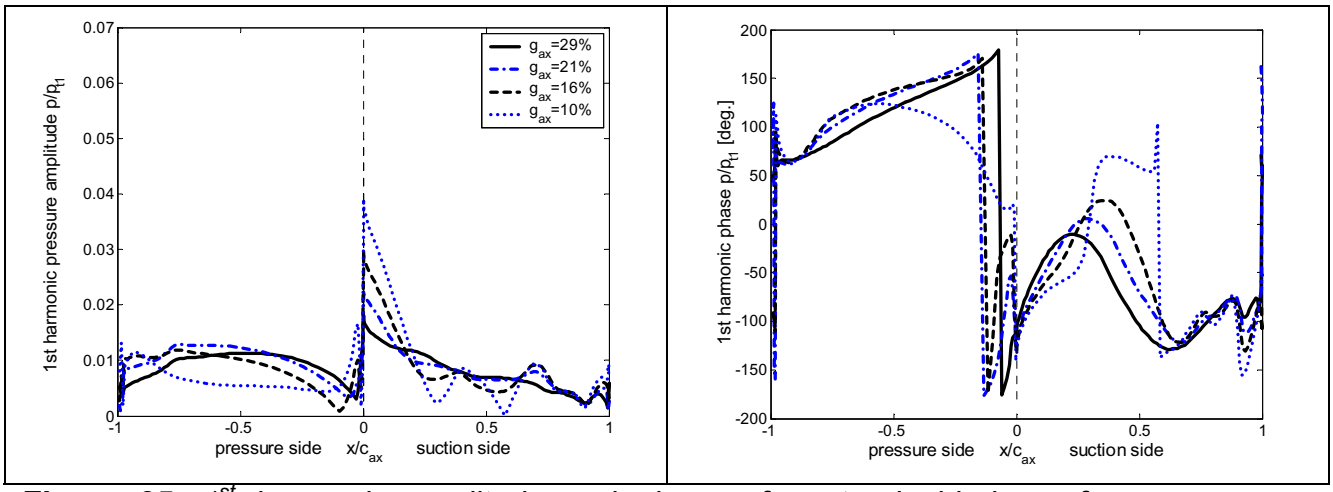

Figure 35: *1st harmonic amplitude and phase of unsteady blade surface pressures, turbopump turbine with varying axial gap, taken from [Jöcker et al. 2002b], publication 6 in the Appendix*

The suction side leading edge peak due to the potential excitation increases as expected with decreased axial gap due to a stronger and spatially wider excitation by the pressure wave behind the stator trailing edge. Both effects together significantly change the harmonic content of the blade forcing as illustrated in Jöcker et al. [2001] (Publication 5 in the Appendix). Whereas at larger axial gaps the excitation is mainly sinusoidal and dominated by a strong excitation wave on the pressure side (see also Figure 26) the

leading edge excitation and successive reflections become dominant at small axial gaps giving rise to higher harmonic excitation. The changes in the leading edge peak and the pressure side excitation are the main variations in the 1st harmonic pressure distribution with axial gap. The phase of excitation events does not change as much as in the ADTurB case (compare Figure 34), especially on pressure side. This is a significant difference to the ADTurB case, where both pressure distribution and phases change significantly with variation of axial gap. The influence of these differences on the excitability is discussed in Chapter 6.4.2. A reason for the differences between the ADTurB subsonic case and the turbopump case might be that the excitation in the latter one is primarily dominated by one pressure wave, which is reflected several times in the rotor passage, whereas the ADTurB stage is characterised at this operating condition by interacting potential waves from two stators. The related excitation mechanisms were outlined in Chapter 6.2.2, the change with axial gap in the ADTurB case was discussed above.

It is concluded from the axial gap study that the increase of this parameter does not necessarily lead to a decrease of aerodynamic excitation. The investigated transonic case OP2 showed that the shock excitation does not change significantly with increased axial gap. The small uncertainty in the study due to the difficulty to compute exactly the same operating conditions in all axial gap configurations with the Q3D method does not change this conclusion. The potential wave excitations could modify due to different axial gap, because the wave propagation and their relative strength could change. In the ADTurB case it was demonstrated that this led to a redistribution of excitation energy from the 1st to higher harmonics with decreased axial gaps. It is also concluded that the excitation modification due to axial gap change might be very different for different turbines or operating conditions. This was demonstrated by a comparison between the subsonic ADTurB case and the turbopump turbine case.

6.3.3 Stator blade count and size

The results presented by Korakianitis [1992a, b, 1993a, b] suggested that the stator to rotor pitch ratio R had a major influence on the rotor excitation. A detailed study of stator vane size and count was included in the pre-design investigation of the turbopump turbine by Jöcker et al. [2001] (publication 5 in the Appendix). The studied variations of stator geometry are described in Chapter 5.2. The findings are summarized below.

As expected, the scaling of the vanes left the mean rotor flow conditions non-affected whereas the reduction of the vane number without scaling increased the mean stator vane load and rotor blade load (Figure 36 left side). This affected accordingly the blade excitation.

The vane scale had a significant influence on the 1st harmonic blade excitation. A half size stator (scaled by 0.5) led to a reduction of the excitation level by more than 50% at almost all blade locations. The enlargement of the stator (scaled by 1.3) as well as the removal of stator vanes (-4 vanes) gave a significant increase of excitation level (Figure 36, right side). The removal of 4 vanes led to even higher excitation levels than the levels reached due to the enlargement of the stator vanes.

Changes of vane count modifies obviously the excitation frequency because the rotor will pass more stator vanes per revolution. This is an important factor concerning the design

because it shifts the resonance condition, which is obvious from a Campbell diagram (Figure 15). Moreover, the change of vane pitch changes the relative time between the shock effects (not present in the turbopump study), the potential effects and the wake effects, because they usually spread in different directions. For example, in Figure 32 the propagation of the wake and the shock behind the ADTurB stator is illustrated. A modification of the pitch would change the relative paths of these trajectories leading to different interactions of these at any location downstream of the stator. Hence the stator pitch is a tool to tune the phase between shock-, potential- and wake effects on the excitation, which is further discussed in Chapter 6.4.1.

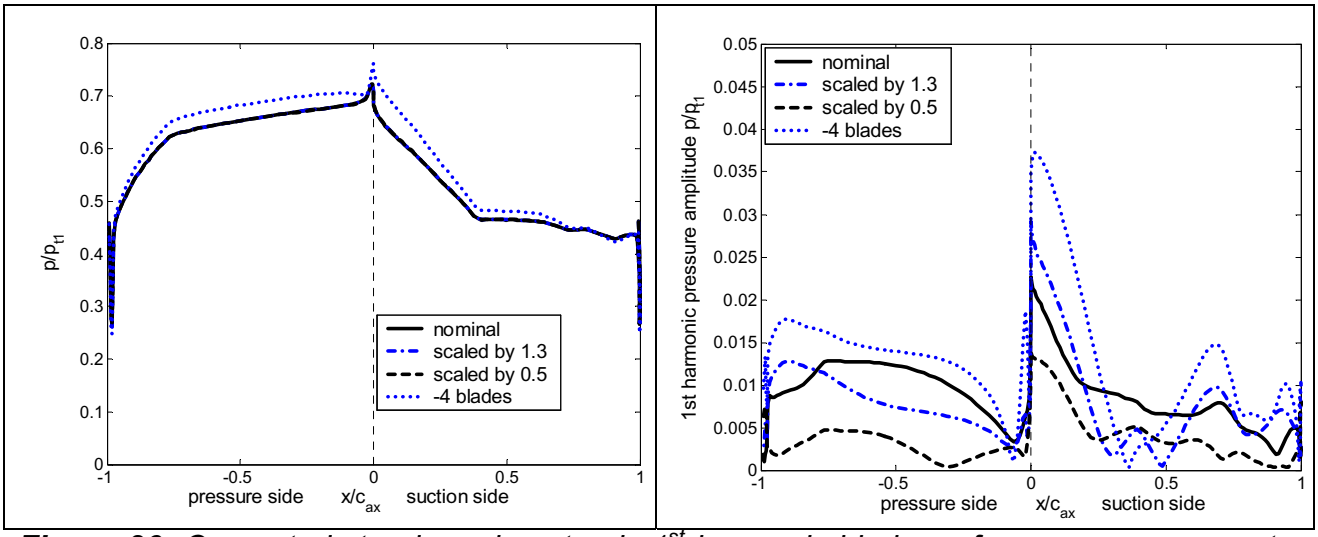

Figure 36: *Computed steady and unsteady 1st harmonic blade surface pressures on rotor due to stator variation, turbopump turbine*

Larger vanes are accompanied by stronger potential fields and stronger wake defects. In the present study it was found that especially the 1st harmonic pressure peak on the pressure side aft part was increased in the cases with stronger potential effects (cases 1.3 and –4, R=2.75). Smaller vanes (case 0.5, R=1.03) gave significantly reduced potential excitation. This case is characterized by the wake influence on most parts on the blade. The potential influence is mainly limited to the leading edge region and comparably weak. If the vane is small enough two (or more) consecutive wakes can influence the flow in one rotor passage at the same time, which can result in a 2nd (or higher) harmonic dominance in the excitation. This has been observed in the present turbopump study.

In [Jöcker et al. 2001] (publication 5 in the Appendix) the results from the stator pitch study have been compared directly to the computations by Korakianitis [1992b] in terms of 1st harmonic axial force. It shows comparable trends even though of different magnitude. The overall conclusion from Korakianitis [1993a] that the excitation is characterised by wake effects at low pitch ratios (R≈1) is also found here, but already at intermediate pitch ratios (R≈2, nominal turbopump case) the wake effects become very small compared to potential effects. Korakianitis [1993a] classified excitations to be dominated by potential effects for pitch ratios R ≥ 3.

For the ADTurB turbine stage it has already been noted in the discussion of operating points (Chapter 6.3.1) that the steady aerodynamics of the two different stators are not identical, which leads also to differences in the steady rotor flow, a comparison of the isentropic surface Mach number is included in Figure 28. The detailed comparison of the

two stators is presented in [Freudenreich et al., 1999] (publication 2 in the Appendix). Due to the small differences in steady load the differences between the 43 NGV and 70 NGV excitations can not be clearly isolated from blade load effects, which may have an influence on excitation.

From a comparison of the 43 NGV case (Figure 24, right side) and the 70 NGV case at 88% rotational speed (OP2s-70NGV, Figure 29, left side) it is seen that the peaks 1, 2 and 3 on suction side are not as observable with 70 NGV excitation as in the case of 43 NGV excitation. Around x/c_{ax} =0.6 on suction side pressure peaks are seen which are related to potential excitations and are accordingly marked with 1 and 2. The peak 3 due to the rotor passage shock is not present, because there is no passage shock in the case with 70 NGVs. With regard to the harmonic excitation of the rotor the shift of peaks 1 and 2 towards the rear of the blade is important because this allows the first harmonic pattern of the excitation on the rotor suction side to be more dominant. This can be observed by regarding the distribution of excitations during one period of excitation in the time space plots (Figure 29): In the 70 NGV cases the positive-negative pattern is much less disturbed than in the 43 NGV cases, which leads to a strong 1^{st} harmonic excitation and less pronounced higher harmonics. On pressure side the P1, P2 and P3 peaks can be found again, even though at different times relative to each other and relative to the peaks on suction side. Hence, the different stator size has a significant influence on the timely appearance of excitation peaks.

It is striking that the leading edge excitation due to 70 NGVs is of the same level as the excitation due to 43 NGVs at the nominal rotational speed (compare Figure 24, right side, Figure 29, left side) whereas the turbopump study above indicates a significant reduction of excitation with smaller vanes. The analyses of the ADTurB stator gusts in [Jöcker et al. 2000b] did indicate much larger velocity deficits behind the 43 NGV stator than behind the 70 NGV stator. This was expected, as smaller stators should lead to smaller wakes and reduced potential waves behind their trailing edges. But the main excitation in this transonic case is due to the trailing edge shock, which is present behind both the 43 and the 70 NGV stator. The excitation strength is obviously not much affected by the stator size in this case. This might be due to remaining excitation strength of the shock behind a smaller vane but also due to the superposition of potential and shock excitation in the small gap cases with 70 NGVs.

It is concluded from this study that the reduction of the vanes can significantly reduce the potential excitation in subsonic cases, but may lead to higher harmonics in the excitation. In transonic cases this seems not necessarily an effective measure to reduce the excitation due to the remaining stator trailing edge shock. Furthermore, it has been pointed out that the modification of vane count does not only change the excitation frequency, it is also a possibility to actively change the temporal relations of excitation mechanisms, which could be used to cancel excitations from different sources. Its potential is discussed in Chapter 6.4.1.

A different aspect of these results concerns the application of blade and vane number adjustment in state-of-the-art CFD codes to enforce periodic boundaries on a relative small sector of the annulus. In the presented turbopump turbine study the scaling had a significant influence on the unsteady blade pressures and it is concluded that scaling of vanes or blades for computational reasons should be avoided.

6.4 Potential for unsteady design improvements

The previous chapter discussed the aerodynamic excitation mechanisms present in the investigated turbine stages and their variation with operation conditions, axial gap and stator design. The analysis of the unsteady aerodynamics concerning the blade vibration excitation is completed in this chapter with the discussion how the found mechanisms and variations with the investigated parameters may be used to improve the high pressure stage design towards the reduction of HCF risk. It is divided in two parts. The first regards the potentiality to modify the excitation sources to generally reduce the stimulus of blade vibration; the second involves the mechanical system in terms of the blade mode shape in the judgement of excitation stimuli.

6.4.1 Modification and interaction of excitation sources

The analysis of the excitation mechanisms indicated several possibilities to reduce the unsteady pressure perturbations on the rotor blade surface, but it also showed that it is difficult to find general rules towards that goal. It follows a critical discussion.

In subsonic cases the increase of the axial gap was usually followed by a reduction in rotor excitation in terms of the 1st harmonic unsteady pressure. Still, exceptions have also been recognized, where local peaks of excitations increased with larger axial gaps. This was related to an energy transfer from the 1st to higher harmonics of excitation at lower axial gaps. When regarding the unsteady blade force harmonics, the trend could be adverse to the 1st harmonic pressure distribution. This was found in the turbopump turbine indicating that the 1st harmonic axial and tangential forces reduced with decreased axial gap whereas higher force harmonics increased. This points out the necessity to relate the changes in excitation due to a design parameter also to the excited mode, which is done in Chapter 6.4.2. The increase of axial gap does not necessarily reduce HCF risk.

Another effective method to reduce excitation stimuli was found to be the increase of vane number (reduction of vane pitch and size) in potential wave excited cases. This has been shown on the turbopump turbine. But this measure is not always efficient in transonic cases, where the excitation by the stator trailing edge shock may not change significantly with stator size. The ADTurB turbine (OP2) demonstrated this. Furthermore, it has been seen that a change in wave reflection pattern due to a different stator count can modify the harmonic content of the excitation. This led to an enforcement of the 1st harmonic excitation pressure with increased vane number in the ADTurB case.

It has been found that the excitation by the stator trailing edge shock is the strongest excitation source in the transonic cases. Hence, the most obvious measure to reduce the stimulus is the Mach number reduction in the gap. The code validations have shown the sensitivity of the excitation level to the stator exit Mach number and the difficulty to provide the correct boundary conditions to capture this excitation source accurately in the computations. This measure seems also to be the most effective in transonic cases, especially with regard to the limitations to reduce the excitation level by axial gap or stator count (see discussion above).

It has been discussed in the open literature [Korakianitis 1992 a, b] that excitations due to wake (vortical) and potential origin can cancel out, if they are counteracting. As these

excitation sources propagate through the axial gap with different speeds and in different directions it is obvious that their relative phase can be modified with the parameters axial gap and stator count. The relative phase is caused by the time difference in appearance of pressure perturbations due to these sources on the rotor blade. Hence, an optimum axial gap and an optimum stator count might exist, at which the excitations cancel most. This measure to reduce excitation has been investigated on the turbopump turbine by computing the excitation due to varied magnitudes of potential and wake (vortical) excitations. The gust computation option in UNSFLO has been used for that to clearly control the vortical and potential contributions to the excitation. The theory is presented in Chapter 4.2. The results are documented and discussed in [Jöcker et al. 2001] (publication 5 in the Appendix). Figure 37 shows the computed axial and tangential forces (f_x and f_y) as well as the moment (m) about a chosen point due to the 1st harmonic excitation pressure in the complex plane. The real part of each vector shows the in phase excitation and the imaginary part the out of phase excitation relative to one excitation period. The absolute phase is arbitrary and depends purely on the definition of start and end of the excitation period, important here are the magnitude and the relative phase of the shown excitations.

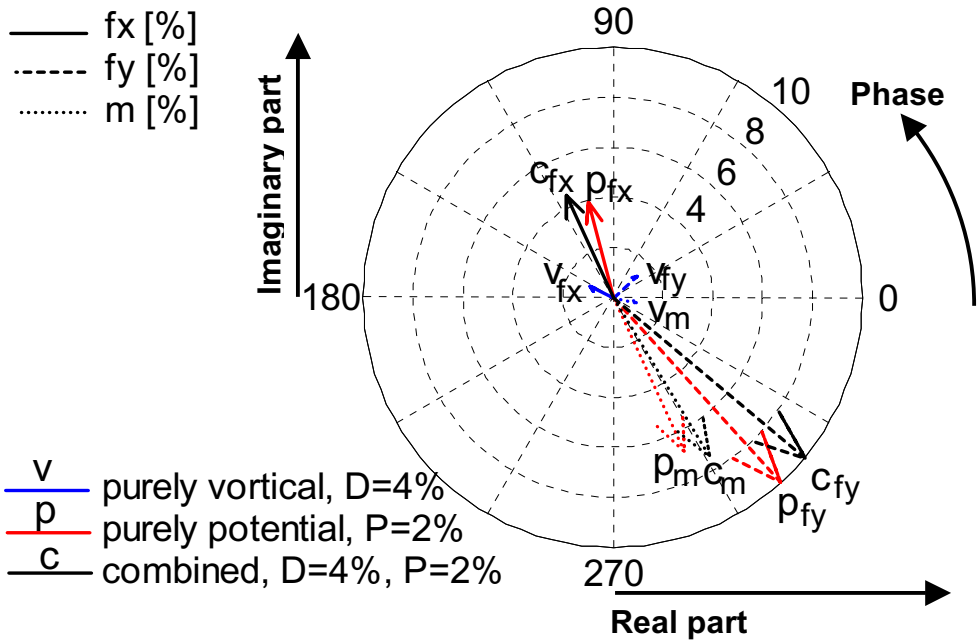

Figure 37: *Splitting into vortical and potential parts of the unsteady aerodynamic force amplitudes*

Three computational results are shown, one due to a purely vortical excitation with a wake deficit D of 4%, then due to a purely potential excitation with a potential amplitude at the inlet boundary of 2%. Third, a combined computation result is shown with both a wake and a potential unsteadiness defined at the inlet boundary. The 1st harmonic magnitudes are given in percent of the steady force and moment components. The presented combination of vortical and potential excitation gives not the closest result to the stage computation result, but is still relative close in terms of 1st harmonic unsteady blade pressure (see [Jöcker et al. 2001], publication 5 in the Appendix). The superposition of the vortical and potential excitation forces seems to be valid in this case, as indicated by the linear behaviour ($\mathbf{v}_{fx} + \mathbf{p}_{fx} = \mathbf{c}_{fx}$ and so on). The possibility that forces due to vortical and potential excitation sources cancel is indicated by the phase shift between them. An optimisation of

the case would try to turn the potential and vortical vectors against each other until they are pointing in opposite directions, for example by modification of axial gap or stator pitch. However, to choose for which force components to optimise the excited mode shape must be known, as discussed in Chapter 6.4.2. In this particular case it appears that the effort to approach such an optimisation is too large compared to the gain, because the vortical excitation impact is relative small compared to the potential. A combination with a reduction of the vanes seems more promising, because then vortically and potentially induced excitations are of more equal level.

In transonic cases the shock excitation has been found so much larger than the wake excitation that a phase tuning of these effects seems not promising. However, it has also been demonstrated in the discussion of the axial gap influence on the ADTurB rotor excitation that a modification of potential wave reflections in relation to the shock excitation can redistribute excitation energy from the 1st harmonic to higher harmonics (see Chapter 6.3.2). Thus, a potential to reduce aerodynamic excitation is given by phase tuning shock and potential wave excitation.

6.4.2 Mode shape sensitivity

The parameter studies in Chapter 6.3 have provided insight in how excitation mechanisms may be modified by the investigated parameters. They have also shown that the analysis of the unsteady blade pressure and blade surface forces may lead to different conclusions regarding the comparative judgement of excitation depending on the evaluation: the evaluation of forces may give different conclusions than the evaluation of pressures (see also discussions in Chapter 6.4.1). Therefore, the mode shape has been regarded to assess the design improvement potential by a mode shape sensitivity study of the excitation [Jöcker et al. 2002b] (Publication 6 in the Appendix). This was partly motivated by the mode shape sensitivity study of flutter stability as presented by Panovsky and Kielb [1998] and later extended by Tchernycheva et al. [2001]. In their work a flutter stability parameter was defined and evaluated for various mode shapes. They found that the mode shape is a sensitive parameter for blade stability and that the dependency on mode shape is similar for various subsonic low-pressure turbine vanes and blades. This was visualised in stability plots, in which the rigid body 2D mode shape was represented as a torsion axis location.

In the present study of forced response sensitivity to the mode shape the excitability of the blade was investigated instead of stability. This parameter was evaluated based on the generalised force on the blade due to mode shapes. The generalized force (or modal force) is an established concept to compute excitations of a mode shape. It is described in Chapter 4.4.4. To visualise the influence of the mode shape on the excitability the mode shape was described in terms of a rotation axis location. This is possible, if 2D rigid-body motions of a blade section are assumed. It includes the description of translational blade motions, for which the torsion axis location is infinite far away from the regarded blade section. Hence, a spatial contour parameter, the torsion axis location, can be used to plot the generalised force for various mode shapes. In order to achieve comparable excitabilities the torsion amplitude of the blade motion was normalised such that the average nodal displacement of the blade was one percent of the rotor blade chord length for all modes. Furthermore, the generalised force due to a mode shape is normalised with the maximum possible generalised force by the pressure field, which is obtained when

local blade displacement and force vectors have the same direction. Therefore, the magnitudes of excitability due to different unsteady loads are not comparable with the chosen normalisation. The detailed equations of the approach are documented in [Jöcker et al. 2002b] (publication 6 in the Appendix).

Figure 38 shows the excitability for the ADTurB turbine stage at transonic conditions (OP2) with different axial gaps. The corresponding 1st harmonic pressure amplitudes and phases are shown in Figure 31. Each contour line in Figure 38 connects the torsion axis locations at which the mode shape excitability due to the computed 1st harmonic unsteady pressure on the blade surface is the same. For example at the smallest axial case the excitability is lowest for a torsion axis near the pressure side surface at about mid chord, it is highest for torsion axes in the upper left and lower right corner. Torsion axis locations in these regions correspond to approximately chordwise bending modes as indicated by the arrow.

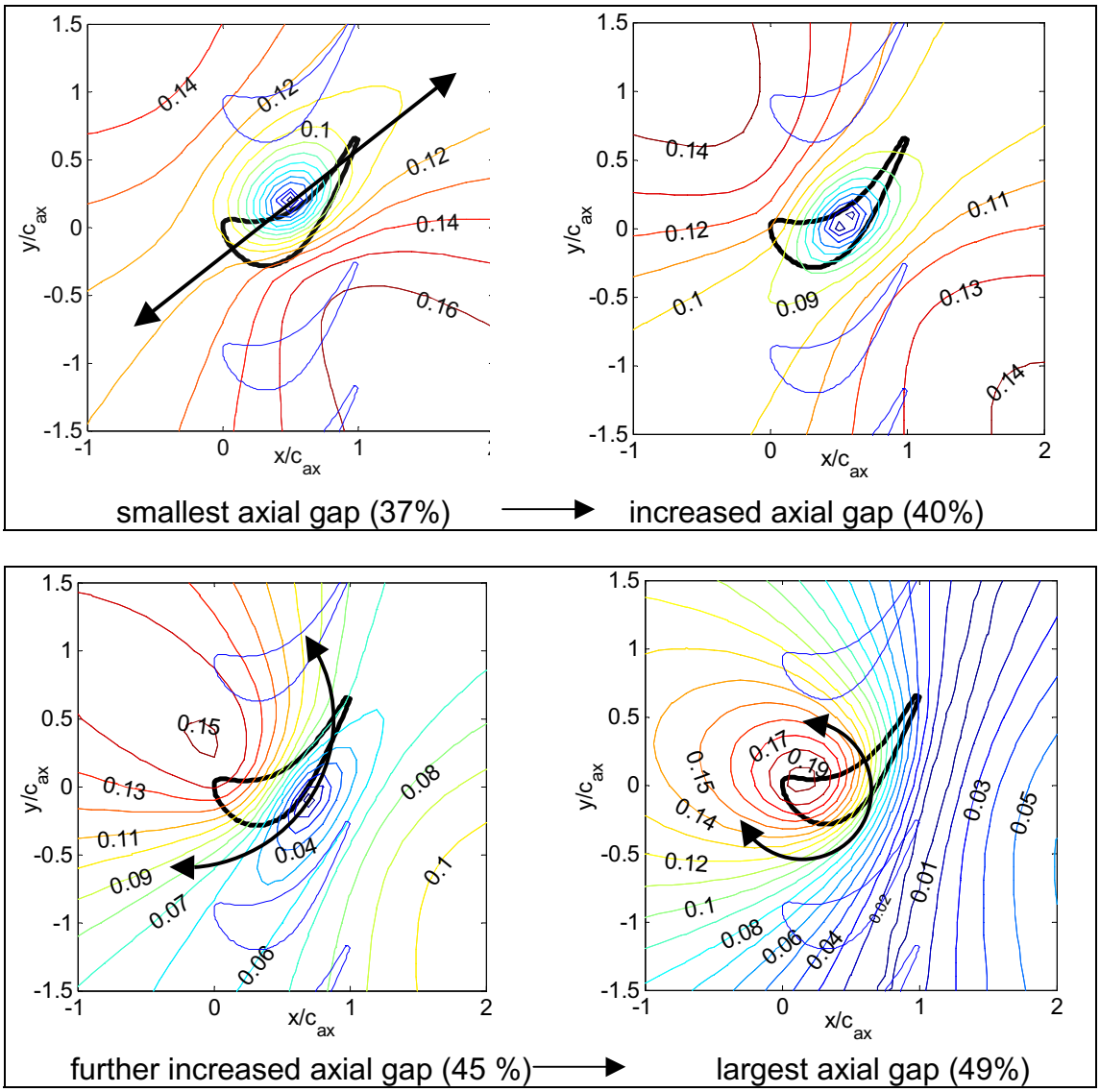

Figure 38: *Excitability of ADTurB cases due to different axial gaps, transonic cases*

One important conclusion from this study is that the excitability is strongly dependent on the mode shape, which is seen in the large gradients in the contours. Regarding the discussions on the excitation mechanisms this was an expected result. Not obvious from

the purely aerodynamic consideration of the excitations was the significant change of strongest excited mode with axial gap variation in the ADTurB case, as seen when comparing the cases in Figure 38.

When the axial gap is increased the most excited mode shape shifts from a chord wise bending mode to a torsion mode with a torsion axis location close to the leading edge. Arrows in the figures indicate this. From a design perspective the least excited mode should be searched. It changes also, when the axial gap is increased. The torsion axis of this mode moves from the pressure side of the blade over the blade thickness and beyond the suction side. Even though the least excited mode shape does not modify as much as the strongest excited mode it should be noted that in the present case the least excited mode shape of the small gap case modifies to a relative strong excited mode in the large gap case. As this mode is close to the 1T mode of the original experimental program (see Campbell diagram, Figure 15), the blade response at this resonance condition could increase with increased axial gap. Still, the 3D mode shape, the 3D excitation and the vibration dependent aerodynamic damping also determine the real blade vibration amplitude.

The main reason for the observed change in excitability with axial gap is the modification of the pressure side excitation, which is discussed in detail in Chapter 6.3.2. The turbopump turbine did not show the same change with axial gap, instead the excitability is similar for all investigated cases. The 1st harmonic pressure amplitude does mainly change in magnitude but not in its distribution on the blade surface and also the phase is not modified significantly by the change of axial gap (Chapter 6.3.2). Therefore, it is always the same mode, which is excited most, an approximately perpendicular to chord bending mode [Jöcker et al. 2002b] (publication 6 in the Appendix).

Excitability variation due to different stators was not investigated, because the aerodynamic variations of these cases were too large resulting in completely different excitability maps. This did not allow conclusions on the excitability variation with change of the stator.

No general trends of the mode shape sensitivity have been found based on the investigated cases. Obviously, both the unsteady pressure distribution on the blade surface and the local surface curvature of a specific blade are parameters with strong influence on excitability so that a common trend for different turbine blades is unlikely.

The observation of excitability plots of larger spatial extension, i.e. with torsion axis locations further away from the blade as shown here, does not change the conclusions. In all cases the contours continue as expected from the figures shown.

The above findings have several implications towards the turbine rotor design with regard to HCF risk reduction:

As the excitability is strongly dependent on the excited mode shape the unsteady aerodynamic blade pressure should only be evaluated with regard to the excited mode shape.

As the most and least excited mode shapes can change significantly with a changed design parameter, as demonstrated above with the axial gap variation in the transonic

ADTurB case, even such relative and small modifications must be evaluated with regard to the excited mode shape in order to ensure that a re-design leads to a HCF risk reduction.

If the mode shape is a parameter, which could be modified in the design process, this offers an effective possibility to reduce the HCF risk due to forced response. From a manufacturing point of view mode shape control is possible by the control of crystal growth during the casting process [Green 1999]. A design recommendation would suggest placing the torsion axis in a region of low excitability and with good margin to the higher gradient.

7 CONCLUSIONS

The validation studies show that the computational results by UNSFLO can be expected to give the trends of unsteady rotor surface pressure due to stator-rotor interaction. It was ensured that the solutions are sufficiently independent from the computational mesh. The comparison of various modelling options of the computational tool lead to the conclusion that most reliable results are obtained with full stage computations combined with the option to account for viscous effects close to the blade surfaces. The difficulty to specify the unsteady inlet gust to the rotor for gust computations has been pointed out. The computed 1^{st} and 2^{nd} harmonics of excitation pressures reflect the measured excitation patterns. Furthermore, confidence in the results is given by comparison to computations published in the open literature. These comparisons suggest that the observed differences at rotor midspan are not due to 3D flow effects. Comparisons to experiments show also that the Q3D predictions give higher Mach number levels in the stator-rotor gap, which has a strong effect on the excitation level at transonic flow conditions but without changing the general pattern. This is explained with the uncertainty of the Q3D method regarding the correct consideration of radial expansion and stream sheet variation. It is also shown that the 3D linearised gust computations with SliQ can predict the measured 1^{st} and 2^{nd} harmonic blade pressure very well even in transonic flow. The requirement of an inlet gust specification according to the experiments to achieve this agreement is stressed. A comparison of numerical results to the vibrating turbine test case STCF11 indicates that UNSFLO computes the main trends of the unsteady flow in a transonic off design case, but this is very sensitive to the choice of time step in the computation.

At the nominal operating conditions of the investigated turbines the excitation mechanisms due to shock, potential waves and wakes are described and related to the work found in the open literature. The differences between subsonic and transonic cases point out the strength of shock excitation leading to pressure excitation levels to be increased by a factor 2 to 3. Potential excitations are discussed on two investigated turbines and it is elaborated that the typical wave type excitation is similar, but that differences in the propagation direction of the waves and the wave reflection pattern in the rotor passage lead to differences in the time and space resolved unsteady pressures on the blade surface. The wake influence on the unsteady pressure on the rotor blade is small in the investigated cases. This is explicitly demonstrated on the turbopump turbine, for which wake and potential excitations are varied separately to study their relative excitation influence.

From the parametric studies the following conclusions were drawn:

- The operating conditions have a significant influence on the excitation mechanism. At low rotational speed separations dominate the unsteady flow behaviour on the rotor suction side with a probably large influence on the unsteady pressure distribution. Limits of the computational method do not allow for further conclusions on these cases. At high rotational speeds the potential excitation is found to reach further into the rotor passage before reflected from the suction side. The change in time averaged pressure on the rotor blade surface and the changes in flow incidence could cause the observed modification of shock and wave propagation. This has a tremendous impact on the 1^{st} harmonic excitation because pressure and suction side are covered by large pressure wave impacts instead of more local impacts at lower rotational speeds. Furthermore,

the time and space distribution of the pressure disturbances on the blade modifies the harmonic content of blade forces, such that the blade force analysis and blade pressure analysis may not indicate the same trends regarding the relative level of excitation.

- The axial gap study shows that the increase of this parameter does not necessarily lead to a decrease of aerodynamic excitation, which is observed in the transonic case OP2. The potential wave excitations are modified due to different axial gap, because the wave propagation and their relative strength change. This can lead to a redistribution of excitation energy from the 1st to higher harmonics with decreased axial gaps. It is also concluded that the excitation modification due to axial gap change might be very different for different turbines or operating conditions. This is demonstrated by a comparison between the subsonic ADTurB case and the turbopump turbine case.

- The reduction of the vane size can significantly reduce the potential excitation in subsonic cases, but can also lead to higher harmonics in the excitation. In transonic cases it appears not necessarily to be an effective measure to reduce the excitation due to the remaining stator trailing edge shock. It has been pointed out that the modification of vane count does not only change the excitation frequency, it is also a parameter to actively change the temporal relations of excitation mechanisms, which could be used to cancel excitations from different sources.

From the assessment of the potential to improve the design of high pressure turbines towards a reduction of HCF failure the following conclusions were drawn:

- In transonic cases the most efficient measure to decrease the excitation level is the decrease of stator exit Mach number to reduce the shock strength. The increase of axial gap and the reduction of vane size show limited potential to decrease the excitation due to the remaining shock excitation strength.

- Axial gap and stator design can be modified to change the interaction between the excitation mechanisms present in the stage. Phase relations between shock and potential wave excitation may be utilised to shift excitation energy to higher harmonics. The wake influence was found to be small in the investigated cases so that a phase tuning of wake excitation to potential and shock excitation seems not efficient, unless it is in subsonic cases combined with a reduction of vane size towards $R \approx 1$ to achieve potential and wake excitations of comparable magnitude.

- The excitability of a blade due to the unsteady pressure is strongly dependent on the mode shape. This is an expected result but it is not obvious from the purely aerodynamic consideration of the blade surface pressures that the most and least excited mode shapes of the ADTurB cases change significantly with axial gap variation. Therefore, it was concluded that the assessment of the aerodynamic excitation should only be made with regard to the excited mode shape. Even relative changes in the aerodynamic excitation due to a modification of a design parameter such as the axial gap should be judged with regard to the excited mode shape. If the mode shape itself is a parameter, which can be modified in the design process, a design recommendation with regard to mode shape excitability suggests placing the torsion axis in a region of low excitability and with good margin to the high gradient regions of excitability.

8 FUTURE WORK

The validation part of the work demonstrated the capability of a 3D linearised gust method to predict the 1st and 2nd harmonic unsteady blade pressure on the rotor of a particular case including shock excitation effects. As such a method is computationally very efficient it would be of interest to examine its limits in terms of allowable shock strength, vane exit Mach number and axial gap to provide a reasonable solution in the harmonics of interest.

The investigation of various operating conditions indicated that at off-design, especially at lower rotational speeds, separations might have a significant impact on the unsteady pressure on the rotor blade. This could be even larger and more dangerous than the excitations investigated in the present work. If new engine designs would need to allow for resonance conditions at such operating points it would be valuable to investigate these off-design conditions experimentally to get a validation basis for computations.

Low engine order excitations are usually present in all real engines. Due to tolerances in the manufacturing process of vanes these are not equal and so is not the excitation from the various vanes assembled in the stator ring. This annular non-uniformity introduces excitations of lower frequency and might also change the excitation content of the vane passing frequency. A generic study to assess the magnitude of these influences would be valuable. Especially, experimental results would be very useful to validate methods to predict such effects.

From the analysis of excitation mechanisms for different turbine stage configurations and at various investigated operating conditions it was seen that excitation mechanisms follow similar patterns mainly governed by pressure and shock wave propagation and reflections in the stage. An ambitious goal for future work would be to generate simple models relating basic design parameters like stator exit flow Mach number, rotor incidence, rotor stagger angle, stator pitch/axial gap ratio or blade curvature to wave propagation behaviour. This should then allow conclusions on the excitation patterns on the rotor blade surface. Such models could then be used very early in the design process to regard possible excitations of the blade mode shape.

The potentiality in the option to stabilize forced response with help of aerodynamic damping was not discussed in this thesis. A generic study would be interesting to sketch the magnitude of aerodynamic damping for different turbine configurations, operating conditions and blade mode shapes in comparison to structural damping. The trends should then be compared to findings regarding the excitation of blades in order to find conclusions on optimum designs to reduce the HCF risk. The consideration of the aerodynamic damping sensitivity to the mode shape should be included.

The demonstrated sensitivity of the excitability of a blade to the mode shape must be proven also on real mode shapes to generalise the findings. Thus, the study should be extended to 3D mode shapes of flexible blades. This could be achieved by computing the generalised forces due to such real mode shapes. As 3D modes cannot be related to a single parameter such as a torsion axis location such a study would be limited to some chosen characteristic or typical mode shapes.

9 REFERENCES

Abell, E. E.; Kielb, R. E.; Henderson, P. J.; 1977
"Structural Analysis of a Cooled Directionally Solidified Turbine Blade"; *Journal of Aircraft, Vol. 14, No. 2; February 1977*

Abhari, R. S.; Guenette, G. R.; Epstein, A. H.; Giles, M. B.; 1992
"Comparison of Time-Resolved Turbine Rotor Blade Heat Transfer Measurements and Numerical Calculations."; *J. of Turbomachinery, Vol. 114, pp. 818-827, 1992*

ADTurB 2, 2000
"Aerolastic Design of Turbine Blades II, Project Web Site"; *Official web site of the EU Research Project No. GRD1-1999-10258; Web address: www.egi.kth.se/ekv/adturb2*

AGARD; 1980
"Multilingual Aeronautical Dictionary"; *AGARD, ISBN 92-835-01666-7, p. 213, 1980*

Adamczyk, John J.; 1999
"Aerodynamic Analysis of Multistage Turbomachinery Flows in Support of Aerodynamic Design"; *ASME paper 99-GT-80*

Arnone, A.; Marconcini, M.; Pacciani, M.; Schipani, C.; Spano, E.; 2001
"Numerical Investigation of Airfoil Clocking in a Three-Stage Low Pressure Turbine"; *ASME paper 2001-GT-0303*

Baldwin, B.; Lomax, L.; 1978
"Thin Layer Approximation and Algebraic Model for Separated Turbulent Flow"; *AIAA Paper 78-257; 197883*

Barter, J.W.; Vitt, P.H.; Chen, J.P.; 2000
"Interaction Effects in a Transonic Stage"; *ASME paper 2000-GT-0376*

Beam, R.M.; Warming, R.F.; 1977
"An Implicit Factored Scheme for the Compressible Navier Stokes Equations"; *Proceedings of the 3rd Computational Fluid Dynamics Conference, Albuquerque, New Mexico, and AIAA Journal, 16:393-403, 1978*

Billonnet, G.; Fourmaux, A; Touissant, C.; 2001
"Evaluation of Two Competitive Approaches For Simulating the Time-periodic Flow in an Axial Turbine Stage"; *Conference Proceedings of the 4th European Conference on Turbomachinery – Fluid Dynamics and Thermodynamics Firenze, 20th-23rd March, 2001, S.G.E., ISBN: 88-86281-57-9*

Birch, T.; 1987
"Navier-Stokes Predictions of Transition, Loss and Heat Transfer in a Turbine Cascade"; *ASME paper 87-GT-22*

Bölcs, A.; Fransson, T.H.;Schläfli, D.; 1989
"Aerodynamic Superposition Principle in Vibrating Turbine Cascades"; *AGARD, 74th Specialist's Meeting of the Propulsion and Energetics Panel on Unsteady Aerodynamic Phenomena in Turbomachines, Luxembourg, Aug. 28 –Sept. 1, 1989*

Bréard, C. ; Vahdati, M. ; Imregun, M. ; Green; J.S.; 2000
"A Resonance Tracking Algorithm for the Prediction of Turbine Forced Response with Friction Dampers", *ASME paper 2000-GT-0372*

Busby, J. A.; Davis, R. L.; Dorney, D. J.; Dunn, M. G.; Haldeman, C. W.; Abhari, R. S.; Venable, B. L.; Delaney, R. A.; 1999
"Influence of Vane-Blade Spacing on Transonic Turbine Stage Aerodynamics Part II: Time-Resolved Data and Analysis.", *Journal of Turbomachinery, Vol. 121, pp. 673-682, 1999 and ASME Paper No. 98-GT-482*

Boussinesq, T.V.; 1877
"Mém. Pres Acad. Sci."; *3rd Ed.; Paris XXIII, p. 46, 1877*
Campobasso, M. S.; Duta, M. C.; Giles, M. B.; 2001
Adjoint Methods for Turbomachinery Design"*; ISABE-2001-1055*
Carstens, V.; Bölcs, A; Körbächer, H.; 1993
"Comparison of Experimental and Theoretical Results for Unsteady Transonic Cascade Flow at Design and Off-Design Conditions"; *ASME Paper 93-GT-100*
Carta, F. O.; 1988
"Aeroelastic Coupling – An Elementary Approach"; *AGARD Manual on Aeroelasticity in Axial Flow Turbomachines, AGARD-AG-298, ISBN 92-835-0467-4, edited by Max F. Platzer and Franklin O. Carta, 1988*
Carta F. O.; 1982
"An Experimental Investigation of Gapwise Periodicity and Unsteady Aerodynamic Response in an Oscillating Cascade (Part 1 of 3)"; *Nasa-CR 3513, 1982.*
Cebeci, T.; Smith, A.M.O.; 1974
"Analysis of Turbulent Boundary Layers", *Academic Press, 1974*
Chen, S. H.; Eastland, A. H., Jackson, E. D.; 1994
"Efficient Method for Predicting Rotor/Stator Interaction."; *AIAA Journal of Propulsion and Power, Vol. 10, No. 3, pp. 337-342*
Clark, J. P.; Aggarwala, A. S. ; Velonis, M. A.; Gacek, R. E.; Magge, S. S.; Price, F. R.; 2002
"Using CFD to Reduce Resonant Stresses on a Single-Stage, High-Pressure Turbine Blade" *ASME paper GT-2002-30320*
Colantuoni, S.; Colella, A.; Santoriello, S.; Kapteijn, C.; 1995
"Aerodesign and Performance Analysis of a Transonic Turbine Inlet Guide Vane with Trailing Edge Coolant Flow Ejection.", *VDI Berichte Nr. 1185, 1995*
Colella, A.; Solazzo, M. A.; 1996
"DLR-Rig Aero Design of Second Stator"; *ADTurB Project Report No. ADTB-ARA-4003, 1996, Confidential*
Collar, A. R.; 1946
"The Expanding Domain of Aeroelasticity", *The Royal Aeronautical Society, pp. 613-636*
Chernobrovkin, A.;Lakshminarayana, B.; 2000
"Unsteady Viscous Flow Causing Rotor-Stator Interaction in Turbines, Part 2: Simulation, Integrated Flowfield, and Interpretation", *Journal of Propulsion and Power, Vol. 16, No. 5, 2000*
Chiang, H. D.; Fleeter, S.;1992
"Analysis of Forced Resonse of Detuned Blade Rows"; *Journal de Physique III, France 2, pp. 527-544, April 1992*
Chiang, H. D.; Kielb, R. E.; 1993
"An Analysis System for Blade Forced Response"; *ASME Paper No. 92-GT-172 and Journal of Turbomachinery, Vol. 115, pp. 762-770, 1993*
Chien, K.Y.; 1982
"Predictions of Channel and Boundary Layer Flows With a Low Reynolds Number Turbulence Model"; *AIAA Journal, Vol. 20, No. 1; pp. 33-38*
Chung, M.-H.; Wo, A. M., 1997
"Navier Stokes and Potential Calculations of Axial Spacing Effect on Vortical and Potential Disturbances and Gust Response in an Axial Compressor"; *ASME Journal of Turbomachinery, Vol. 119, pp. 472 – 481, July 1997*

Clark, J.P.; Stetson, G.M.; Magge, S.S.; Ni, R.H.; Haldeman, C.W.; Dunn, M.G.; 2000
"The Effect of Airfoil Scaling on the Predicted Unsteady Loading on the Blade of a 1 and 1/2 Stage Transonic Turbine and a Comparison with Experimental Results"; *ASME paper No. 2000-GT-0446*

Dawes, W. N.; 1993
"Simulating Unsteady Turbomachinery Flows on Unstructured Meshes Which Adapt Both in Time and Space"; *ASME paper no 93-GT-104*

Dénos, R.; Arts, T.; Paniagua, G.; Michelassi, V.; Martelli, F.; 2000
"Investigation of the Unsteady Rotor Aerodynamics in a Transonic Turbine Stage", *ASME paper No 2000-GT-0435*

Dénos, R.; Sieverding, C.H.; Arts, T.; Brouckhaert, J.F.; Paniagua, G.; 1999
"Experimental Investigation of the Rotor Aerodynamics of a Transonic Turbine Stage"; *Proceedings of the 3rd Euopean Conference on Turbomachinery – Fluid Dynamics and Thermodynamics, London, UK, March 2-5, 1999, Professional Engineering Publishing, ISBN: 1 86058 196 X*

Doorly, D. J.; Oldfield, M. J.; 1985
"Simulation of the Effects of Shock Wave Passing on a Turbine Rotor Blade." *Journal for Gas Turbines and Power, Vol. 107, Oct. 1985, p. 998-1006*

Eulitz, F.; Engel, K.; Nürnberger, D.; Schmitt, S.; Yamamoto, K.; 1998
"On Recent Advances of a Parallel Time-Accurate Navier-Stokes Solver for Unsteady Turbomachinery Flow", *Computational Fluid Dynamics 1998, proc. 4. ECCOMAS, Ed. Papailiou et a., Vol.1, Part 1, pp. 252-258, John Wiley & Sons*

Erdos, J.I., Alzner, F., MCNelly, W.; 1977
"Numerical Solution of Periodic Transonic Flow through a Fan Stage", *AIAA Journal, Vol.15, pp 1559-1568, 1977*

Eriksson, L.-E., 1990
"A Third Order Accurate Upwind-biased Finite Volume Scheme for Unsteady Compressible Flow", *VFA report 9370-154, Volvo Aero Corporation, Trollhättan, Sweden*

Eriksson, L. E.; 1995
"Development and Validation of Highly Modular Flow Solver Versions in G2DFLOW and G3DFLOW Series for Compressible Viscous Reacting Flow.", *Technical Report 9970-1162 Volvo Aero Corporation, Sweden, 1995*

Fan, S.; Lakshminarayana, B.; 1996
"Time-Accurate EulerSimulation of Interaction of Nozzle Wake and Secondary Flow with Rotor Bladein an Axial Turbine Stage Using Nonreflecting Boundary Conditions."; *ASME Journal of Turbomachinery, Vol. 118, pp. 663-678, 1996 and ASME Paper No. 95-GT-230*

Feiereisen. J. M.; Fleeter, S.; 1998
"Unsteady Potential Effects on Rotor Wake and Stator Unsteady Aerodynamic Response"; *AIAA Paper No. 98-3432, 1998*

Feiereisen, J. M.; Montgomery, M. D.; Fleeter, S.; 1993
"Unsteady Aerodynamic Forcing Functions – A Comparison Between Linear Theory and Experiment."; *ASME Paper No. 93-GT-141, 1993*

Fielding, Leslie; 2000
"Turbine Design"; *ASME Press, New York, 2000 ISBN: 0-7918-0086-5*

Florea, R.; Hall, K. C.; 2001
"Sensitivity Analysis of Unsteady Inviscid Flow Through Turbomachinery Cascades"; *AIAA Journal, Vol. 39, No. 6; June 2001*

Fourmaux, A.; 1986
"Unsteady Flow Calculation in Cascades"; *ASME paper No. 86-GT-178; 1986*

Fransson, T.H.; Jöcker, M.; Bölcs, A.; Ott, P.; 1998
"Viscous and Inviscid Linear/Nonlinear Calculations Versus Quasi 3D Experimental Cascade Data For a New Aeroelastic Turbine Standard Configuration", *Journal of Turbomachinery, Vol. 121, No. 4, Oct. 1999, pp. 717ff.*;
Fransson, T.H.; Verdon, J.M.; 1992
"Updated Report on Standard Configurations for Unsteady Flow Through Vibrating Axial-Flow Turbomachine Cascades"; *Report No TRITA/KRV/92-009,, Royal Institute of Technology, Stockholm, Sweden, available on internet via http://www.egi.kth.se/ekv/stcf*
Fransson, T.H., Verdon, J.M.; 1991
"Standard Configurations for Unsteady Flow Through Vibrating Axial-Flow Turbomachine Cascades", *Unsteady Aerodynamics, Aeroacoustics and Aeroelasticity of Turbomachines and Propellers, H.M. Atassi (ed.), Springer Verlag, New York, pp. 859-889, 1993*
Fransson, T.H.; Bölcs, A.; Platzer, M.F.; 1989
"Numerical Simulation of Inviscid Transonic Flow Through Nozzels With Fluctuating Back Pressure", *Journal of Turbomachinery, Vol. 111, pp. 169-180, 1989*
Fransson, T.H.; Pandolfi, M.; 1986
"Numerical Investigation of Unsteady Subsonic Compressible Flows Through an Oscillating Cascade"; *ASME Paper 86–GT-304*
Freudenreich, K.; Jöcker, M.; Fransson, T. H.; 2001a
"Gust and Forcing Function in a Transonic Turbine" *Conference Proceedings of the 4th European Conference on Turbomachinery – Fluid Dynamics and Thermodynamics Firenze, 20th-23rd March, 2001, S.G.E., ISBN: 88-86281-57-9*
Freudenreich, Kai; 2001b
"Experimental Investigation of Velocity Gust in High Pressure Turbines"; *Doctoral Thesis at the Department of Energy Technology, Division of Heat and Power Technology, KTH Stockholm, 2001, ISSN 110-7990, TRITA-KRV-2001-1*
Freudenreich, Kai,; 1999
"Velocity and Turbulence Intensity Measurements in Two Annular Stator Configurations Using a Three-Dimensional Laser-Two-Focus Anemometer"; T*eknologi Licetiat Thesis at the Department of Energy Technology, Division of Heat and Power Technology, KTH Stockholm, 1999, ISSN 110-7990, TRITA-KRV-1999-1, ISBN 91-7170-376-4*
Freudenreich, K.; Jöcker, M.; Rheder, H.-J.; Höhn, W.; Fransson, T.H.; 1999
"Aerodynamic Performance of Two Isolated Stators in Transonic Annular Cascade Flow", *Proceedings of the 3rd Euopean Conference on Turbomachinery – Fluid Dynamics and Thermodynamics, London, UK, March 2-5, 1999, Professional Engineering Publishing, ISBN: 1 86058 196 X*
Friedrichs, S.; 2001
"Unsteady Flow and Aeroelasticity in Turbomachines"; *Cambridge Turbomachinery Course, Whittle Laboratory, June 2001*
Gerolymos, G.A.;1993
"Advances in the Numerical Integration of the Three-Dimensional Euler Equations in Vibrating Cascades"; *Journal of Turbomachinery, Vol. 115, pp. 781, 1993*
Giles M.; Heimes, R.; 1993
"Validation of a Numerical Method for Unsteady Flow Calculations"; *Journal of Turbomachinery, Vol. 115(1), pp 110-117, 1993*
Giles, M.; 1992
"An Approach for Multi-Stage Calculations Incorporating Unsteadiness"; *ASME paper No. 92-GT-282*

Giles, M.; 1991
"UNSFLO: A Numerical Method For The Calculation Of Unsteady Flow In Turbomachinery", *GTL Report #205*
Giles, M. B.; 1990
"Stator/Rotor Interaction in Transonic Turbine"; *Journal of Propulsion and Power, Vol. 6, No. 5, Sept. – Oct. 1990*
Giles, M. B.; 1989
"Non-Reflecting Boundary Conditions For Euler Equation Calculations", *AIAA Journal, Vol. 28, No. 12, pp 2050-2058*
Giles, M. B.; 1988a
"Non-Reflecting Boundary Conditions for the Euler Equations",
Report No. CFDL-TR-88-1, February 1988
Giles, M. B.; 1988b
"Calculation of Unsteady Wake-Rotor Interaction"; *AIAA J. of Propulsion, Vol. 4, No. 4; pp.356-362; 1988*
Goldstein, M. E.; 1978
"Unsteady vortical and entropic distortions of potential flows round arbitrary obstacles", *Journal of Fluid Mechanics, 1978, Vol. 89, part 3, pp. 433-468*
Green, J.S.; 1999
"Forced Response Predictions: Applications within the Design Process (Dealing with Orientation Scatter in Single Crystal Blades)"; *4th National Turbine Engine HCF Conference, Monteray, CA, USA. 9-11 Feb 1999.*
Green, J.S.; 2001
"AdturB Project Synthesis Report"; *Report No ADTB-RR-0011*
Groth, J.P.; Mårtensson, H.; Eriksson, L.E.; 1996
"Validation of a 4D Finite Volume Method for Blade Flutter"; *ASME paper 96-GT-429*
Grüber, B.; Carstens, V.; 1996
"Computation of the Unsteady Transonic Flow in Harmonically Oscillating Turbine Cascades Taking Into Account Viscous Effects"; *ASME Paper 96-GT-338*
Haldeman, C.W.; Dunn, M.G.; Abhari, R.S.; Johnson, P.D.; Montesdeoca, X.A.; 2000
"Experimental and Computational Investigation of the Time-Averaged and Time-Resolved Pressure Loading on a Vaneless Counter-Rotating Turbine", *ASME paper No. 2000-GT-0445*
Hall, K. C.; Lorence, C. B.; 1992
"Calculation of Three-Dimensional Unsteady Flows in Turbomachinery Using the Linearized Harmonic Euler Equations", *ASME Paper 92-GT-136*
Hall, K. C.; Crawley, E. F.; 1987
"Calculation of Unsteady Flows in Turbomachinery Using the Linearized Euler Equations", *Proceedings of the 4th international symposium on "Unsteady Aerodynamics and Aeroelasticity of Turbomachines and Propellers", pp. 15-38, Aachen, Germany, September 6-10, 1987.*
He, L; 1992
"Method of Simulating Unsteady Turbomachinery Flows with Multiple Perturbations"; *AIAA Journal, Vol. 30, No. 11, pp. 2730-2735, 1992*
He, L.; 1999
"Three-Dimensional Unsteady Navier-Stokes Analysis of Stator-Rotor Interaction in Axial-flow Turbines";IMECHE 99 paper C557/049/99, *Proceedings of the 3rd Euopean Conference on Turbomachinery – Fluid Dynamics and Thermodynamics, London, UK, March 2-5, 1999, Professional Engineering Publishing, ISBN: 1 86058 196 X*

He, L.; 2001
"Unsteady Flow and Aeroelasticity in Turbomachines"; *Cambridge Turbomachinery Course, Whittle Laboratory, June 2001*
Henderson, G. H.; Fleeter, S.; 1993a
"Forcing Function Effects on Unsteady Aerodynamic Gust Response. Part 1: Forcing Functions."; *Journal of Turbomachinery, Vol. 115, pp. 741-750, 1993*
Henderson, G. H.; Fleeter, S.; 1993b
"Forcing Function Effects on Unsteady Aerodynamic Gust Response. Part 2: Low Solidity Airfoil Row Response."; *Journal of Turbomachinery, Vol. 115, pp. 751-761, 1993*
Hennings, H. , Elliott, R.; 2002
"Forced Response Experiments in a High Pressure Turbine Stage", *ASME paper GT-2002-30453*
Hennings, H.; 2002b
"Private Communications"
Hilbert, G.R.; Ni Ron Ho; Takahashi, R. K.; 1997
"Forced Response Prediction of Gas Turbine Rotor Blades", *paper presented at the 1997 ASME Winter Annual Meeting*
Hilditch, M. A.; Smith, G. C.; Singh, U. K.; 1998
"Unsteady Flow in a Single Stage Turbine."; *ASME Paper No. 98-GT-531*
Hodson, H.P; 1985
"An Inviscid Blade to Blade Prediction of a Wake-Generated Unsteady Flow"; *ASME paper 84-GT-43 and J. of Turbomachinery, Vol. 107, pp 337- 344*
Hodson, H. P.; 1998
"Bladerow Interactions in Low Pressure Turbines"; *VKI Lecture Series 1998-02; Blade Row Interference Effects in Axial Turbomachinery Stages, 1998*
Holmes, D. G.; Mitchell, B. E.; Lorence, C. B.; 1997
"Three Dimensional Linearized Navier-Stokes Calculations for Flutter and Forced Response"; *Proceedings of the 8th International Symposium on Unsteady Aerodynamics, Aeroacoustics and Aeroelasticity of Turbomachines, Stockholm, Sweden, Kluwer Academic Publishers, ISBN0-7923-5040-5*
Hummel, F.; 2001
"Wake Wake Interactions and its Potential for Clocking in a Transonic High Pressure Turbine"; *ASME paper 2001-GT-0302*
Hwang, C. J.; Liu, J .L.; 1993
"Analysis of Steady and Unsteady Turbine Cascade Flows by a Locally Implicit Hybrid Algorithm"; *J. of Turbomachinery, Vol. 115, Oct. 1993*
Jameson, A.; 1986
"Current Status and Future Directions of Computational Transonics"; *Computational Mechanics-Advances and Trends, pp.329-367, ASME Ed. A.K. Noor, 1986*
Jareland, H.M.; Csaba, G.; 2000
"Friction Damper Mistuning of a Bladed Disk and Optimization With Respect to Wear"; *ASME paper 2000-GT-0363*
Jay, R. L.; Fleeter, S.; 1988
"Unsteady Aerodynamic Measurements in Forced Vibration Research"; *AGARD Manual on Aeroelasticity in Axial Flow Turbomachines, AGARD-AG-298, ISBN 92-835-0467-4, edited by Max F. Platzer and Franklin O. Carta, 1988*
Jeanpierre, J.; Fransson, T.; 1997
"Task 2, Forced Response Analysis, Subtask A2.1.1, Prediction of the Excitation Pressure Level on the Blades – 43 NGV", *Report No ADTB-KTH-2005, Internal report No. 97/26 November 1997, Confidential*

Johnson, A. B.; Rigby, M. J.; Oldfield, M. L. G.; 1989
"Unsteady Aerodynamic Phenomena in a Simulated Wake and Shock Wave Passing Experiment", *AGARD Conference Proceedings No. 468, "Unsteady Aerodynamic Phenomena in Turbomachines", pp. 9.1-9.13, Luxembourg, August 28-30, 1989.*
Johnston, R.T.; Feiereisen, J. M.; Fleeter, S.; 1998
"Measured Rotor Wake and Potential Forcing Functions, Including Blade Row Interactions"; *AIAA Journal of Propulsion and Power, Vol. 14 No. 2, pp. 191-198, 1998*
Jöcker, M.; Fransson, T.; 2002a
"Brite EuRam ADTurB: "Task 2 DLR Rig – Validation of Excitation Pressure Computations", *Report No. ADTB-KTH-2020, Internal Report No. KTH-HPT 25/02, February 2002, Confidential*
Jöcker, M.; Fransson, T.H.; 2002b
"Modeshape Sensitivity of the High Pressure Turbine Rotor Excitation Due to Upstream Stators", presented at *the 47th ASME TURBO EXPO 2002, paper No. GT-2002-30452*
Jöcker, M.; Hillion, F.X.; Fransson, T.;Wåhlén, U.; 2001
"Numerical Unsteady Flow Analysis of a turbine Stage with Extremely Large Blade Loads", *46th ASME Int. Gas Turbine and Aeroengine Congress, Exposition and User Symposium, paper No. 2001-GT-0260 and J. of Turbomachinery, Vol. 124, No. 3, pp.429ff, July 2002*
Jöcker, M.; Hillion, F.X.; Fransson, T.; 2000a
"Final Report, Design and Analysis of a Turbine with Extremely Large Blade Loads, Phase 2", *Report KTH-HPT-00/07, March 20700, Confidential*
Jöcker, M.; Freudenreich, K.; Rehder, H.-J.; Fransson, T. H.; 2000b
"Parametric Studies of the Aerodynamic Excitation in High Pressure Turbines.", *Proceedings of 9th International Symposium on Unsteady Aerodynamics, Aeroacoustics and Aeroelasticity of Turbomachines, Lyon, France, 2000, ISBN: 2 7061 1052 X*
Jöcker, M.; Fransson, T.; 1998a
Brite Euram ADTurB: Task 2: "Forced Response Analysis, Prediction of the Excitation Pressure Level on the Blades, 70 NGV", *Internal Report KTH-HPT-98/29, KTH/HPT, Stockholm, 1998, Confidential*
Jöcker, M.; Fransson, T.; 1998b
"Report on UNSFLO Calculations", Project "Design and Analysis of a Turbine Blade with Extremely Large Blade Loads", KTH Study Part 2: Numerical Parameter Study of the Axial Gap and the Stator Pitch on the Forced Response", *Report No. KTH-HPT-30/98, Nov. 98, Confidential*
Jöcker, M.; 1994
"Validation of Unsteady Aerodynamic Prediction Models on the Turbine Configuration TCT III"*, Project Study, KTH Stockholm, 1994, Confidential*
Jung, A. R.; Mayer, J. F.; Stetter, H.; 1996
"Simulation of 3D-Unsteady Stator/Rotor Interaction in Turbomachinery Stages of Arbitrary Pitch Ratio",*ASME paper 96-GT-69*
Kahl, G.; 1997
"Structural Mistuning and Aerodynamic Coupling in Turbomachinery Blades"; *Proceedings of the 8th International Symposium on Unsteady Aerodynamics, Aeroacoustics and Aeroelasticity of Turbomachines, Stockholm, Sweden, Kluwer Academic Publishers, ISBN0-7923-5040-5*
Kahl, G.; Klose, A.; 1991
"Time Linearized Euler Calculations for Unsteady Quasi-3D Cascade Flows"; *Unsteady Aerodynamics, Aeroacoustics and Aeroelasticity of Turbomachines and Propellers, H.M. Atassi (ed.), Springer Verlag, New York, pp.109–126, 1993*

Kielb, J. J.; Abhari, R. S.; 2001
Experimental Study of Aerodynamic and Structural Damping in a Full-Scale Rotating Turbine"; *ASME paper No 2001-GT-0262*
Kielb, R.E.; 2000
"CFD for Turbomachine Unsteady Flows – An Aeroelastic Design Perspective"; *Proceedings of 9th International Symposium on Unsteady Aerodynamics, Aeroacoustics and Aeroelasticity of Turbomachines, Lyon, France, 2000, ISBN: 2 7061 1052 X*
Kielb, R. E.; Chiang, H. D.; 1992
"Recent Advancements in Turbomachinery Forced Response Analyses"; *AIAA 92-0012, January 6-9, 1992, Reno, NV*
Korakianitis, T.; 1991
"Axial Gap Effects on the Propagation of Unsteady Flow in Cascades"; *proceedings of the 6th International Symposium on Unsteady Aerodynamics, Aerocoustics and Aeroelasticity of Turbomachines and Propellers, University of Notre Dame, September 15-19. 1991*
Korakianitis, T.; 1992a
"On the Prediction of Unsteady Forces on gas Turbine Blades: Part 1 – Description of the Approach", *Journal of Turbomachinery, 114, pp. 114-122, 1992*
Korakianitis, T.; 1992b
"On the Prediction of Unsteady Forces on gas Turbine Blades: Part 2 –Analysis of the Results", *Journal of Turbomachinery, 114, pp. 123-131, 1992*
Korakianitis, T.; 1993a
"On the Propagation of Viscous Wakes and Potential Flow in Axial-Turbine Cascades", *Journal of Turbomachinery, 115, pp. 118-127, 1993*
Korakianitis, T.; 1993b
"Influence of Stator-Rotor Gap on Axial-Turbine Unsteady Forcing Functions"; *AIAA Journal, Vol. 31, No. 7, July 1993*
Koya, M.; Kotake, S.; 1985
"Numerical Analysis of Fully Three-Dimensional Periodic Flows Through a Turbine Stage"; *J. of Engineering for Gas Turbines and Power, Vol. 107, pp. 945-952; 1985*
Lakshminarayana, B.; Chernobrovkin, A.; Ristic, D.; 2000
" Unsteady Viscous Flow Causing Rotor-Stator Interaction in Turbines, Part 1: Data, Code, Pressure ", *Journal of Propulsion and Power, Vol. 16, No. 5, 2000*
Laumert, B.; Mårtensson, H.; Fransson, T.F.; 2002
"Simulation of Rotor/Stator Interaction With a 4D Finite Volume Method"; *ASME paper No. GT-2002-30601*
Laumert, B.; Mårtensson, H.; Fransson, T.F.; 2001a
"Investigation of Unsteady Aerodynamic Blade Excitation Mechanisms in a Transonic Turbine Stage, Part 1: Phenomenological Identification and Classification"; *ASME paper 2001-GT-0258*
Laumert, B.; Mårtensson, H.; Fransson, T.F.; 2001b
"Investigation of Unsteady Aerodynamic Blade Excitation Mechanisms in a Transonic Turbine Stage, Part 2:Analytical Description and Quantification"; *ASME paper 2001-GT-0259*
Laumert, B.; Mårtensson, H.; Fransson, T.H.; 2000
"Investigation of the Flowfield in the Transonic VKI BRITE EURAM Turbine Stage with 3D Steady and Unsteady N-S Computations "; *ASME paper No. 2000-GT-0433*
Launder, B.E.; Spalding, D.B.; 1974
"The Numerical Computation of Turbulent Flow"; *Computational Methods in Applied Mechanics and Engineering, Vol. 103, pp.269-289, 1974*

Lewis, J.P.; Delaney, R. A.; Hall, E.J.; 1987
"Numerical Prediction of Turbine Vane-Blade Interaction"; *AIAA 87-2149; 1987*
Liamis, N.; Couaillier, V.; 1994
"Unsteady Euler and Navier-Stokes Flow Simulations With an Implicit Runge-Kutta Method", *Proceedings of the 2nd ECCOMAS Computational Fluid Dynamics Conference, 5-8 September 1994, Stuttgart, Germany, John Wiley & Sons 1994*
Liepman, H. W.; Roshko, A.;1957
"Elements of Gas Dynamics"*; Wiley, New York*
Manwaring, S. R.; Rabe, D. C.* Lorence, C. B.; Wadia, A. R.; 1997
"Inlet Distortion Generated Forced Response of a Low-Aspect-Ratio Transonic Fan." *Journal of Turbomachinery, Vol. 115, pp. 724-740, 1997 ASME Paper 96-GT-376*
Manwaring, S. R.; Wisler, D. C.; 1993
"Unsteady Aerodynamics and Gust Response in Compressors and Turbines."; *Journal of Turbomachinery, Vol. 115, pp. 724-740, 1993*
Marshall, J.G.; Giles, M.B.; 1997
"Some Applications of a Time-Linearized Euler Method to Flutter and Forced Response in Turbomachinery", *Proceedings of the 8th International Symposium on Unsteady Aerodynamics, Aeroacoustics and Aeroelasticity of Turbomachines, Stockholm, Sweden, Kluwer Academic Publishers, ISBN0-7923-5040-5*
Marshall, J.G.; Imregun, M.; 1996
"A Review of Aeroelasticity Methods With Emphasis on Turbomachinery Applications"; *Journal of Fliuds and Structures (1996) 10, 237-267*
Michelassi, V.; Martelli, F.; 1998
"Numerical Simulation of Unsteady Stator-Rotor Interaction in Brite-Turbine Stage"; *VKI Lecture Series 1998-02; Blade Row Interference Effects in Axial Turbomachinery Stages, 1998*
Montgomery, M.D.; Verdon, J. M.; 1997
"A 3D Linearized Euler Analysis for Blade Rows, Part 1: Aerodynamic and Numerical Formulations"; *Proceedings of the 8th International Symposium on Unsteady Aerodynamics, Aeroacoustics and Aeroelasticity of Turbomachines, Stockholm, Sweden, Kluwer Academic Publishers, ISBN0-7923-5040-5*
Moss, R. W.; Ainsworth, A. W.; Sheldrake, C. D.; Miller, R.; 1997
"The Unsteady Pressure Field Over a Turbine Blade Surface: Visualisation and Interpretation of Experimental Data", *ASME paper 97-GT-474*
Moyroud, F.; Cosme, N.; Jöcker, M.; Fransson, T.H.; Lornagex, D.; Jacquet-Richardet, G.; 2000
"A Fluid-Structure Interfacing Technique for Computational Aeroelastic Simulations"; *Proceedings of 9th International Symposium on Unsteady Aerodynamics, Aeroacoustics and Aeroelasticity of Turbomachines, Lyon, France, 2000, ISBN: 2 7061 1052 X*
Murthy, D. V.; Morel, M. R.; 1993
"Turbine Blades Forced Response Prediction using Freps", *Presented at the 1993 SAE Aerospace Atlantic Conference and Exposition in Dayton, Ohio, USA, April 20-23, 1993*
Pandolfi, M.; 1980
"Numerical Experiments on Unsteady Flows Through Vibrating Cascades "; *Proceedings of the 2nd International Symposium on Unsteady Aerodynamics and Aeroelasticity in Turbomachines, Sept. 1980, Lausanne, Switzerland*
Panning, L.; Sextro, W.; Popp, K.; 2000
"Optimization of Interblade Friction Damper Design"; *ASME paper 2000-GT-0541*
Panovsky, J.; Kielb, R.E.; 1998; "A Design Method to Prevent Low Pressure Turbine Blade Flutter"; *ASME paper 98-GT-575*

Rai, M.M.; 1989
"Three Dimensional Navier Stokes Simulations of Turbine Rotor-Stator Interaction"; *J. of Propulsion and Power, Vol. 5, No. 3, 1989, pp. 305-319*
Rangwalla, A. A.; Madavan, N. K.; Johnson, P. D.; 1992
"Application of an Unsteady Navier-Stokes Solver to Transonic Turbine Design."
AIAA Journal of Propulsion and Power, Vol. 8, No. 5, pp. 1079-1086
Rao, K. V.; Delaney, R. A.; Dunn, M. G.; 1994
"Vane Blade Interaction in a Transonic Turbine: Part I: Aerodynamics."; *Journal of Propulsion and Power, Vol. 10, No. 3, pp. 305-311, 1994*
Roe, P.; 1986
"Characteristic Based Schemes for the Euler Equations"; *Ann. Rev. Fluid Mech., 18:337-65, 1896*
Ruffles, P.C.; 2001
"Expanding the Horizons of Gas Turbine in Global Markets"; *ISABE 2001-1010*
Santoriello, G.; Colella, A.; Colantuoni, S.; 1993
"Rotor Blade Aerodynamic Design"; *Internal Project Report Alfa Romeo Avio, IMT Area 3 Turbine Project (AER2-CT-92-0044), Confidential*
Saxer, A. P.; Giles, M. B.; 1994
"Predictions of Three-Dimensional Steady and Unsteady Inviscid Transonic Stator/Rotor Interaction with Inlet Radial Temperature Nonuniformity."; *Journal of Turbomachinery, Vol. 116, pp. 347-357, 1994*
Saxer, A. P.; Giles, M. B.; 1993
"Quasi-Three-Dimensional Nonreflecting Boundary Conditions for Euler Equation Calculations*"; J. of Propulsion and Power, Vol. 9, No. 2, 1993, pp. 263-271*
Schmitt, S.; Eulitz, F.; Nürnberger, D.; Carstens, V.; Belz, J.; 2001
"Simulation of Propfan Forced Response Using a Direct Fluid-Structure Coupling Method"; Proceedings of the 4th European Conference on Turbomachinery – Fluid Dynamics and Thermodynamics Firenze, 20th-23rd March, 2001, S.G.E., ISBN: 88-86281-57-9
Sextro, W.; 2000
"The Calculation of the Forced Response of Shrouded Blades with Friction Contacts and Its Experimental Verification"; *ASME paper 2000-GT-540*
Shahpar, S.; 2001
"Three-Dimensional Design and Optimisation of Turbomachinery Blades using the Navier Stokes Equations"; *ISABE-2001-1053*
Sharma, O. P.; Pickett, G. F.; Ni, R. H.; 1992
"Assessment of Unsteady Flows in Turbines" *J. Turbomachinery, Vol. 114, pp. 79-90, and ASME Paper No. 90-GT-150*
Sidén, G.; 1991
"Numerical Solution of Viscous Compressible Flows Applied to Turbomachinery Blade Flutter"; *Ph. D. Thesis, Chalmers University of Technology, Göteborg 1991*
Silkowski, P.D.; Rhie, C.M.; Copeland, G.S.; Eley, J.A.; Bleeg, J.M.; 2001
"CFD Investigation of Aeromechanics"; ASME paper 2001-GT-0267
Silkowski, P.D.; Hall, K.C.; 1997
"A Coupled Mode Analysis of Unsteady Multistage Flows in Turbomachinery", *ASME paper 97-GT-186*
Singh, G.; Hall, D.M.; 1996
"Validation of Unsteady Methods Against Turbine Data"; *ImechE, 1996, No. S461/003/96, 1996*

Smith, S.N.; 1972
"Discrete Frequency Sound Generation in Axial Flow Turbomachines"; *Reports and Memoranda No. 3709, Cambridge 1972*
Spallart, P.R.; Allmaras, S.R.; 1992
"A One-Equation Turbulence Model for Aerodynamic Flows"; *AIAA paper 92-0439*
Suddhoo, A,; Stow, P.; 1990
"Simulation of Inviscid Blade Row Interaction Using a Linearized Potential Code"; *AIAA paper 90-1916, 1990*
Takeishi, K.; Matsuura, M.; Aoki, S.; Sato, T.; 1989
"An Experimental Study of Heat Transfer and Film Cooling on Low Aspect Ratio Turbine Nozzles", *ASME Paper No. 89-GT-187, ASME Journal of Turbomachinery, Vol.112, pp. 488-496*
Tchernycheva, O.; Kielb, R.E.; Barter, J.; Fransson, T.; 2001; "Comperative Analysis of Blade Mode Shape Influence on Flutter of Two Dimensional Turbine Blades"; *15th ISOABE 2001, Bangalore, India*
Ubaldi, M.; Zunino, P.; Cattanei, A.; Campora, U.; 2001
"Effect of Trailing Edge Cooling Flow on Turbine Wake Unsteady Flow Characteristics"; *Conference Proceedings of the 4th European Conference on Turbomachinery – Fluid Dynamics and Thermodynamics Firenze, 20th-23rd March, 2001, S.G.E., ISBN: 88-86281-57-9*
Vahdati, M.; Sayma, A.; Imregun, M.; 1998
"Prediction of High and Low Engine Order Forced Responses for an LP Turbine Blade"; *AIAA paper no AIAA-98-3719, 1998*
Venable, B. L.; Delaney, R. A.; Busby, J. A.; Davis, R. L.; Dorney, D. J.; Dunn, M. G.; Haldeman, C. W.; Abhari, R. S.; 1999
"Influence of Vane-Blade Spacing on Transonic Turbine Stage Aerodynamics Part I: Time-Averaged Data and Analysis.", *Journal of Turbomachinery, Vol. 121, pp. 663-672, 1999 and ASME Paper No. 98-GT-481*
Van den Braembussche, R. A.; 2001
"Design and Optimisation of Turbomachinery Components"; *Conference Proceedings of the 4th European Conference on Turbomachinery – Fluid Dynamics and Thermodynamics, Firenze, 20th-23rd March, 2001, S.G.E., ISBN: 88-86281-57-9*
Verdon J. M.; Caspar J. R.; 1984
"A linearized unsteady aerodynamic analysis for transonic cascades."; *J. Fluid Mech., Vol. 149, pp. 403-429,1984.*
Von Hoyningen-Huene, M.; Hermeler, J., 1999a
"Comparison of Three Approaches to Model Stator-Rotor Interaction in the Turbine Front Stage of an Industrial Gas Turbine", *Proceedings of the 3rd Euopean Conference on Turbomachinery – Fluid Dynamics and Thermodynamics, London, UK, March 2-5, 1999, Professional Engineering Publishing, ISBN: 1 86058 196 X*
Von Hoyningen-Huene, M.; Hermeler, J., 1999b
"Time-Resolved Numerical Analysis of the 2-D Aerodynamics in the First Stage of an Industrial Gas Turbine for Different Vane-Blade Spacings"; *ASME paper 99-GT-102*
Von Hoynigen-Huene, M.; Jung, A.R.; 1999c
"Comparison of Different Acceleration Techniques and Methods for Periodic Boundary Treatment in Unsteady Turbine Stage Flow Simulations", *ASME paper 99-GT-155*
Von Hoyningen-Huene, M.; Frank, W.; Jung, A.R.; 2000a
"Three-Dimensional Time-Resolved Flow Field in the First and Last Turbine Stage of a Heavy Duty Gas Turbine, Part I: Secondary Flow Field", *ASME paper 2000-GT-0438*

Von Hoyningen-Huene, M.; Frank, W.; Jung, A.R.; 2000b
"Three-Dimensional Time-Resolved Flow Field in the First and Last Turbine Stage of a Heavy Duty Gas Turbine, Part II: Interpretation of Blade Pressure Fluctuations", *ASME paper 2000-GT-0439*
Weaver, M.M.; Abhari, R.S.; Dunn, M.G.; Manwaring, S.R.; Salay, M.J.; Frey, K.K.; Heidegger, N.; 2000
"Forcing Function Measurements and Predictions of a Transonic Vaneless Counter Rotating Turbine"; *ASME paper 2000-GT-0375*
Whitehead, D.S.; Newton, S.G.; 1985
"A Finite Element Solution of Unsteady Two-Dimensional Transonic Flows in Cascades"; *International Journal of Numerical Methods in Fluids, Vol. 5, pp. 115-132, 1985*
Whitehead, D.S.; 1987
"Flutter of Turbine Blades", *Proceedings of the 4th International Symposium on Unsteady Aerodynamics and Aeroelasticity of Turbomachines and Propellers, pp. 437-452, Aachen, Germany, September 6-10, 1987.*
Whitehead, D. S.; 1990
"A Finite-Element Solution of Unsteady Two-Dimensional Flow in Cascades", *International Journal for Numerical Methods in Fluids, Vol. 10, pp. 13-34, 1990.*
Wilson, D. G.; Korakianitis, T.; 1998
"The Design of High-Efficiency Turbomachinery and Gas Turbines"; *ISBN 0-13-312000-7, Upper Saddle River, N.J.: Prentice Hall, 2nd ed.; 1998*
Wisler, D. C.; 1998a
"Blade Row Interaction and Unsteady Effects in Axial Flow Compressors and Fans"; *VKI Lecture Series 1998-02; Blade Row Interference Effects in Axial Turbomachinery Stages, 1998*
Wisler, D. C.; 1998b
"The Technical and Economic Relevance of Understanding Blade Row Interaction Effects in Turbomachinery"; *VKI Lecture Series 1998-02; Blade Row Interference Effects in Axial Turbomachinery Stages, 1998*
Wölfel, H.P.; 2001
"Umdruck zur Vorlesung Maschinendynamik"; *TU Darmstadt, WS 91/92*
Yen, H.-Y.; Herman Shen, M.-H.; 2000
"Development of a Passive Turbine Blade Damper Using Magnetomechanical Coating"; *ASME paper 2000-GT-36*